REPAIR OF SUB-LETHAL DAMAGE FOLLOWING SINGLE AND SPLIT-DOSE IRRADIATION USING ^{60}Co-GAMMA AND p(66)/ Be NEUTRONS

M A ZERABRUK

December 2005

REPAIR OF SUB-LETHAL DAMAGE FOLLOWING SINGLE AND SPLIT-DOSE IRRADIATION USING ^{60}Co-GAMMA AND p(66)/ Be NEUTRONS

Medhanie Abraha Zerabruk

This dissertation is submitted to the Cape Peninsula University of Technology as fulfilment of the requirement for the Master Technologiae in Biomedical Technology in the Faculty of Applied Sciences.

December 2005

Supervisor: Dr K A Meehan (Ass Prof) **Co-Supervisor:** Dr J P Slabbert

Faculty of Applied Sciences   Department of Radiobiology

Cape Peninsula University of Technology   iThemba LABs , Faure

Table of contents

CHAPTER 1

GENERAL INTRODUCTION AND LITERATURE REVIEW

CHAPTER 2

RADIOBIOLOGY

CHAPTER 3

CRYPT STEM CELL SURVIVAL ASSAY

CHAPTER 4

IMMUNOHISTOCHEMISTRY

CHAPTER 5

MICRONUCLEI (MN) ASSAY

CHAPTER 6

DIRECTION TO FUTURE STUDY

Declaration

I, the undersigned student hereby declare that the work contained in this dissertation is my own original work and has not been previously submitted, in its whole or in part, to any University of Technology or Technikon as fulfilment for the purpose of Master's or any other degree, for that matter.

Signature:................................ Date:......21|7|07......

Abstract

In clinical radiotherapy, experiments are performed to determine optimal conditions of the radiation prior to radiotherapy. These experiments focus on the relative biological effectivness(RBE) determination and are predominantly applied in high linear energy transfer (LET) radiations i.e. fast neutrons, as the RBE values for such radiations vary greatly. In general, the RBE of a certain radiation relative to a given reference radiation (^{60}Co gamma) varies widely with the energy, dose, dose rate, fractionation, type of tissue and end-point used.

Experience with neutron therapy at iThemba LABS has shown that treatment with more fractions and lower doses per fraction may be beneficial for some patients. To calculate the iso-effective treatment dose needed, an appropriate α/β ratio for early effects is needed. In this study, the repair of mouse jejunum was measured for split-dose irradiations to determine if a suitable α/β ratio for neutrons could be estimated using the known value for gamma rays and the applicable RBE.. Crypt stem cell survival was measured 3.5 days after split-dose exposures to p(66)/Be neutrons and ^{60}Co gamma rays. Dose response curves for both treatment modalities and for both acute and fractionated exposures were constructed by counting crypts of Leiberkhün at the base of the villi in haematoxylin and Eosin-stained sections of mouse jejunum. Using a RBE value of 1.64 and an α/β ratio of 7Gy noted for the fractionated photon exposures, an α/β ratio of 11.5

could be estimated for neutrons. With this, the neutron biological effective dose for a two treatment – that is iso-effective to an acute exposure of 8Gy- is calculated to be 9.6Gy. This compares to a value of 10.1 observed from the actual split-dose data for neutrons. It is concluded that a reasonably accurate α/β ratio for early neutron effects can be estimated using the values previously determined for photons.

Immunohistochemistry was performed using collagen –I and –IV to identify fibrosis; p53 as an apoptosis marker and CD34 as a marker of stem cells. Mouse tissue sections were stained after single and split-dose exposure to both gamma and neutron irradiations. Although p53 did not show evidence of dose response after both single- and split-dose exposures, and similar results were observed using CD34 as marker due o technical challenges, results from collagen type –I and –IV were encouraging and showed an increase in intensity as the dose and radiation energy increased. As collagen deposition is an indication of early radiation effect, this could prove an invaluable marker in the clinical setting.

Micronuclei (MN) frequencies can be used to evaluate the LET dependence repair kinetics of gamma and neutron irradiation. In this study, MN frequencies were lower after neutron exposure than gamma irradiation. A radiosensitive cell-line, CHO-XRS1 showed an increased biological damage compared to the CHO-K1 cells after both radiation modalities. These results can also be applied in the clinical setting as patients requiring radiotherapy may vary in their radiosensitivity.

Dedication

This thesis is dedicated to my Mom and Dad who have always been my mentors and source of inspiration. Thanks Mom and Dad for working hard to make me the person I am today.

Acknowledgements

When I started the project, I had neither a clue nor a guess of what radiobiology meant. But through the genuine help of many experts and fellow people I have managed to pick up each piece and completed the puzzle. I would like to thank.......

List of Tables

List of Figures

single crypt and five crypts are seen under the villus, at x400 magnification and (B) a cross-sectional view of control mouse jejunum with its villi (finger-like projections) and many crypts adjacent to one another at the base of the villi (x100).

Figure 3.5 Haematoxylin and Eosin (H & E) stained cross sections of mouse jejunum exposed to ^{60}Co-gamma; x50 magnification. (a) shows unirradiated (0 Gy) control mouse tissue; (b), (c), (d) and (e) are single fraction doses given as 11, 12, 13 and 14Gy, respectively. Likewise, slides (f), (g), (h) and (i) show the split-dose fraction given as 7+7, 7.5+7.5, 8+8 and 8.5+8.5Gy from the same radiation.

Figure 3.6 Haematoxylin and Eosin (H & E) stained cross sections of mouse jejunum exposed to p(66)/Be neutrons; x50 magnification. (a) shows unirradiated (0 Gy) control mouse tissue; (b), (c), (d) and (e) are single fraction doses given as 7, 8, 9 and 10Gy, respectively. Likewise, slides (f), (g), (h) and (i) show the split-dose fraction given as 4+4, 4.5+4.5, 5+5 and 5.5+5.5Gy. Villi denudation is seen in the higher dose of single fraction (slides d and e).

Figure 3.7 Dose dependent response of surviving crypts of Leiberkhün in mice exposed to single (heavy dark vertical lined bars) and split-dose fraction (light horizontal lined bars) using ^{60}Co-gamma irradiations (A) and p(66)/Be neutrons (B). Histogram bars show mean values of surviving crypts of three mice.

Figure 3.8 Dose response curves for crypt cell survival following exposure to single (▼, ■) or split-doses (◆, ▲) of both ^{60}Co-gamma rays and p(66)/Be neutron beam. The clear increase in total dose needed to remain iso-effective is a measure of the repairable damage induced by each treatment modality. Each dose-point is the mean number of surviving crypt cells counted in tissue from three mice.

Figure 4.1 Immunohistochemical staining of collagen-I. (a) Human placenta tissue and (b) unirradiated (0Gy) mouse tissue stained with primary antibody were used as positive control. (c) unirradiated (0Gy) mouse tissue stained without primary antibody but with ancillary reagents and (d) vice versa were used as internal negative controls. (e), (f) and (g), (h) show collagen-1 staining for low- and high-dose single-dose and split-dose exposures of ^{60}Co-gamma rays, respectively.

Figure 4.2 Shows subsequent immunohistochemical collagen-1 staining of the second experiment when a dextran labelled polymer (envison) was used in the attempt to reduce background staining. Slides (a) (b), (c) and (d) show low-

and high-dose response of single- and split-dose fraction of ^{60}Co-gamma rays, respectively. Controls as seen in Fig. 4.1.

List of Abbreviations

μ	micron
BN	bi-nucleated
Bq	Becquerel
CHO cells	Chinese hamster ovarian cells
Ci	curie
cm	centimetre
Cyt-B	cytochalasin B
DAB	di-amino-benzidine
EDTA	ethylenediamine tetra-acetic acid
FCS	foetal calf serum
GI	gastrointestinal
Gy	gray
KeV	kilo electron volt
H and E	haematoxylin and eosin
HPCR	high-pressure cooking antigen retrieval
LET	linear energy transfer
m	milli
α-MEM	eagle minimum essential medium
MeV	milli electron Volt
ml	millilitre

MN	micronuclei
PBS	phosphate buffered saline
rad	radiation absorbed dose
rem	radiation equivalent man
RBE	relative biological effectiveness
Sv	sievert
DNA	deoxy ribonucleic acid
SSB	single-strand break
DSB	double-strand break
LD	lethal damage
PLD	potentially lethal damage
SLD	sublethal damage
TBS	tris-buffer solution
UNSCEAR	United Nations Scientific Committee on the Effects of Atomic Radiation
NCRP	National Council on Radiation Protection and Measurements
ICRU	International Commission on Radiological Units and Measurements
ICRP	International Commission on Radiation Protection

Chapter 1

GENERAL INTRODUCTION AND LITERATURE REVIEW

1.1 Background

Years ago people suffered badly from radiation exposure and traces still appear to bear witness on the survivors of Hiroshima and Nagasaki. Hundreds of thousands of people lost their lives and survivors of these incidents are still facing the sequels of that tragic event (Smith, 2000). Considering past experience like this, the use of radiation as an instrument for treatment of deadly diseases such as cancer was never considered. However, while a risk of exposure to radiation still exists, radiation has become useful through the integrity of many dedicated scientists over the last few decades.

Today, radiation is used widely and efficiently and has proved its validity by sparing many lives from deadly disease. With the rapid growth in medical applications, radiation is the primary treatment for the long-term monitoring of life threatening anomalies (Travis, 2000).

A breakthrough in radiation discovery was seen in the nineteenth century. In 1895 the German physicist, Roentgen, discovered a ray that was emitted from a gas test tube. According to Roentgen, it was given the name "X", representing unknown radiation (X-

Chapter 1

GENERAL INTRODUCTION AND LITERATURE REVIEW

1.1   Background

Years ago people suffered badly from radiation exposure and traces still appear to bear

witness on the survivors of Hiroshima and Nagasaki. Hundreds of thousands of people

lost their lives and survivors of these incidents are still facing the sequels of that tragic

event (Smith, 2000). Considering past experience like this, the use of radiation as an

instrument for treatment of deadly diseases such as cancer was never considered.

However, while a risk of exposure to radiation still exists, radiation has become useful

through the integrity of many dedicated scientists over the last few decades.

Today, radiation is used widely and efficiently and has proved its validity by sparing

many lives from deadly disease. With the rapid growth in medical applications, radiation

is the primary treatment for the long-term monitoring of life threatening anomalies

(Travis, 2000).

A breakthrough in radiation discovery was seen in the nineteenth century. In 1895 the

German physicist, Roentgen, discovered a ray that was emitted from a gas test tube.

According to Roentgen, it was given the name "X", representing unknown radiation (X-

radiation) (Dowd & Tilson, 1999). In the beginning of 1896, the first medical use of this unknown radiation (X-radiation) was reported. In the same year Daniel reported hair loss after radiation exposure and in 1897 another German surgeon, Wilhelm Alexander Freud reported the loss of a hairy mole after the use of X-radiation for treatment (Hall, 2000). In 1898, Antoine Henri Becquerel investigated radioactivity, and Pierre and Marie Curie discovered radium, a radioactive element. The same year Villard also discovered the gamma ray (Dowd & Tilson, 1999).

These discoveries resulted in experiments on one's own body. Becquerel carried a radium container in his pocket that resulted in skin erythema and ulceration, and he thus became the first person to become aware of the biological effects of irradiation. Pierre Curie also deliberately exposed his forearm skin to ionising radiation and observed the acute biological effect of irradiation (Hall, 2000).

In the years between 1920-1930 French researchers introduced another concept, that of the fractionated use of radiation, in an attempt to sterilize the testes of a ram. They noted that sterilisation of ram testes with a single radiation dose resulted in massive skin damage of the scrotum. However, breaking down the single dose into smaller doses and applying it over an extended period of time in successive irradiations resulted in sterilization with little or no skin reaction on the scrotum (Hall, 2000).

Different committees and organisations, such as the UNSCEAR, NCRP, ICRU, and ICRP (see abbreviations), were set up since 1928 to develop radiation safety rules. In some countries protocols and protection recommendations were already developed as

early as 1913 to 1915 (Taylor, 1996; Dowd & Tilson, 1999). Small pocket devices were developed to measure the amount of radiation received during occupational exposure and these instruments were capable of detecting high and low radiation energy and also the type of radiation encountered during exposure (Dowd & Tilson, 1999).

1.2   Medical use of radiation

In this modern era the application of radiation energy goes beyond one's expectation by being used in food preservation and sterilization, medical sterilization, generation of medical and industrial X-rays, tracking the progress of medicines through the body with radioisotopes, nuclear medicine radiobiology, nuclear power, sewage treatment, artificial lighting, smoke detectors and tracing back to date archaeological and geological events (Taylor, 1996).

Due to their easy interaction with matter, poor penetration ability, and subsequent life risks, alpha particles are not used medically. If they gain access to the body, e.g. through inhalation, they are very hazardous and damage the cells and are not easily detected by personnel monitoring devices (Casarett, 1980; Dowd & Tilson, 1999). Beta particles are medically recognised to have several advantages, such as reducing fluid accumulation in the serosal cavities in metastatic carcinoma and treatment of thyroid cancer (Dowd & Tilson, 1999). X-rays are mainly used for medical diagnostic purposes and radiotherapy (Dowd & Tilson, 1999; Taylor, 1996) and gamma radiation is used in brachytherapy and teletheraphy for cancer treatment (Dowd & Tilson, 1999).

Despite all the shortcomings of fast neutrons described by Bewley (1989), some therapeutic indications for fast neutrons have become evident for treatment use and are reviewed by Wambersie *et al* (1994). Neutrons could have some advantage in treating X-ray resistant tumours, slowly progressing cancers and some highly developed cancers with a greater ratio of poorly oxygenated (hypoxic) cells (Joiner, 2002).

1.3   Types of radiation

But what is radiation all about? Radiation is a broad term used to portray a conceptual fact about the energy released from a radioactive atom either as waves or particles (Hall, 2000). According to Dowd & Tilson (1999) "it is the energy in transit".

Table 1.1. Types of radiations, their source and physical characteristic (Dowd & Tilson, 1999)

Type	Mass (amu)	Charge	Description	Production source
Alpha particle	4	+2	Doubly ionised helium atom	Radioactive decay, mostly heavy atoms
Beta particle (negation)	0.00055	-1	Negative electron	Radioactive decay
Beta particle (positron)	0.00055	+1	Positive electron	Radioactive decay, pair production
Protons	1	+1	Hydrogen nuclei	Van de Graff generators, cyclotrons
Negative pi-mesons	0.15	-1	Negative particle	accelerators
Heavy nuclei	Varies	Varies	Atom stripped off one or more electrons	accelerators
Neutrons	1	0	Neutron of atom	Atomic reactor, cyclotrons
Gamma rays	0	0	Electromagnetic radiation	Radioactive decay radiation
X-ray	0	0	Electromagnetic radiation	X-ray tube; rearrangement of orbital electrons

Radiation can be generated from two different sources: natural and artificial (man-made). Radiation from natural sources includes cosmic rays, radioactive substances found in rocks, and artificial sources such as X-rays (Taylor, 1996).

Regardless of what the source might be, radiation always exists as waves (electromagnetic radiation) or as particles (Taylor, 1996). **Table 1.1** briefly summarises the different types of radiation, their source and physical characteristics. Electromagnetic radiation comprises a large class of radiation which is divided into two categories, namely: the non-ionising and ionising radiations. Non-ionising radiation includes radio waves, microwaves, infra red, visible light and ultra violet; and ionising radiation consists of mainly X-rays, gamma rays and cosmic rays (Nias, 1990).

Unlike the electromagnetic radiations, the particulate radiation comprises only ionising radiation and includes the alpha, beta, electrons, neutrons, negative π-mesons, protons, and heavily charged ions (Nias, 1990).

1.4   Physics of radiation

All matter is made up of atoms and all atoms consist of an electron, proton and neutron (Dowd & Tilson, 1999). An atom is always in an electrically balanced state (neutral) and electrons are always in a constant motion revolving around the nucleus in their orbit. However, sometimes an atom can be unstable, as it encounters radiation, and changes continuously forming isotopes of the original atom (Taylor, 1996).

When ionising radiation comes into contact with biological matter, it may undertake either surface reflection, or be transmitted through the matter without interacting with atoms and molecules, but can also be totally or partially absorbed by the matter. The first two encounters are of no biological significance. However, absorption of radiation transfers energy and will lead to one of the following processes: **Excitation**, occurs when the energy of ionising radiation is only able to shift the orbit of an electron to a higher energy level and **ionisation** occurs when the absorbed energy is strong enough to "kick-off" an electron out of its orbit from an atom or molecule (Nias, 1990). A radioactive substance (radical) is formed in the process and continuously seeks a stable state. Such unstable atoms are chemically very reactive. Some radicals are so reactive that they exist only for as short a time as a microsecond (Taylor, 1996).

Any form of radiation quality is evaluated according to its energy deposition into or its absorption by the matter, and the consequential effect it will have on the specific target. The primary difference between photons and particulate radiation is that photons interact mostly by absorption but particulate radiations interact by ionisation (Dowd & Tilson, 1999).

This absorbed or deposited energy has a traditional unit *rad*, (old unit) which stands for the *radiation absorbed dose* and is measured per unit mass of the absorbing target. The SI unit of a dose is Gray (Gy), which is equal to 100rads (Dowd & Tilson, 1999).

Other units used to indicate different parameters of radiation dose include the *rem* (radiation equivalent man, old unit) and *sievert* (Sv; SI unit) which are units of biological

effect and are commonly used for personnel radiation monitoring. The **curie** (Ci; old unit) and **becquerel** (Bq; SI unit) are units of radioactivity and measure the rate of nuclear integration of a material (Taylor, 1996; Dowd & Tilson, 1999).

1.5 Factors affecting the quality of radiation

1.5.1 Dose

Radiation exposure could be of high or low dose. High doses, above 0.2 mSv, are considered harmful and could result in acute effects shown either instantly as somatic effects or as genetic effects appearing in the next generation of the person being exposed. Low doses are below 0.2 mSv where the effect is not usually noticed and can usually be received without being noticed by the recipient until a cumulative effect emerges over an extended period of time (Meltz, 2001).

In clinical radiotherapy a single high-dose is not usually administered to treat cancer patients but in order to spare the tissues from the damage brought about by high-doses, the single dose is broken down into smaller doses and delivered uniformly over an extended period of time. This method of dose distribution is known as *fractionation* (Hall, 2000). The conventional predictable dose used by most radiotherapy centres world-wide is 2Gy per day, 5 days a week and a total dose of 60-70Gy. However, variations on the schedules have developed in some countries depending up on the type and sensitivity of the cancer and also whether the radiotherapy is done in combination with surgery or not (NCRI, 2003).

1.5.2   Dose rate

The dose rate of any radiation exposure is "the radiation dose delivered per unit time" (Hall, 2000). The effect of exposure to high dose radiation could differ as a result of the rate of delivery. For instance an acute exposure of 2 mSv of gamma radiation within half an hour would cause nausea and vomiting, however, the same high dose distributed over days or months would result in a much less severe effect and could even pass unnoticed (Taylor, 1996). Therefore the rate at which the radiation is delivered to matter, especially to the human body, determines the effect and quality of the radiation.

1.5.3   LET of radiation

Another fundamental factor that accounts for the radiation quality is the linear energy transfer (LET) of a radiation. LET is the term widely used in radiobiology referring to "the density of ionisation in particle tracks". It has the unit keV/μm, which represents the density of the ionisation energy (keV) deposited per distance travelled (1 μm) across the tissue (Joiner, 2002).

X- and gamma-rays are considered to be low-LET radiations, and the alpha and beta particles are referred to as high-LET radiations (Casarett, 1980). High-LET radiations are densely ionising with a high rate of ion pair formation and poor penetration as a result of the quick release of energy. On the other hand, low-LET radiations are sparsely ionising with a low rate of ion pair formation, thus a good penetration with a slow release of

energy (Hall, 2000). **Figure 1.1** shows a schematic representation of the radiation energy distribution tracks within biological matter.
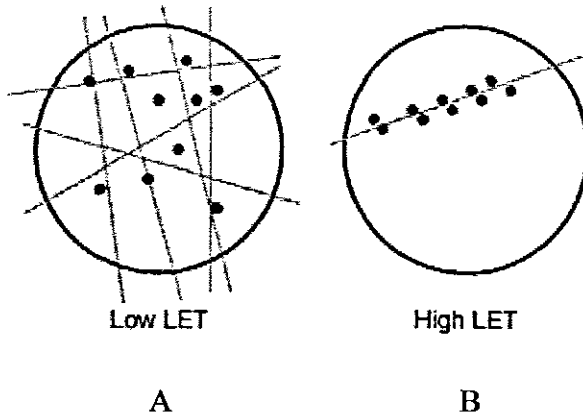
Figure 1.1. (A) Schematic illustration of low- and (B) high-LET radiations. Low-LET radiations are sparsely ionised and scattered in tortuous tracks where as high-LET radiations are densely ionised along one track.

Neutrons are regarded as high-LET radiation even though they carry no charge. The reason being that neutrons have the characteristics of reacting with atomic nuclei to produce radionuclides. It is this formation of a radionuclide that proves and qualifies a neutron beam as high-LET radiation (Casarett, 1980).

Although radiation is by-and-large categorized as high- or low-LET, it is not conclusive that a radiation incident has specific LET because of its energy. As radiation is not monoenergetic, the LET value given for a radiation is the average value of all the energies that a specific radiation carries (Dowd & Tilson, 1999). **Table 1.2** shows the average LET values for the different radiations.

Table 1.2. Average LETs for different radiations (Dowd & Tilson, 1999)

Types of Radiations	LET in keV/μm
Gamma rays	~0.1-0.3
10-MeV x-ray	~0.4-0.7
Diagnostic x-ray	1-3
Fast neutrons	~65
5-MeV alpha particles	100
Heavy nuclei	1000

1.5   The Biology of Radiation

As radiation enters a living cell it starts interacting with the cell components and takes a millionth of a second to insult the cell resulting in temporary and/or permanent damage (Steel, 2002). As it happens very fast, it is not well known which of the many chemicals or biochemical reactions brought about are responsible for initiating the damage. However, the possible interactions are: (1) *direct* and (2) *indirect* interactions (Bolus, 2001).

1.6.1   Direct and indirect interaction

In *direct* interactions the radiation is in direct contact with the macromolecule and results in serious modification or damage to the constituents of the macromolecule. This modification or damage depends upon the type of radiation and the amount of energy absorbed.

The absorbed dose may cause ionisation of different atoms and molecules and important macromolecules such as DNA (Schulte-Frohlinde & Bothe, 1991; Lett, 1992) lipids and proteins (Köteles, 1979; Daninak & Tann, 1995). There is a great possibility of breaking

a macromolecule more than once with densely ionising radiation (high-LET) than the sparsely ones (low-LET) (Casarett, 1980).

In single strand breaks the insult may not be very serious as there is another complementary strand from which the cell can repair. However, the damage becomes serious enough and may be beyond the cell's ability to repair if a double strand break occurs as shown in **Figure 1.2** (Sadrozinski, 2003). Sometimes separation of the two strands of a DNA molecule can happen if the bases are damaged. At times a DNA or protein crosslink may occur. This could be lethal as the crosslink will not pull apart during cell division (Travis, 2000). The most common types of DNA damage is shown in **Figure 1.2**.

Indirect interactions of radiation with other molecules, such as a water molecule, produces free radicals by the process called radiolysis of water (McMillan & Steel, 2002). Such free radicals are highly reactive and cytotoxic to the macromolecule (Steel, 2002). As the majority (70%-80%) of the cytoplasm is water, its abundance causes absorption of most of the incident radiation and the production of free radicals. Therefore, the main radiation damage to the cell is the result of the *indirect* interaction of the free radicals and the macromolecules (Casarett, 1980; Livesey *et al.*, 1985).
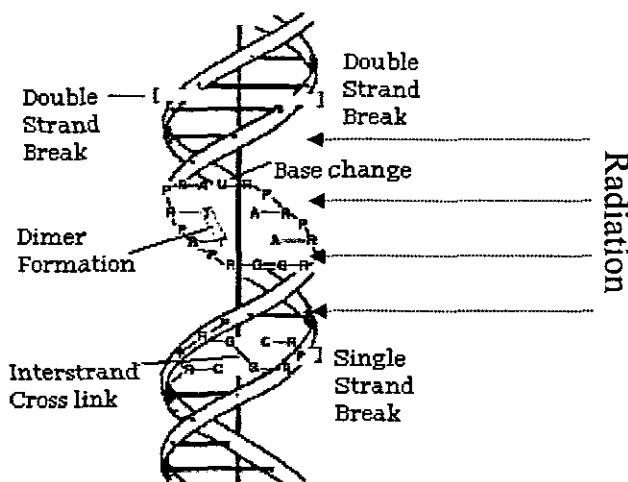
Figure 1.2. Shows the most common types of DNA damages and/or modifications after exposure to radiation.

1.6.2   Radiation-induced DNA damage

The primary site for radiation damage in the cell is the nucleus (DNA), though it damages all components of the cell. DNA is the centre of information for all the activities performed and thus the most sensitive part of the cell (Somosy, 2000; Travis, 2000). Radiation-induced damage to DNA can therefore be as much as ten times more than to the rest of the components of the cell. The radiation response of cell organelles is well reviewed by Somosy, (2000).

The interaction of ionising radiation with the cell, especially with macromolecules such as DNA, could result in one of the following phenomena: a cell hit by radiation can encounter a single- (SSB) and/or double-strand breaks (DSB), base pair change, dimer formation between base pairs, or interstrand cross link formation (Travis, 2000).

Since early 1966, studies have been carried out on DNA damage from radiation and its associated cell death. Extensive work involving unicellular organisms (bacteria and yeast) and multicellular organisms (mammalian cells) has provided the following four important points relating to the induction and repair of strand breaks as follows: (1) Double-strand breaks which have failed to repair aggravate cell damage by leading to chromosome aberrations and failure of cell division; (2) cell repair could either be error prone, where the repair is done but incorrectly; or error free, where the repair is made and normal function is attained; (3) all strand breaks are not lethal, only those sites critical to bring about cell death; and (4) quantification of strand breaks and their repair could be completely ambiguous as their presence or absence only indicates either the amount of energy deposited or the cells ability to repair non-lethal damage (George & Cramp,1987).

1.6.3   Radiation effects on chromosomes

A cell encountering ionising radiation is susceptible to many forms of chromosomal aberrations (Evans, 1962; Savage, 1976; Travis, 2000). Such aberrations are cell cycle dependent and are mainly evident in G_0/G_1 and $G_2/$ S phase and involve both chromatids of a chromosome (IAEA, 2001). Chromosomal aberrations can be grouped into unstable (including acentrics, dicentrics and centric rings) and stable aberrations (including reciprocal translocations, non-reciprocal translocations and interstitial translocations) (IAEA, 2001). For this study purpose we will only look at unstable aberrations.

When one arm of two different chromosomes is broken during radiation exposure the resultant effect is one set of chromosome fragments with no centromere and another set

of chromosome fragments with a centromere, each set having broken sticky ends (**Figure 1.3A**). If the broken sticky ends do not rejoin again (restitution) the two chromatids without a centromere will join to form an ***acentric*** chromatid, and the other set of chromatids with centromeres will also join to form a ***dicentric*** chromatid, as shown in **Figure 1.3A** (Travis, 2000).

(A)   (B)
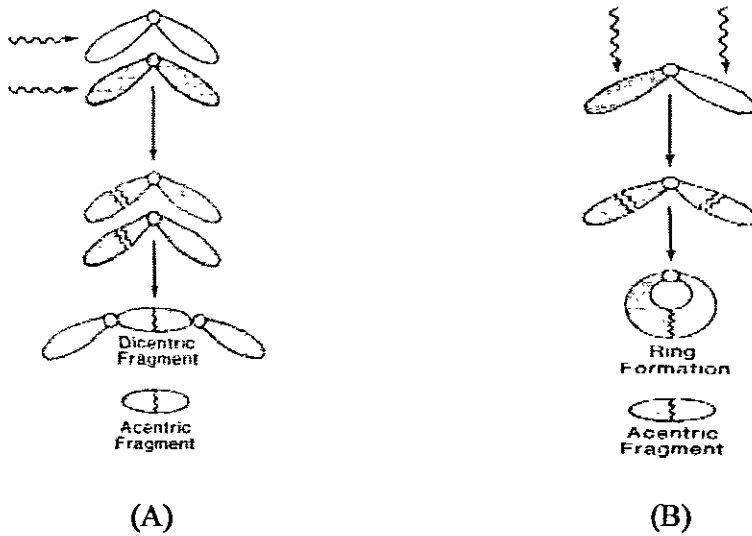
Figure1.3. Shows the possible chromosome breakages and re-unions after exposure to radiation resulting in (A) dicentric and acentric; and (B) ring and acentric fragment arrangements.

After irradiation each arm of one chromosome can also break resulting in one set of chromosome fragments with one broken end and another set of chromosome fragments with a centromere and broken on both ends. Thus the former set will give rise to an ***acentric*** fragment, and the latter will form either a normal or twisted ***centric*** ring as shown in **Figure 1.3B** (Travis, 2000).
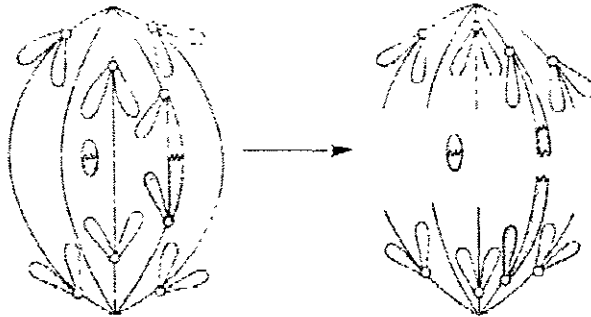
Figure 1.4. Shows the loss of genetic information due to *acentric* and *dicentric* chromosomal breakage, when chromosomes are pulled to opposite sides in the anaphase of the cell cycle (Travis, 2000).

During anaphase the acentric fragment does not attach to the spindle of the cell and stays in the original cell; however the two centromeres of the dicentrics will attach to the spindle and another break occurs as the spindle tries to pull the chromosome to the two opposite sides, as shown in **Figure 1.4.** In each case the daughter cells lose some of the genetic information (Travis, 2000).

Chromosome fragments (acentrics, centrics and dicentrics) and whole chromosomes that are unable to attach to the spindle at metaphase, lag behind at anaphase, and are not included in the daughter nuclei during nuclear division. This results in a small separate nucleus formation along with the main nucleus, hence the term micronuclei (Fenech *et al.*, 1999).

Micronuclei, which are derived from chromosomal aberrations, can be used as an indirect measurement for chromosomal damage (Fenech, 2000). The study of DNA damage at the chromosome level is important as such aberrations form the basis for radiobiological and

DNA-repair theory and contribute a lot in the fields of clinical cytogenetics, environmental monitoring and biological dosimetery (Streffer *et al.*, 1998).

References:

Bewley, D.K. 1989. The physics and radiobiology of fast neutron beams. Bristol: Adam Higler.

Bolus, N.E. 2001. Basic review of radiation biology and terminology. *Nuclear Medicine Technology*, 29(2):67-73.

Casarett, G.W. 1980. *Radiation histopathology.* Florida: CRC Press: Vol 1.

Daninak, N. & Tann, B.J. 1995. Utility of biological membranes as indicators for radiation exposure: alterations in membrane structure and function over time. *Stem Cells*, 13: 142-152.

Dowd, S.B. & Tilson, E.R. 1999. *Practical radiation protection and applied radiobiology.* 2nd ed. Philadelphia: Saunders.

Evans, H.J. 1962. Chromosome aberrations induced by ionisation radiations. *Int. Rev. Cytol.*, 13: 221-321.

Fenech, J. 2000. The *in vitro* micronucleus technique. *Mutation Research*, 455: 81-95.

Fenech, J., Holland, N., Chang, W.P., Zeiger, E. & Bonassi, S. 1999. The Human Micronuclei Project-An international collaborative study on the use of the micronucleus techniques for measuring DNA damage in humans. *Mutation Research*, 428: 271-283.

George, A.M. & Cramp, W.A. 1987. The effects of ionising radiation on structure and function of DNA. *Progress in Biophysics and Molecular Biology,* 50(3):121-169.

Hall, E.J. 2000. Radiobiology for the Radiologist. 5th ed. Philadelphia, PA: Lippincott Williams & Wilkins. 67-87

IAEA, 2001. Cytogenetic Analysis for Radiation Dose Assessment, A manual, Technical Report Series No. 405, Vienna.

Joiner, M.C. 2002. Particle beams in radiotherapy. In Basic Clinical Radiobiology, 3rd ed. Edited by G.G. Steel. London: Arnold. 205-216.

Köteles, G.J. 1979. New aspects of cell membrane radiobiology and their impact on radiation protection. *Atomic Energy Review,* 17: 3-30.

Lett, T.T. 1992. Damage to Cellular DNA from particulate radiation, the efficacy of its processing and the radiosensitivity of mammalian cells: emphasis on DNA strand breaks and chromatin break. Radiation and Environmental Biophysics, 31: 257-277.

Livesey, J.C., Reed, D.J. & Adamson, L.F. 1985. Radiation-Protective Drugs and Their Reaction. *Research,* 69: 459-474.

McMillan, T.J. & Steel, G.G. 2002. DNA damage and cell killing. In Basic Clinical Radiobiology, 3rd ed. Edited by G.G. Steel. London: Arnold. 71-83.

Meltz, M. 2001. Ionising Radiation and its Biological and Human Health Effects. Proceedings of the Symposium of the University of Texas Health Science Center, San Antonio, updated July 2001 [24 June 2004].

NCRI Progress Review Group. 2003. Report of the Radiotherapy and Related Radiobiology. [Online], 27 August. Available: http://www.ncri.org.uk/publications/index.cfm?NavSub=20 [16 September 2005].

Nias, A.H.W. 1990. An Introduction to Radiobiology. London: Wiley

Sadrozinski, H.F.W. 2003. Radiation effects in life sciences. Nuclear Instruments and Methods in Physics research Section A: Accelerators, Spectrometers, Detectors and Associated Equipment. Proceedings of the 4th International Conference on Radiation Effects on Semiconductor Materials, Detectors and Devices. 514(1-3): 224-229, [Online] September 2003. Available: doi:10.1016/j.nima.2003.08.109 [28 April 2004].

Savage, J.R.K. 1976. Classification and relationships of induced chromosomal structural changes. *J. Med. Genet.*, 13: 103-122.

Schulte-Frohlinde, D. & Bothe, E. 1991. The development of chemical damage of DNA in aqueous solution, In: Fielden, E.M., O'Neils, O. (Eds.), The Early Effects of Radiation in DNA, NATO ASI Series H: Cell Biology, 54. Springer, Berlin, 317-332.

Smith, M. 2000. "Hiroshima was no longer a city". International Socialist Review, Issue 13, [Online] August/September. Available: http://www.isreview.org/issues/13/Hiroshima-Nagasaki.shtml [7 July 2004].

Somosy, Z. 2000. Radiation response of the cell organelles. Micron, 31: 165-181

Steel, G.G. 2002. Introduction: the significance of radiobiology for radiotherapy. In Basic Clinical Radiobiology. 3rd ed. Edited by G.G. Steel. London: Arnold.1-7

Streffer, C., Müller, W.-U., Kryscio, A. and Böcker, W. 1998. Micronuclei – biological indicator for retrospective dosimetery after exposure to ionising radiation. Mutation Research, 404: 101-105.

Taylor, L.S. 1996. WHAT YOU NEED TO KNOW ABOUT RADIATION. [Online]. Available: http://www.physics.isu.edu/radinf/lstintro.htm [17 June 2005].

Travis, E.L. 2000. Primer of Medical Radiobiology. 2nd ed. St. Louis: Mosby

Wambersie, A., Richard, F. & Breteau, N. 1994. Development of fast neutron therapy worldwide. *Acta Oncol.*, 34: 261-274.

Chapter 2

RADIOBIOLOGY

2.1 Background

In 1896, after a skin reaction from the radium bar carried by Becquerel in his pocket, and hair loss reported from radiation exposure by Daniel, radiobiology was introduced as a new science (Dowd & Tilson, 1999). Radiobiology is the combination of two disciplines: - the physics and the biology of radiation. This new science focused on the interaction of ionising radiation with biological systems, its biological effect at cellular level and the factors that change the course of interaction within the biological system.

The principles of radiobiology governing radiation interaction with matter explain that charged particles produce a unique radiation effect compared to photons. Photons, such as X-rays, interact by absorption, however; charged particles interact by ionisation (Dowd & Tilson, 1999).

2.2 Biophysical properties of biological damage

The biological damage caused by high-LET radiation is immense yet relatively low with low-LET. There is an optimal LET above which the damage caused will no longer be in a linear relationship with the increase of LET (Hall, 2000). The reason for this is that very densely ionising, high-LET radiation is less efficient when too many particles hit the

same spot on the double-strand DNA molecule causing the same damage (Joiner, 2002).

At the same time, sparsely ionising low-LET radiation is also less efficient when little

damage is induced by a single particle hit to one of the strands of the DNA molecule

(Hall, 2000). Therefore, somewhere in between is the optimal LET at which the

maximum damage is done.

The relationship between the diameter of a double-strand DNA molecule (20Å) and the

average separation distance of ionisation density reveals that the two measurements

almost coincide at about 100 keV/μ (Hall, 2000). **Figure 2.1** illustrates the RBE change

in relation to increased LET of a radiation and the point at which double-strand breaks

occur at the maximum LET. At this optimal LET the maximum biological damage occurs

as a result of double-strand breaks of the DNA molecule. However, it differs with cell

type, range of LET values in the radiation beam, and the average LET (Joiner, 2002).
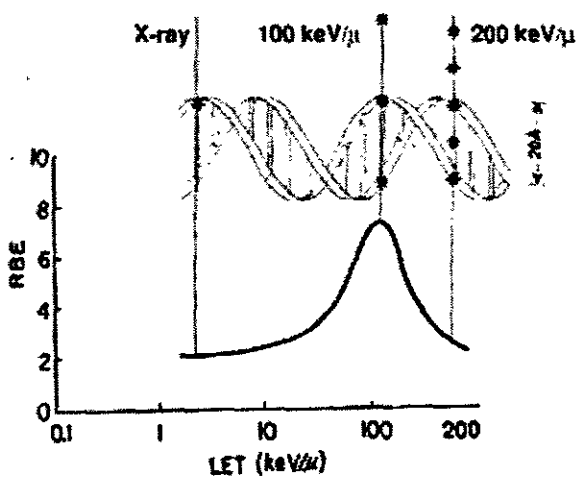
Figure 2.1. Shows the RBE dependence on LET of radiation and
the optimal biological damage of DNA double-strand breaks at
the maximum LET. (Redrawn from Hall, 2000).

In a plotted graph, using RBE as a function of LET, the rise of RBE values is gradual, approaching 10 KeV/μ then suddenly increases to attain a maximum value at around 100 KeV/μ. Beyond 100 KeV/μ the curve shows a quick fall in value again explaining the phenomenon of overkill. This optimal LET, where the maximum biological effect is attained remains much the same for a wide range of mammalian cells, from mouse to humans (Hall, 2000).

Depending on the damage induced, the cell may either respond to repair the damage or remove itself as a whole before the incorrect information is transferred to the next daughter cell. The repair processes may involve stimulation of enzymatic reactions and enhancement of cell proliferation should there be a need for cell replacement (Steel, 2003). However, damage (especially in DNA) that fails to repair may lead to programmed cell death, known as *apoptosis,* presumably initiated with incident radiation (McMillan & Begg, 2002).

2.3   Types of damage

Generally there are three possible types of radiation damage that can occur during radiation exposure, namely: lethal damage, sub-lethal damage and the potentially lethal damage, of which only sub-lethal and potentially lethal damage can be repaired (Hall, 2000).

Lethal damage (LD) is a complete, irreversible and non-repairable damage that ultimately leads to cell death. Here the cell damage overrides cell repair capacity and cells lose reproductive integrity, therefore no recovery is expected (Nias, 1990).

- 23 -

However, with the potentially lethal and sub-lethal damage, the damage is basically lethal but with a special treatment before or after irradiation some damage is spared to the cell (Travis, 2000).

Potentially lethal damage (PLD) has the potential to recover provided a suitable environment, pre- or post-irradiation treatment is obtained for the cell to repair the damage. The importance of the pre- or post-irradiation treatment is the delay of the mitotic phase of the cell cycle in order to create enough time for the cell to repair its DNA damage before attempting any cell division (mitosis) (Nias, 1990; Travis, 2000). The degree of repair may differ and the repair probability will also vary from one cell line to another (Hall, 2000).

In **sub-lethal damage (SLD)** the repair of the surviving fraction of the cell is enhanced and the damage is less than the equivalent single dose as a result of the cumulative repair from the two split-doses given in a certain time interval. The resulting effect was termed by Elkind as the "recovery from sub-lethal damage" or simply known as Elkind repair (Elkind & Sutton, 1960). Fractionation tends to spare normal tissue due to the repair of sub-lethal damage between dose fractions as well as re-growth or repopulation of cells. On the other hand fractionation increases the induced damage to the tumour cells because of the reoxygenation and reassortment in the cell cycle (Nias, 1990).

2.4 Cellular response to radiation damage

2.4.1 Cell cycle and radiosensitivity

Proliferating cells normally reproduce themselves by entering a process called the cell cycle. This cell cycle is generally divided into two major phases; the interphase, which is subdivided into G-1, S, and G-2 phases and the mitotic phase (M) including its subdivisions: prophase, metaphase, anaphase, telophase, and cytokinesis (Van De Graaff, 2000). Mammalian cell cycling times vary greatly due to the differences in time spent in G-1 phase and to a lesser degree in S- and M-phases. Overall, cells in M and G-2 phase are the most radiosensitive and the most resistant ones are those in late S-phase as well as early G-1 cells with a longer cycling time and a considerably prolonged G-1 phase (Hall, 2000).

Exposure of proliferating cells to radiation may cause substantial delays in most of the cell cycle phases. Such phenomena correlate with the delay of metabolic pathways associated with the cell-proliferation cycle. The delay varies considerably within the different phases of the cell cycle, where the shortest delay is from early G-1, with a greater delay from late G-1 to S, and keeps increasing through the S-phase to G-2. Most of all, the greatest delay is seen from G-2 to M (Casarett, 1980).

When DNA is hit by radiation, the cell responds with three main cell progression delays. The first delay is in the cell cycle checkpoint (Sorrentino, 1996; Bolus, 2001 & Meltz, 2001). This involves stimulation of enzymatic reactions to repair damage and enhance cell proliferation in case there should be a need for cell replacement (Steel, 2003).

The delay allowing for repair to occur; in the G-1 phase, could lead to the second cell progression delay which is the slowing down of DNA synthesis. As cell synthesis is delayed in S-phase, cells cannot complete the M-phase on time and this leads to the third delay of the cell division (Sorrentino, 1996). In general, the more the radiation damage occurring before M-phase, the greater the chance for the cell to repair errors and less delay to cell division (Casarett, 1980).

Therefore, as a result of an overall decrease or failure of cells to proliferate, cell death occurs. Proliferating cells fall short in completing mitosis either instantly or after a few successive divisions following irradiation and this leads to cell death (Thomson & Suit, 1969 and Bolus, 2001). Cells can undergo mitotic death in the first or within a few successive cell divisions due to unrepaired or improperly repaired chromosomal damage (Dewey, *et al.*, 1970), or can undergo interphase death (e.g. lymphocytes, spermatogonia) a relatively rapid cell death induced by the apoptotic mechanism of the cell (Stephens, *et al.*, 1991; Hendry & West, 1997; Bolus, 2001).

2.4.2 Radiation and cell sensitivity

Different cells have different radiosensitivities. Some are very sensitive, some intermediate and others are resistant (Casarett, 1980). In 1906 Bergonie and Tribondeau discovered that cells which have a high division rate, high metabolic rate, are not differentiated, and well-nourished are generally more likely to be radiosensitive and stated: "The radiosensitivity of a tissue is directly proportional to its reproductive capacity and inversely proportional to its degree of differentiation" (Dowd & Tilson,

1999). Except for a few cell types, the law remained the rule-of-thumb in radiobiology.

Cells such as nerve and muscle cells are known to be radioresistant and liver cells, partially differentiated are also radioresistant, but less so. Cells that serve to support other tissue, such as the epithelial cells of the blood vessels and the fibre of the connective tissue, are intermediate in radiosensitivity (Casarett, 1980). On the other hand, the precursor cells called *stem cells*, such as in the crypt of Leiberkhün at the base of the villi are one of the most sensitive cells to radiation. They continuously divide and as they move about along the villi they partially differentiate and keep differentiating until they are fully differentiated and functional (Potten, 2004). The characteristic high turnover rate of radiosensitive cells enables them to overcome low-dose exposures with complete damage repair. However, in higher doses; due to an increase in cell death, the normal cells of the particular organ are destroyed resulting into a severe negative effect on the organ.

Elkind and his colleagues (1965), revealed an increase of the cell surviving fraction from 0.005 to 0.02 using cultured Chinese Hamster cells when a single dose of 15.58Gy was given in two fractions, with a time window of 2 hours between doses. At room temperature, cells showed a rapid increase of recovery and the maximum cell survival was attained after a 2 hour gap between split-doses. An additional time gap between the spilt-doses did not show much difference in cell survival score. However, when the cells were grown at 37 °C the trend of the survival graph seemed to change, showing different growth patterns, as shown in **Figure 2.2** (Elkind *et al.*, 1965).

In the first two hours the pattern stays the same as the repair starts shortly after initial damage. After that, the survival curve slowly drops for the next 4 hours if the time gap in-between the fractionated doses is increased. A further increase in the time gap is accompanied by an increase of cell survival only if the time interval exceeds the cell cycle, once again the pattern of the curve slowly rises upwards (Hall, 2000). This curve illustrates the characteristics of the cell cycle, namely: the **Repair**, the **Reassortment** and the **Re-growth** (Re-population), known as the three R's of radiobiology, as shown in **Figure 2.2.**
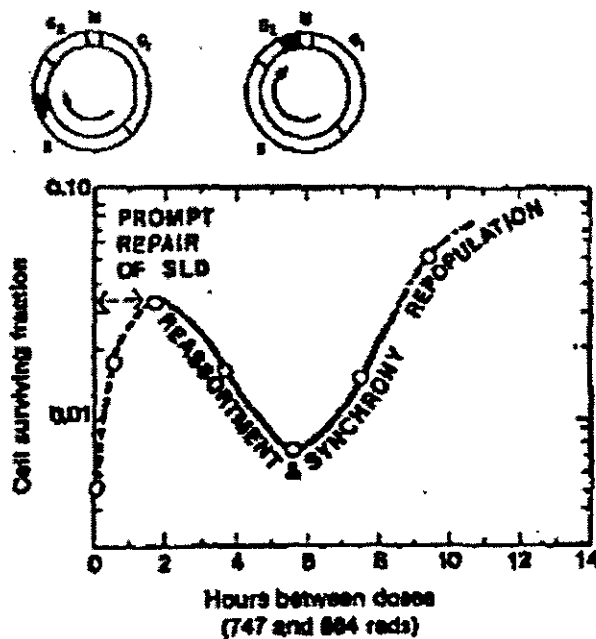
Figure 2.2. Shows the three R's of radiobiology from survival experiment of Chinese hamster cells exposed to split-dose X-ray radiation (Hall, 2000).

The **Repair** normally starts after induced damage, such as the sub-lethal damage already described above. Cells in the S-phase of the cell cycle are the most notable survivors after the first induced damage and are able to progress further, while cells in the rest of the phases (radiosensitive) die (Steel, 2002). If time allows, they reassort (synchronise) themselves into more radiosensitive phases of the cell cycle, hence the **Reassortment** phase (Hall, 2000). Studies investigating the age of a cell or the synchronous and non-synchronous cell populations through the cell cycle explain that the reassortment of a cell is due to the fact that radiosensitivity is high in the G-2 and mitosis phase, and usually less so during late S-phase (Elkind, *et al.*, 1965; Hall, 2000). **Repopulation** of cells occurs due to cell division if the time between fractionation exceeds the cell cycle time. Cells thus quickly repopulate from the reassortment (synchronous) phase (Elkind, *et al.*, 1965).

2.5 Relative biological effectiveness (RBE)

According to the International Commission on Radiological Protection (ICRP), the effectiveness of different types of radiations for inducing the same biological endpoint is commonly known as the *Relative Biological Effectiveness* (RBE) of a radiation (ICRP, 2003). The RBE of a given radiation is defined as: "the comparison of a dose of test radiation to the dose of 250 keV x-ray that produces the same biological response" (Travis, 2000).

The RBE is expressed as:

$$RBE = \frac{\text{Dose in Gy from 250 keV X-ray or reference beam}}{\text{Dose in Gy from another test radiation delivered under the same conditions to produce the same biological effect}}$$

Low-LET radiation is usually used as a reference and is a 250 KeV/μ X-rays. Depending on the dose and the biological damage, as shown by many endpoints, the RBE of a given radiation increases with an increase in LET (IAEA, 2001; Joiner, 2002). Therefore, RBE of a given radiation is highly dose dependent; hence different RBE's could be measured for a given biological damage corresponding to a specific dose point (Hall, 2000) as shown in **Figure 2.3**. At doses below 0.5Gy, the possibility of a double-strand break (DSB) is very much lower; however, as the dose increases the incidence of DSB increases accordingly (IAEA, 2001). Hence the dose-response curve for the survival fraction will be a combination of both the single- and double-strand breaks as the former explains events at low and the latter at high doses fitting the following linear-quadratic equation:

$$SF = \alpha D + \beta D^2$$

where: D is the dose, α is the linear coefficient of the lethal damage and β is the dose squared coefficient of the sub-lethal damage. Therefore, the maximum RBE (RBE_m) is obtained as the ratio of the α-coefficients of the high- and low-LET dose response curve yield equations (IAEA, 2001). The α/β ratio has the unit dose (Travis, 2000) and is the "dose at which the linear and quadratic components of a radiation damage are equal"

(Hall, 2000 & IAEA, 2001). This ratio is used to divide the normal tissues as acute and late responding in terms of a linear-quadratic relationship between effect and dose, which plays a significant role in clinical radiotherapy (Hall, 2000).

For the same radiation energy applied either as a single dose or a dose per fraction, the RBE varies considerably among different tissues used as end-points. Broerse and Barendsen (1973) and their co-workers examined five different cell types, from mouse and humans, after exposure to 300-kV X-rays and 15 MeV neutrons. They obtained a wide range of radiosensitivities with a wide shoulder for X-rays. For neutrons a similar range of radiosensitivities produced a smaller shoulder. The width of the shoulder indicates the range of variability, where X-rays have large variability and neutrons have small variability (Hall, 2000).
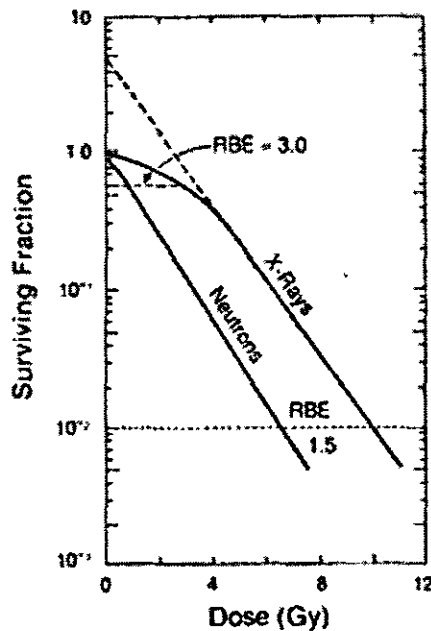
Figure 2.3. Shows the RBE dependence for a given biological end-point chosen at specific dose points (Hall, 2000).

2.6   Neutrons

2.6.1 Early neutrons and their clinical practice

Neutrons are generated by reactors through a fission process, from the bombardment of targets with a low atomic number, such as beryllium, with high energy positive ions accelerated in cyclotrons and by using small and inexpensive accelerators. Detailed sources and energy deposition characteristics of fast neutrons are discussed by Broerse & Barendsen, (1973) and Bewley, (1989).

Between 1937 and 1943 neutrons were applied in radiotherapy but without any medical and/or radiobiological advantage over other radiations e.g. X-rays, and were generated from 37-in. and 60-in. cyclotrons at Berkeley with a modal energy of 4 and 7 MeV, respectively (Stone, 1948). However, in 1943 radiation practice using fast neutrons was stopped when serious late effects on skin and subcutaneous tissue was noticed (Barendsen, 1966). Findings of higher RBE values of fast neutrons for these late effects in normal tissue than for early effects on skin could be one of the reasons why such treatments were stopped. In addition, fast neutrons had some other drawbacks, such as very low tissue penetration, significant scattering properties, and showed variation in dose per fraction, total dose and overall treatment time (Barendsen, 1966).

An initiative was taken by Fowler and his colleague to re-evaluate neutrons generated by the MRC cyclotrons at Hammersmith Hospital in London, with the intention of fast neutrons could be used in clinical radiotherapy (Fowler *et al.*, 1963). On measuring the RBE of fast neutrons relative to photons (X-rays) given as a single and split-dose

it was noticed that the RBE in the split-dose treatment was higher compared to the single fraction (Bewley 1966; Fowler & Morgan, 1963). Such findings were adequately interpreted on the basis of the radiobiological factors; such as the shape of survival curves, repair of sub-lethal damage and the oxygen effect, from experiments using dose-effect relationship comparisons between photons and fast neutrons (Barendsen, 1962; Barendsen *et al.*, 1963; Barendsen & Walter, 1964). Therefore, based on such interpretations suggestions were made about the possible advantage of fast neutrons in the clinical practice of radiotherapy for tumours responding poorly to photon treatments (Barendsen, 1966). Moreover, it was suggested that the possible explanation for the adverse effect noticed by Stone was partly from an over exposure of irradiation (Barendsen, 1966).

2.6.2   Factors affecting the RBE of fast neutrons

In general, the RBE for fast neutrons depends on the radiation energy spectrum, dose, dose per fraction for the specific treatment protocol, and the type of end-point used and tissue involved (Broerse & Barendsen 1973; Bewley, 1989).

2.6.2.1   Energy spectrum

The RBE of neutron beams varies considerably with their energy spectrum, and depends on the energy of the event particles and their nuclear interaction to generate the neutron beam (Hall *et al.*, 1979; Beauduin *et al.*, 1988; Gueulette *et al.*, 1996). Experiments performed for different rapidly proliferating tissues such as the bone-marrow and small

intestine also confirmed that the RBE values generally decrease with the increase in

neutron energy (Hornsey *et al.*, 1965; Davids, 1970; Broerse, 1974; Gueulette, *et al.*,

1996). The variation for neutron energy spectra is dependent on the internal design of the

local therapy centres, on the facilities' target construction, collimation, and beam

filtration systems, which have a large influence on the physical characteristics of the

generated beam (Gueulette *et al.*, 1996). **Table 2.1** reviews the study by Gueulette *et al.*,

(1996) to investigate the characteristics of the neutron beam generated at the different

therapy centres and the RBE values measured relative to the ^{60}Co-gamma radiation.

Table 2.1. Summary of the RBE values measured at different neutron therapy centres. Intestinal crypt survival was used as an end-point and values obtained after single fractions (*Gueulette, et al.*, 1996).

Therapy centre and nuclear reaction	Beam orientation and collimination system	Target, Backing and additional filtration	SSD	RBE relative to^{60} Co-γ
Orléns p(34)+Be (France)	Vertical beam Removable inserts	5 mm Be 2.5 mm C+2 mm Cu 36-mm polyethylene	169	1.79 ± 0.10^2 (depth= 5 cm)
Riyadh p(26)+ Be (Saudi Arabia)	Isocentric Removable inserts	Beryllium target 40-mm polyethylene	125	1 84 ± 0.07 (depth= 5 cm)
Ghent d(14)+ Be (Belgium)	Isocentric Removable inserts	Thin beryllium target No additional filtration	135	2.24 ± 0.11 (depth= 5 cm)
Faure p(66)+ Be (South Africa)	Isocentric Removable inserts	19 6 mm Be, 1 mm Cu 25-mm polyethylene	150	1.55 ± 0 04 (depth= 5 cm) 1.50 ± 0 04 (depth= 13 cm)
Detroit d(48)+ Be (USA)	Isocentric Multirod coll	15-mm beryllium glancing target, no additional filtration	183	1.50 ± 0.03 (depth= 2 cm) 1.51 ± 0 03 (depth= 10 cm)
Nice p(65)+ Be (France)	Vertical beam Multileaf coll	18.4 mm Be, 7.5-mm graphite 20-mm polyethylene	190	1.49 ± 0.05 (depth= 2 cm) 1.50 ± 0 04 (depth= 7 cm)
Louvain-la-Neuve p(65)+Be (Belgium)	Vertical beam Multileaf coll	17 mm Be, 8 5 mm Cu 20-mm polyethylene	162.5	1.52± 0.04 (depth= 5 cm)

2.6.2.1 Dose and dose per fraction

The summary of experimental data on RBE values of fast neutrons and the effects on

various normal tissues by Broerse (1974) showed that there is a general tendency of

increasing the RBE value with a decrease in dose or dose per fraction. In order to

evaluate the potential therapeutic gain of fast neutrons, comparing the RBE for tumour cell killing and normal tissue sparing is very important. Therefore, it was noticed that the most significant RBE values suitable for clinical neutron therapy fall between the dose range of 0.5Gy and 2.5Gy (Broerse, 1974; Broerse & Barendsen, 1973).

2.6.2.3 Tissue sensitivity

The RBE values obtained from photons and fast neutrons (8 MeV and 15 MeV) for the damage of different types of normal tissue show differences that can be attributed to the intrinsic differences in radiosensitivity between the normal tissues (Broerse & Barendsen, 1973). In addition the experimental data obtained for certain tumours using both 8 MeV and 15 MeV fast neutrons indicated that the RBE values for normal tissue tolerance are smaller than tumour cell killing. Hence, therapeutic gain from fast neutrons is evident if the RBE values for tumour killing are larger than for the damage to normal tissue.

Single dose high energy p(66)/Be neutron experiments in 15 human tumour cell lines with differing radiosensitivities showed an overlap of tumour sensitivity between ^{60}Co-gammas and p(66)/Be neutrons (Britten _et al._, 1992 and Slabbert _et al._, 1996). However, though weak, a significant relationship was established between p(66)/Be neutron RBE and the mean inactivation dose, suggesting a possible RBE advantage of p(66)/Be neutrons over certain photon-resistant tumours (Slabbert _et al._, 1996). In another similar experiment of 30 human cell lines, using 4 MeV photons and p(62)/Be neutrons, assessment of the neutron RBE also predicted a certain therapeutic potential gain for p(62)/Be neutrons over some photon resistant pathologies (Warenius _et al._, 1994).

2.6.2.4 Fractionation

In radiotherapy single high doses are divided into several treatment fractions as the amount of damage which normal tissue can sustain is a dose limiting factor. This allows normal tissue, which undergoes sub-lethal damage from the previous fraction, to actually repair and recover, while killing the tumour cells unable to sustain the first fraction. The majority of cells exposed to low-LET radiations experience a higher chance of sub-lethal (repairable) damage than those with high-LET radiations (Jones, 2001). When a single dose is divided into two fractions, an additional dose is required to compensate for repair. This additional dose is dependent on the size of the single dose and the relative size of the two smaller fractions and achieves a maximum effect when equal (Withers, 1970). Withers *et al* (1982) also emphasised that the relative effectiveness of fractionated radiotherapy is determined by the size of the dose-per-fraction not by the total number of fractions.

For doses less than 3Gy per fraction, the relationship between the increase in total dose and the number of fractions is very weak, as long as the overall treatment time is kept constant. When higher doses per fraction (>3Gy) with increased number of fractions are used, the increase in total dose depends on the size of the fraction (Wambersie *et al.*, 1974). The dependency on fraction size is somehow associated with the type of tissue involved; usually epithelial tumours and acute responding tissues are less influenced by the fraction size than the overall treatment time, whereas late responding tissues seem to be highly influenced by fraction size (Withers *et al.*, 1982). Moreover, when Withers *et*

al., (1982) plotted the increase of total iso-effective dose against decreasing dose-per-fraction, rather than the size of increasing fractions, he noticed that late-responding tissues showed a much steeper variation of total dose with a change in fraction size than early-responding tissues.

2.7 Neutron fractionation therapy at iThemba LABs

Current fractionation neutron therapy at iThemba LABS is given in a total dose of ≈ 20.4Gy, 3days per week, over 4 weeks at 1.7Gy per fraction. This is one third compared to the conventional, international standard use of radical fractionation schedules, which is given in a total dose of 60-70Gy, 5days per week, over 6-7 weeks delivered at 2Gy per day/ fraction (NCRI, 2003). High doses using small fraction numbers currently applied in p(66)/Be neutron therapy promotes late complications in irradiated tissues, and this can be attributed to the hindrance of the full potential therapeutic gain of the p(66)/Be neutrons over primary tumours (Slabbert *et al.,* 2000). But such potential therapeutic gain from fast neutrons is only certain if the depth-dose distribution can meet the level obtained with high energy X-rays (Broerse & Barendsen, 1973).

2.8 Aim of study

Changing the fractionation protocol of the radiation dose given influences the biological factor of the radiation in addition to the total dose and overall time increase (NCRI, 2003). The aim of increased number of fractions in p(66)/Be neutron therapy is to separate the early and late effects of radiation. While the overall treatment time stays the

same, the total dose may increase as the dose per fraction decreases. This results in increased early effects but reduced late effects. Manipulation of the trend of fractionation along with the increase of the total dose and its distribution should lead to a better neutron therapeutic gain.

The primary focus of this study was to increase the iso-effectiveness of fractionated p(66)/Be neutron radiations by increasing the number of fractions and lowering the dose-per-fraction, *i.e.* to attain the same biological effect when radiation is given as a single fraction. This may result in an increase of the total dose and it is assumed there would be sub-lethal damage repair, thus requiring an additional dose to compensate for the repair after irradiation. Regarding the repair of sub-lethal damage, an estimated alpha/beta ratio of 11.5Gy and 7Gy were chosen for ^{60}Co-gamma and p(66)/Be neutrons, respectively.

In this study, 16-week old Balb/C mice and Chinese hamster ovarian (CHO) cells were used in an *in vivo* and an *in vitro* experiment, respectively. For the *in vivo* experiment whole-body radiation was applied to two treatment modalities – either as single doses of 11, 12, 13 and 14Gy for ^{60}Co-gammas and 7, 8, 9 and 10Gy for p(66)/Be neutrons, or as split-doses of 7, 7.5, 8 and 8.5Gy for ^{60}Co-gammas and 4, 4.5, 5 and 5.5Gy for p(66)/Be neutrons. For the *in vitro* experiments CHO-K1 and – XRS1 cells cultivated in a Petri dish were exposed to radiation given as single doses of 3Gy and 1Gy in ^{60}Co-gammas and; 1.5Gy and 0.5Gy in p(66)/Be neutrons, respectively. Split-doses of 1.5Gy and 0.5Gy for ^{60}Co-gammas and; 0.75Gy and 0.25Gy for p(66)/Be neutrons were given to CHO-K1 and CHO-XRS1 cells, respectively. Time gaps between 1 to 3 hours were given for the

in vitro and 4 hours for the *in vivo* experiments. Samples were collected 24 hours after irradiation for the *in vitro* study and 3.5 days after irradiation for the *in vivo* study.

Intestinal crypt regeneration was used in the assessment of repairable damage as an early response of radiation damage after single and split-dose for both radiation exposures. This end-point was chosen as the tissue contains radiosensitive stem cells. A single stem cell is capable of regenerating into a crypt showing a high capacity to repair sub-lethal damage. A CD34 monoclonal antibody, commonly used to mark stem cells, was applied to mouse tissue in order to identify the position of the stem cells. Further assessments for other early effect indicators, such as accumulation of collagen fibrils, (collagen-I and collagen-IV) and apoptosis were assessed. The micronuclei formation, which is cell cycle dependent and a good indicator of DNA damage, was also assessed in cytokinase-blocked binucleated Chinese hamster ovarian (CHO) cells to determine the repair kinetics.

References:

Barendsen, G.W. & Walter, H.M.D. 1964. Effects of different ionising radiations on human tissue culture. IV. Modification of radiation damage, *Radiation Research*, 21: 314.

Barendsen, G.W. 1962. Dose-survival curves of human cells in tissue culture irradiated with alpha-, beta-, 20-kV X- and 200 kV X-radiation. *Nature*, 193: 1153.

Barendsen, G.W. 1966. Possibilities for the Application of Fast Neutrons in Radiotherapy: recovery and oxygen enhancement of radiation induced damage in relation to linear energy transfer. *European Journal of Cancer*, 2: 333-345.

Barendsen, G.W., Walter, H.M.D., Fowler, J.F. & Bewley, D.K. 1963. Effects of different ionising radiations on human cells on tissue culture. III. Experiments with cyclotron-accelerated alpha particles and deuterons, *Radiat. Res.* 18: 106.

Beauduin, M., Gueulette, J., Grégoire, V., De Coster, B.M., Vynckier, S., & Wambersie A.1988. Practical problems raised by the comparison of clinical results of neutron therapy, Clinical RBE and clinical neutron potency factor as a function of neutron energy. Survey of the literature, In: Chauvel P, Wembersie A, eds. Proc EULIMA workshop on Potential Value of Light Ion Beam Therapy. Publ no Eur 121165 EN, CEC, Sci Tech Commun Unit

Bewley, D.K. 1966. Radiobiological research with fast neutrons and the implications for radiotherapy. *Radiology* 86, 251

Bewley, D.K. 1989. The physics and radiobiology of fast neutron beams. Bristol: Adam Higler.

Bolus, N.E. 2001. Basic review of radiation biology and terminology. *Nuclear Medicine Technology*, 29(2):67-73.

Britten, R.A, Warenius, H.M, Parkins, C. et al., 1992. The inherent cellular sensitivity to p(62.5)/Be neutrons of human cells differing in photon sensitivity. *Int. J. Radiat. Oncol. Biol. Phys.*, 61: 805-812.

Broerse, J.J. & Barendsen, G.W. 1973. Relative biological effectiveness of fast neutrons for effects on normal tissues. *Current Topics in Radiation Research Quarterly*, 8: 305-350.

Broerse, J.J. 1974. Review of RBE values of 15 MeV Neutrons for the effects on normal tissues. *European Journal of Cancer*, 10: 225-230.

Casarett, G.W. 1980. *Radiation histopathology*. Florida: CRC Press: Vol 1.

Davids, J.A.G. 1970. Bone-marrow syndrome in CBA mice exposed to fast neutrons of 1.0 MeV mean energy: effect of syngeneic bone-marrow transplantation. *Int. J. Radiat. Biol.*, 17: 173.

Dewey, W.C., Furman, S.C. & Miller, H.H. 1970. Comparison of lethality and chromosomal damage induced by X-rays in synchronized Chinese hamster cells in vitro. *Radiation Research*, 43: 561-581.

Dowd, S.B. & Tilson, E.R. 1999. *Practical radiation protection and applied radiobiology*. 2nd ed. Philadelphia: Saunders.

Elkind, M.M. & Sutton, H. 1960. Radiation response of mammalian cells grown in culture: I. Repair of X-ray damage in surviving Chinese hamster cells. *Radiat Res* 13: 566-593.

Elkind, M.M., Sutton-Gilbert, H., Moses, W.B., Alescio, T. & Swain, R.B. 1965. Radiation response of mammalian cells in culture: temperature dependence of the repair of X-ray damage in surviving cells (aerobic and hypoxic). *Radiation Research*, 25 (5): 359-376.

Fowler, J.F. & Morgan, R.L. 1963. The long-term injury to normal tissues. *Brit. J. Radiol.*, 36: 115.

Fowler, J.F., Morgan, R.L., Wood, C.A.P., Bewley, D.K., Thomlinson, R.H., Hornsey, S., Silint, G., Alper, T., Silvester, J.A. & Turner, B.A. 1963. Papers presented at the symposium on Pretherapeutic experiments with fast neutron beam from the MRC cyclotron. Annual Congress of the British Institute of Radiology, 1962. *Brit. J. Radiol.*, 36: 77-121.

Gueulette, J., Beauduin, M., Grégoire, V., Vynckier, S., De Coster, B.M., Octave-Prignot, M., Wambersie, A., Strijkmans, K., De Schrijver, A., El-Akkad, S., Böhm, L., Slabbert, J.P., Jones, D.T.L., Maughan, R., Onoda, J., Yudelev, M., Porter, A.T., Powers, W.E., Sabbattier, R., Breteau, N., Courdi, A., Brassart, N. & Chauvel, P. 1996. RBE variation between fast neutron beams as a function of energy. Intercomparison involving 7 neutron therapy facilities. Bull Cancer/ Radiother., 83 (Suppl 1): 55s-63s.

Hall, E.J. 2000. Radiobiology for the Radiologist. 5th ed. Philadelphia, PA: Lippincott Williams & Wilkins. 67-87

Hall, E.J., Withers, H.R., Geraci, J.P., et al., 1979. Radiological intercomparison of fast neutron beams used for therapy in Japan and the United States, *Int. J. Radiat. Oncol. Biol. Phys.*, 5: 227-233.

Hendry, J.H. & West, C.M.L. 1997. Apoptotic and mitotic cell death: their relative contributions to normal-tissue and tumour radiation response. *Int. J. Radiat. Biol.*, 71: 709-719.

Hornsey, S., Vatistas, S., Bewley, D.K. & Parnell, C.J. 1965. The effect of fractionation on 4 – day of survival of mice after whole-body neutron irradiation. *Brit. J. Radiol.*, 38: 878.

ICRP PUBLICATION 92, 2003. Relative biological effectiveness (RBE), quality factor (*Q*), and radiation weighting factor (w_R). [Online], 33(4) December. Available: http://www.sciencedirect.com/science [28 April 2004].

IAEA, 2001. Cytogenetic Analysis for Radiation Dose Assessment, A manual, Technical Report Series No. 405, Vienna

Joiner, M.C. 2002. Particle beams in radiotherapy. In Basic Clinical Radiobiology, 3rd ed. Edited by G.G. Steel. London: Arnold. 205-216.

Jones, D.T.L. 2001. Fast neutron therapy: cures for the incurable. In Archive edition of IRPS bulletin. [Online], 15(2) July. Available: http://www.dmt.canberra.edu.au/irps/Archives/vol15no2/welcome.html [12 September 2005].

McMillan, T.J. & Begg, A.C. 2002. Genetic control of the cellular response to ionising radiation. In Basic Clinical Radiobiology, 3rd ed. Edited by G.G. Steel. London: Arnold. 84-93.

Meltz, M. 2001. Ionising Radiation and its Biological and Human Health Effects. Proceedings of the Symposium of the University of Texas Health Science Center, San Antonio, updated July 2001 [24 June 2004].

NCRI, Progress Review Group. 2003. Report of the Radiotherapy and Related Radiobiology. [Online], 27 August. Available: http://www.ncri.org.uk/publications/index.cfm?NavSub=20. [16 September 2005].

Nias, A.H.W. 1990. An Introduction to Radiobiology. London: Wiley

Potten, C.S. 2004. Radiation, the Ideal Cytotoxic Agent for studying the Cell biology of Tissues such as the Small Intestine. *Radiat. Res.*, 161(2): 123-136.

Slabbert, J.P., Theron, T., Serafin, A., Jones, D. T.L., Böhm, L., Schmitt, G. 1996. Variations in the radiosensitivity of different cell types exposed in vitro to p(66)/Be neutrons and ^{60}Co gamma rays. *Strahlenther. Onkol.*, 172:567-572.

Slabbert, J.P., Theron, T., Zölzer, F., Streffer, C., Böhm, L. 2000. A comparison of the potential therapeutic gain of p(66)/Be neutrons and d(14)/Be neutrons. International Journal of Radiation Oncology Biology Physics 47, 1059–1065.

Sorrentino V. 1996. The cell cycle, In Cell Proliferation in Cancer, Pustazi L; Lewis CE; Yap E, NewYork: Oxford. 27-41

Steel, G.G. 2003. The biological base of Radiotherapy. [Online], Available: http://www.oup.co.uk/pdf/0-19-262926-3_4-2.pdf. [24 November 2003].

Steel, G.G. 2002. Introduction: the significance of radiobiology for radiotherapy. In Basic Clinical Radiobiology. 3rd ed. Edited by G.G. Steel. London: Arnold.1-7

Stephens, L.C., Schultheiss, T.E., Price, R.E., et al., 1991, Radiation apoptosis of serous acinar cells of salivary and lacrimal glands. *Cancer*, 67: 1539-1543.

Stone, R.S. 1948. Neutron therapy and specific ionization. *Amer. J. Roentgenol*, 59: 771.

Thomson, L.H. & Suit, H.D. 1969. Proliferation kinetics of X-radiation mouse L cells studied with time-lapse photography. *Int. J. Radiat. Biol.*, 15: 347-362.

Travis, E.L. 2000. Primer of Medical Radiobiology. 2nd ed. St. Louis: Mosby

Van De Graaff, K.M. 2000. Human Anatomy. 5th ed. USA: McGraw-Hill.

Wambersie, A., Dutreix, J., Gueulette, J. & Lellouch, J. 1974. Early recovery for intestinal stem cells, as a function of dose per fraction, evaluated by survival rate after fractionated irradiation of the abdomen of mice. *Radiat Res.*, 58: 498-515.

Warenius, H.M., Britten, R.A., Browning, P.G., Morton, I.E. & Peacock, J.H. 1994. Identification of human in vitro cell lines with greater intrinsic cellular radiosensitivity to 62.5 MeV (p + Be+) neutrons than 4 MeV photons. *Int. J. Radiat. On-col. Biol. Phys.*, 28: 913-920.

Withers, H.R. & Elkind, M.M. 1970. Microcolony survival assay for cells of mouse intestinal mucosa exposed to radiation. *Int. J. Radiat. Biol.*, 17(3): 261-267.

Withers, H.R., Thames, H.D. & Peters, L.J. 1982. Differences in the fractionation response of acute and late-responding tissues. In *Progress in Radio-Oncology, Vol II*, K.H. Karcher, H.D. Kogelnik and G. Reinartz Eds. Raven Press, New York, pp. 287-296.

Withers, H.R. 1970. Recovery in normal and malignant tissue. In Proc. of IVth International Congress of Radiat. Res. (Evian, June 29-July 4, 1970). Gordon and Breach, NY, in press.

Chapter 3
CRYPT STEM CELL SURVIVAL ASSAY

3.1   Introduction and literature review

Sparing normal surrounding cells or tissue, while inducing maximum damage to cancer cells remains the key issue regarding the biological effect of clinically used radiations (NCRI, 2003). Radiation is one of the most cytotoxic agents (Potten, 2004) and when used in clinical practice safety measures should always be taken. Preclinical experiments are always required to establish the dose, dose per fraction and total dose applied, in order to observe the damage to cells and tissues in animals and provide a basis before extrapolation to man.

As differences in physical, chemical and biological factors among radiations were evident, new approaches to radiotherapy treatment were required. Between 1920 and 1930, Regaud and his colleagues discovered fractionation therapy while attempting to sterilise ram testes without necrosing scrotal skin (Regaud & Ferroux, 1927). This work showed tissue sparing was possible by splitting high-dose radiation into two or more smaller fractions resulting in a more desirable biological effect.

The introduction of fractionation therapy lead to the elucidation of Elkind repair or sub-lethal damage repair of radiation-induced injury in cells. Fractionation allows cells to repair their sub-lethal injury with a time gap given between fractions (Elkind & Sutton,

1959). Cellular repair begins immediately after injury and is assumed to be completed after some hours, depending on the type of tissue and type of radiation involved (Withers & Elkind, 1969). Late responding tissues, such as spinal cord and kidney, have a large capacity to repair sub-lethal damage and this is reflected by the low (1-5Gy) α/β ratio, in contrast to early responding tissues, such as skin that has a large (6-13Gy) α/β ratio (Hall, 2000). Considerable repair is evident after X-rays but is relatively ineffectual after neutron exposure (Broerse & Barendsen, 1973).

The second generation of high energy clinical neutron beams, such as p(66)/Be, came into practice in the 1980's with a better depth dose distribution that could meet the requirements of modern linear accelerators (Hussey *et al.*, 1983). High energy p(66)/Be neutrons, in addition to their better depth dose distribution, also resulted in better skin sparing but with lower radiobiological effectiveness (RBEs) (Böhm *et al.*, 1990, and Böhm *et al.*, 1992). Furthermore, the therapeutic gain indications for fast neutrons are evident in certain tumours and are reviewed by Griffin *et al.*, (1984) and Wambersie *et al.*, (1994). Although the therapeutic gain from neutrons has always been a divisive issue, in principle it appears better with lower neutron energies (Slabbert *et al.*, 2000).

In order to evaluate the possible potential therapeutic gain of fast neutrons, comparing the RBE for tumour cell killing and normal tissue sparing is essential as it is a dose-limiting factor. The RBE values for fast neutrons for damage to normal tissue, in general, are dependent on the radiation energy spectrum, the dose, the dose per fraction for the

specific treatment protocol and the type of normal tissue involved (Broerse & Barendsen, 1973).

Comparisons of RBE values of fast neutrons using both 8 MeV and 15 MeV for damage to normal tissue and tumour cell killing, showed that the RBE values of the tumours examined were larger than the RBE's for a number of normal tissues (Broerse & Barendsen, 1973). Therefore, it is obvious that there is a therapeutic gain from fast neutrons if the RBE values for tumour killing are larger than for the damage to normal tissue. Investigation for better RBE values by manipulation of fractionation along with the increase of the total dose and its distribution should therefore lead to a better neutron therapeutic gain.

Experience with p(66)/Be neutron therapy at iThemba LABS has shown that treatment with more fractions and lower doses per fraction may be beneficial for some patients. Therefore, in this study the repair of sub-lethal damage in crypts of Leiberkhün of mouse jejunum was observed following single- and split-dose irradiation in order to calculate the extra treatment dose need to be applied. Although intestinal crypts are considered an early responding tissue, survival is highly quantitative. Furthermore, crypt survival is also characterised by a large repair capacity, hence the end-point is suitable to determine the additional dose required to compensate the repair when treatment is delivered in a fractionated manner. For this reason, crypt stem cell survival was used as an end-point to study the repair characteristics of single and fractionated ^{60}Co-gamma and p(66)/Be neutron irradiation.

3.2   MATERIALS AND METHODS

3.2.1   Experimental animals

Adult 16-week-old male Balb/C mice, weighing approximately 40g and 6-8 cm long were purchased from the Animal Unit of the University of Cape Town (UCT), South Africa, breeding facility. Prior to and after exposure to radiation the animals were maintained in plastic cages and housed at the animal house of the Cape Peninsula University of Technology. Mice were given standard clean water and food.

Both the experimental and control groups were randomized as a function of the type of radiation and/or the dose. Both control and experimental animals were maintained under identical conditions as regards room temperature ($20 \pm 2°C$), air ventilation, and 12-hrs illumination.

3.2.2   Irradiation procedure

Two sources of radiation were used in this study. The gamma irradiations were performed at the Department of Radiation Oncology at Tygerberg Hospital using a ^{60}Co-gamma unit (Theratron 780C, Theratronix International). The dose-rate was 2Gy per minute at a source to surface distance (SSD) of 100 cm, a field size of 20 cm x 20 cm and a gantry angle of 0°. To ensure full charged particle equilibrium, mice were positioned behind 5 mm Perspex. Backscatter was achieved by placing the mouse jig on a 5 cm sheet of polyethylene. A similar set-up was used for neutron irradiations. Neutron

irradiation was carried out at iThemba LABS, Faure, delivering at a dose-rate of 0.4Gy

per minute generated by 66 MeV protons bombarding a 19.6 mm thick beryllium target.

p(66)/Be neutron radiation was applied at a field size of 29 cm x 29 cm, SSD of 150 cm

and a gantry angle of 0°. Mice were placed at the centre of the beam source on a 9 cm

thick Perspex, which served as a backscatter material and a 2 cm thick polyethylene

block placed on spacers which served as build up material. ^{60}Co-gamma rays were used

as a reference beam and p(66)/Be neutron beam as a clinical test beam.

Whole-body radiation exposures were applied with both radiation treatment modalities.

During exposures the mice were stabilised in a specially designed 10 cm by 10 cm by 4

cm Perspex jig (**Figure 3.1**A) providing enough ventilation during exposure. Three mice

per dose point were positioned at the centre of the radiation field as shown in **Figure**

3.1B.
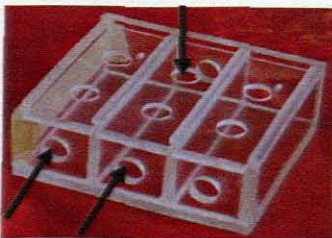
(A)   (B)

Figure 3.1. (A) Photograph showing a specially designed Perspex jig. Arrows
show the ventilation holes on the top and front side of the jig, and (B) showing
three mice stabilised prior to irradiation.

3.2.3   Dose estimation

Notwithstanding the fact that crypt cell survival is characterised by a large shoulder, the dose response curve is very steep once sufficient radiation energy has been delivered. For this reason the success of an experiment starts with an accurate estimation of the doses needed to be applied. Ideally, data should be generated where the mean number of crypts that survived the radiation treatment is between about 100 and 5 crypts per circumference. Furthermore, as this is a repair experiment, the samples for fractionated treatments need to be exposed to higher radiation dose levels to compensate for repair between fractions, thus allowing the dose response curve to remain between 100 and 5 crypts per circumference. To estimate the doses that should be administered the sensitivity of the crypt cells to the treatment modalities should be known, as well as the repair capabilities of jejunum to ^{60}Co-gamma rays and high energy p(66)/Be neutrons.

Based on a study by Böhm *et al.*, (1988) to determine the relative biological effectiveness (RBE) of a single fraction exposure of ^{60}Co-gamma and for an unfiltered p(66)/Be neutron beam, we calculated an RBE value of 1.64 at a survival level of 20 crypts per circumference as shown in **Figure 3.2**. This is in close agreement with the RBE value of 1.65 determined by Cohen and Awschalom (1976). Using this RBE value of 1.64, the α/β ratio for p(66)/Be neutrons was estimated as follows. The α/β ratio of 7Gy for ^{60}Co-gamma rays noted by Gueulette *et al.*, (2001) was multiplied by the RBE. The value of 11.5Gy obtained was then used to estimate how much additional dose should be added

for neutron treatments given in two fractions, separated by 4 hours, to be iso-effective

with the acute exposures. The biological effective doses (BED) for single fraction data

were thus calculated first using the appropriate α/β ratio and then the doses needed to be

given in each fraction estimated. The calculation method was first tested using data of

Gueulette *et al.*, (2001), where iso-effective doses for three fractions were estimated

(open circles) and compared to experimental values (inverted triangles) , as shown in

Figure 3.3. The two sets of data were in close agreement.
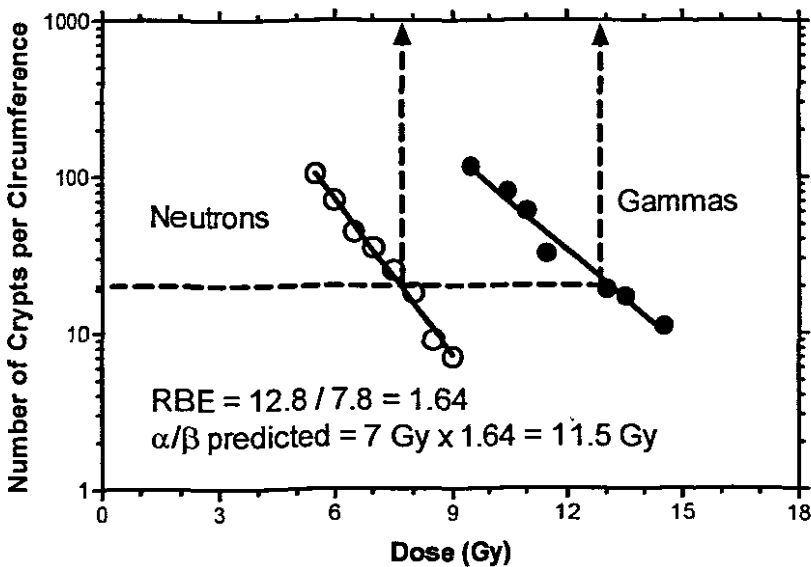
Figure 3.2. Shows the RBE measured at 20 crypts per circumference
from experimental data of Böhm *et al.*, (1988) to estimate the α/β ratio
for neutrons (11.5Gy). Open (O) and closed (●) circles represent data
for single fraction neutron and gamma exposures, respectively.
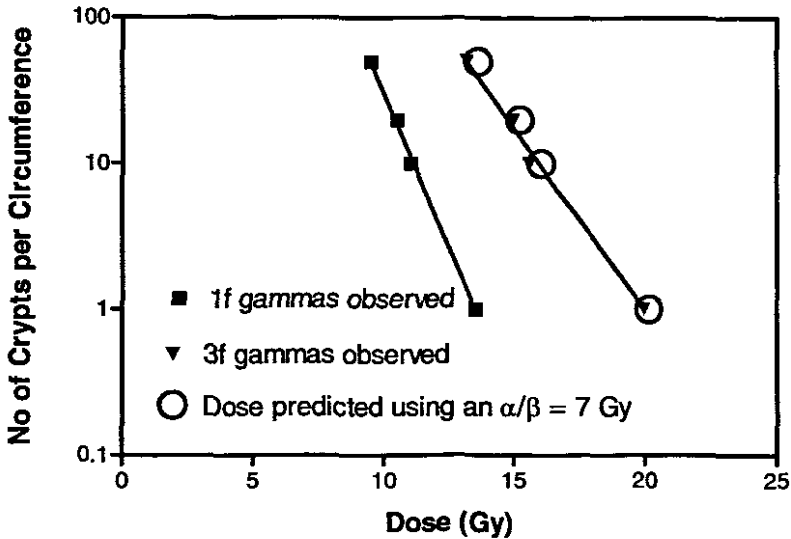
Figure 3.3. The total doses predicted that needs to be given in a 3 fraction treatment (O) and calculated data using acute exposures (■) are compared to that observed experimentally (▼).

The same procedure was applied using an α/β ratio of 7Gy for ^{60}Co-gamma rays and 11.5Gy for p(66)/Be neutrons to estimate the doses needed to be given in each of 2 fractions. The following values were obtained: for single (one-fraction) doses of 11, 12, 13 and 14Gy for ^{60}Co-gamma irradiations, and 7, 8, 9 and 10Gy for p(66)/Be neutron exposures; and as split-doses (two-fractions) of 7, 7.5, 8 and 8.5Gy per fraction for ^{60}Co-gamma and 4, 4.5, 5 and 5.5Gy per fraction for p(66)/Be neutrons. A gap of 4 hours inbetween split-doses was allowed for cells to repair their sub-lethal damage.

The above estimated doses were applied and the three mice irradiated for each dose point. After irradiation, mice were returned to their cages and observed regularly over the following 3.5 days. After 3.5 days post irradiation all mice were sacrificed using

chloroform inhalation in a drop jar. Mice were dissected along the length of the abdomen

under aseptic conditions and tissues were harvested.

3.2.4   Tissue preparation and staining

A 5 cm section of jejunum was removed 2 cm away from the pylorus from each mouse

and immediately fixed in a solution of 10% buffered formalin, pH 7.4 overnight. Tissue

samples were then cut into 3 mm pieces and placed into labelled cassettes and processed

in an automated tissue processor overnight. Six small (3 mm each) segments of intestine,

from the entire length of the jejunum were bundled together and embedded in wax

blocks. Two blocks were made for each mouse.

Transverse sections of 3μm, each having six jejunal sections, were cut for Haematoxylin

and Eosin staining. Sections were collected on clean glass slides from the water bath,

mounted on albumin-coated slides and incubated at 60°C to ensure proper adhesion.

Sections of jejunum from both control and irradiated mice were de-waxed in xylene,

hydrated in graded alcohol to water and stained with Haematoxylin and Eosin. Sections

were then de-hydrated through graded alcohol, cleared in xylene, mounted in Entellen,

and coverslipped. Sections were examined under a light microscope at x400

magnification for the assessment of crypts of Leiberkhün at the base of the villi as shown

in **Figure 3.4**.

(A)   (B)
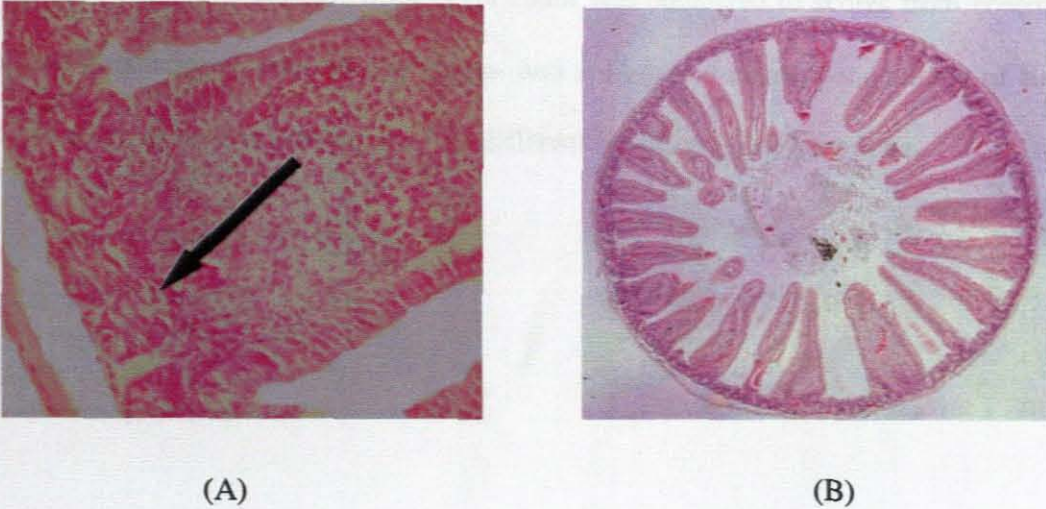
Figure 3.4. Haematoxylin and Eosin (H & E) stained sections of mouse jejunum showing crypts of Leiberkhün at the base of the villus. (A) arrow indicates a single crypt and five crypts are seen under the villus at x400 magnification and (B) a cross-sectional view of control mouse jejunum with its villi (finger-like projections) and many crypts adjacent to one another at the base of the villi (x100).

3.2.5   Scoring

Crypts of Leiberkhün were counted based on the Withers and Elkind (1970) technique that involved the objective overall look of a regenerated crypt at the base of the villi. This was supported with a live screen picture captured from a Zeiss AuxioHOME computer driven microscope. To be considered a surviving crypt, certain objective criteria were met. As shown in **Figure 3.4A** (arrow) a crypt should have a flask shape, contain ten or more cells, each with a prominent nucleus and scant cytoplasm. Cells take up basophilic stain on an eosinophilic background and appear packed together forming a lumen at the centre (Martin *et al.*, 1998). Crypts of Leiberkhün were visible at the base of the villi of mouse gut sections and enumerated. Counts recorded represented the number of crypts

per circumference. The exposed mice crypt count was compared to scores from control

mice, and comparisons between the single- and split-dose treatment modalities of the

same radiation, as well as between the two different radiation types were done.

Figure 3.5. Haematoxylin and Eosin (H & E) stained cross sections of mouse jejunum exposed to ^{60}Co-gamma; x50 magnification. (a) shows unirradiated (0Gy) control mouse tissue; (b), (c), (d) and (e) are single fraction doses given as 11, 12, 13 and 14Gy, respectively. Likewise, slides (f), (g), (h) and (i) show the split-dose fraction given as 7+7, 7.5+7.5, 8+8 and 8.5+8.5Gy from the same radiation.

Figure 3.6. Haematoxylin and Eosin (H & E) stained cross sections of mouse jejunum exposed to p(66)/Be neutrons; x50 magnification. (a) shows unirradiated (0Gy) control mouse tissue; (b), (c), (d) and (e) are single fraction doses given as 7, 8, 9 and 10Gy, respectively. Likewise, slides (f), (g), (h) and (i) show the split-dose fraction given as 4+4, 4.5+4.5, 5+5 and 5.5+5.5Gy. Villi denudation is seen in the higher dose of single fraction (slides d and e).

3.3   RESULTS

Surviving crypts were counted per circumference of mouse jejunum in Haematoxylin and Eosin stained sections per dose point as shown in **Figure 3.5**, **Figure 3.6** and the data in **Table 3.1**. Three sections per mouse from both control and irradiated mice were enumerated to estimate the average value, and from this the mean of three mice was calculated.

For the unirradiated (0Gy) mice, the number of surviving crypts was found to have a mean value of 120 crypts per circumference, compared with 90 crypts in CBA/Rij x C57BL/Rij F1 hybrid mice (Broerse & Barendsen, 1973) and 160 crypts in CDF_1 hybrid mice (Withers & Elkind 1970). **Figure 3.5(a)** and **Figure 3.6(a)** show normal crypts in unirradiated, control mouse jejunal section (x50). The crypts can be seen at the base of the villi adjacent to one another.

For the ^{60}Co-gamma single dose irradiation the mean score for the surviving crypts per circumference decreased from 49 at 11Gy to 5 at 14Gy and for the split-doses the mean value of surviving crypts decreased from 34 per circumference at a total dose of 14Gy to 7 at 17Gy. **Figure 3.7(A)** shows the histogram data plot for both single- and split-dose ^{60}Co-gamma irradiations. Similarly, the mean score of surviving crypts per circumference for the single dose p(66)/Be neutron irradiations reduced from 3 at 7Gy to 0.22 at 10Gy and for the split-dose p(66)/Be neutron irradiations the mean value of surviving crypts reduced from 14 at a total dose of 8Gy to 0.2 at 11Gy. Both single- and split-dose data are shown in histogram plot in **Figure 3.7(B)**.

Table 3.1. The mean number of crypts of Leiberkhün counted per circumference in Haematoxylin and Eosin stained cross-sections (Mic-1, Mic-2 and Mic-3) from the two protocols using ^{60}Co-gamma rays and p(66)/Be neutron beam irradiations. Data for unirradiated mice are also shown (C-1, C-2, and ...C-6). Data for Mic-2 and Mic-3 respectively from 7Gy and 10Gy neutrons are not shown due to the death of both mice.

Control								
Dose	C-1	C-2	C-3	C-4	C-5	C-6	Total	Mean
0 Gy	117.75	123.5	124.3	120.5	117	120.75	723.8	120.63

[60]Co-gamma rays			
Single-dose	Mic-1 Mean	Mic-2 Mean	Mic-3 Mean	Total Mean
11 Gy	52.33	48.67	46.57	49.19
12 Gy	21.24	28.67	17.70	22.53
13 Gy	10.37	4.03	17.47	10.63
14 Gy	7.08	4.88	2.86	4.94
Split-dose			
7+7 Gy	27.62	31.54	42.57	33.91
7.5+7.5 Gy	25.36	42.88	23.13	30.46
8+8 Gy	5.79	10.31	7.95	8.02
8.5+8.5 Gy	11.75	5.35	5.59	7.57

p(66)/Be neutron			
Single-dose			
7 Gy	4.25	-	2.5	3.38
8 Gy	1.7	0.75	0.9	1.12
9 Gy	0.91	0.27	0	0.39
10 Gy	0.26	0.17	-	0.22
Split-dose			
4+4 Gy	29.36	8.33	7	14.90
4.5+4.5 Gy	2.82	1.48	2.58	2.29
5+5 Gy	1.71	1.13	1.88	1.57
5.5+5.5 Gy	0.55	0	0.05	0.30
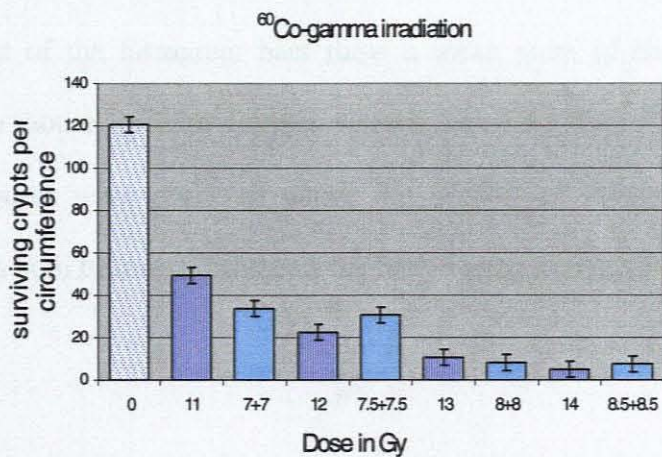
(A)
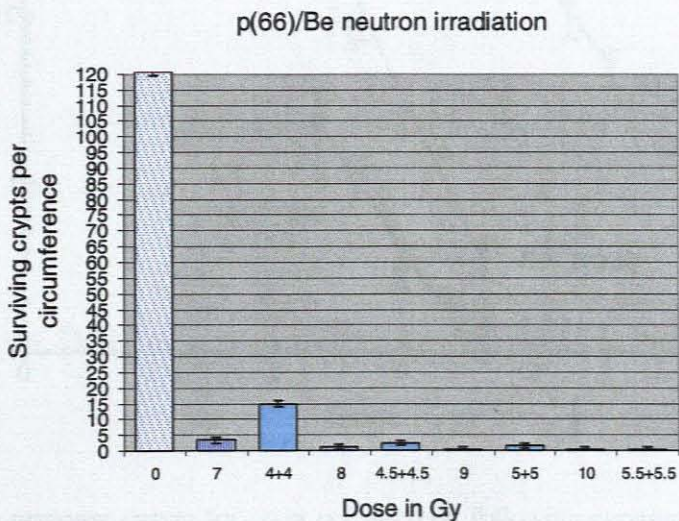
(B)

Figure 3.7. Dose dependent response of surviving crypts of Leiberkhün in mice exposed to single (heavy dark vertical lined bars) and split-dose fraction (light horizontal lined bars) using ^{60}Co-gamma irradiations (A) and p(66)/Be neutrons (B). Histogram bars show mean values of surviving crypts of three mice.

The dose-effect response data are represented graphically in **Figure 3.7** (A) and (B) where the height of the histogram bars show a mean score of the crypt survival per circumference in mouse jejunum sections when assayed 3.5 days after irradiation. Dose dependent responses were observed where the number of crypts decreased with an increased dose in both treatment protocols for both treatment modalities and are shown in **Figure 3.8**.
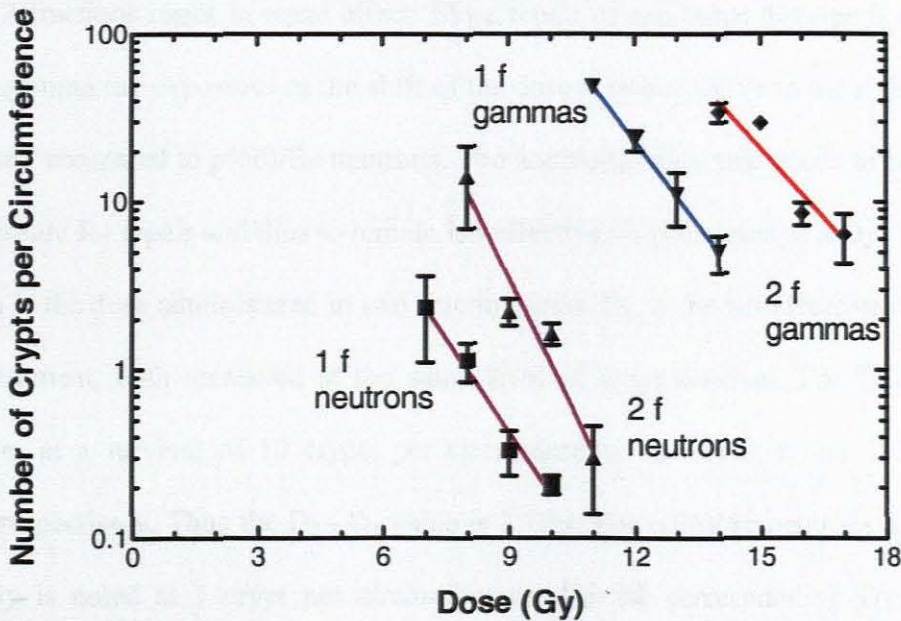
Figure 3.8. Dose response curves for crypt cell survival following exposure to single (▼, ■) or split-doses (◆, ▲) of both ^{60}Co-gamma rays and p(66)/Be neutron beam. A clear increase in the total dose needed to remain iso-effective is evident and this is a measure of the repairable damage induced by each treatment modality. Each dose-point is the mean number of surviving crypt cells counted in tissue from three mice.

For ^{60}Co-gamma irradiation, the doses applied – both single and fractionated – appear to be suitable as crypts between 120 and 5 were obtained. For neutrons, clear dose response curves are noted but at much lower levels of crypt cell survival. For both treatment modalities considerable repair of sub-lethal damage that occurred during the 4 hours between the fractionated exposures are clearly observed in **Figure 3.8**.

The repair is indicated by the shift of the graphs to the right. That is, the higher doses given in 2 fractions result in equal effect. More repair of sub-lethal damage is noted for the ^{60}Co-gamma ray exposures as the shift of the dose response curve to the right is more pronounced compared to p(66)/Be neutrons. The additional dose that needs to be applied to compensate for repair and thus to remain iso-effective, is calculated as a $D_2 - D_1$ value, where D_2 is the dose administered in two fractions and D_1 is the iso-effective dose for a single treatment, both measured at the same level of crypt survival. For ^{60}Co-gamma irradiation, at a survival of 10 crypts per circumference these values are 16.2Gy and 13.1Gy, respectively. Thus the $D_2 - D_1$ value is 3.1Gy. For p(66)/Be neutrons a D_1 value of 8.0 Gy is noted at 1 crypt per circumference and the corresponding D_2 value of 10.1Gy. The $D_2 - D_1$ value for neutrons is thus 2.1Gy. This is considerably less than that seen with ^{60}Co-gamma rays.

3.3   DISCUSSION

The dose response curves show an exponential decrease in the number of crypt survival as the dose increases. This forms a straight line when plotted on a semi-logarithmic graph, as shown in **Figure 3.8**. This shape of dose-response curves is noted for both single and split-dose treatment protocols as well as for both radiation modalities. A marked shoulder that reflects the accumulation of sub-lethal damage is noted for both neutrons and gamma rays. This large shoulder is needed in a study that follows repair of radiation damage as it reflects a large amount of repairable damage induced by the different radiation treatments. By comparison, cells treated *in vitro* have much smaller shoulders (Nias, 1990). For crypt cells in the jejunum a good measure of repairable damage is seen and this is likely the result of cells being in physical contact with one another.

The large shoulder of some 10Gy seen for single dose gamma radiations is reduced to as little as about 3Gy for neutrons. This is consistent with the increase in ionization density of the different treatment modalities. The ionization density of gamma rays is typically around 1 keV / μm and this increases to about 20 keV/ μm for the p(66)/Be neutron beam. For neutrons more lethal and less sub-lethal damage is induced compared to ^{60}Co-gamma rays.

The relative biological effectiveness (RBE) for the p(66)/Be neutrons applied in a single fraction is calculated to be 2.6 at 10 crypts per circumference. For the split-dose exposures the RBE decreases to 2. This reduction is not expected as it indicates that the

neutrons repair relatively more than the gamma rays. This is not so. The repairable damage

was indeed much more manifest after ^{60}Co-gamma irradiations than after p(66)/Be neutron

treatments.

An inter-comparison of single and split-dose fractions between ^{60}Co-gamma and

p(66)/Be neutron irradiations show the relevance of crypt survival in response to sub-

lethal damage from both irradiations. Both data set curves in **Figure 3.8** showed a shift to

the right, reflecting the relative importance of repairable damage in each instance. The

shift of the graph for gamma ray treatments is in fact more than for neutrons. This is seen

when comparing the difference between D_2 and D_1 values. A D_1 value is the dose needed

to induce a level of biological damage when the dose is administered in a single fraction

and the D_2 value is that for split exposures. The difference is a direct measure of how

much extra radiation energy needs to be given to compensate for repair. For gamma rays

this was calculated to be 3.1Gy. By contrast the D_2 - D_1 value for neutrons is only 2.1Gy.

As such, less repair of sub-lethal damage is measured from the current data for gut

exposed to neutrons.

The lower RBE seen for split-dose irradiations and the smaller D_2 - D_1 value seen for

neutrons is thus at variance with one another. This can be explained in part as the D_2 - D_1

values for neutrons and gamma rays were not calculated at the same level of biological

damage. Due to the nature of the data the D_2 - D_1 value for neutrons had to be calculated

at 1 crypt per circumference and that for gamma rays was estimated at 10 crypts per

circumference. Ideally the dose response curves for neutrons and gamma rays should

have been parallel to one another and data should have reflected the same levels of crypt cell survival.

In analysing this data it is of major importance to establish if the α/β ratio estimated for neutrons was indeed correct. The latter was obtained as the product of the RBE and the known α/β for gamma rays. A value of 11.5Gy was estimated – see **Figure 3.2**. Using the actual neutron data observed in this experiment, a dose of 8.01Gy is needed to reduce the number of crypts per circumference to a value of 1. Using the α/β value 11.5 estimated, the iso-effetive dose for a split dose exposure is calculated to be 9.6Gy. This compares to a value of 10.1Gy observed from the actual split- dose data for neutrons. As such, a reasonable agreement between the α/β estimated using neutron RBE and that calculated from the neutron experiment is obtained.

From the above discussion it is clear that considerable repair from neutron radiation damage can be expected when cells are treated *in vivo*. This is important as the protocol for neutron patient treatments is at present under discussion. Up to now a total of 18Gy has been given to target tissue over 12 fractions i.e. 1.5Gy per fraction. However, there are clinical indications suggesting that a lower dose per fraction should be given, thus more treatments will be needed to complete the course of neutron therapy. In lowering the dose per fraction the, α/β ratio for neutron patient treatment protocol may change and needs to be estimated correctly as early effects of the therapy varies with protocol. Therefore, in this current research it was observed that a reasonably accurate α/β ratio for

early neutron therapy effects can be estimated using values previously determined for

photons.

References:

Böhm, L., De Roubaix, S., Jones, D.T.L. & Yudelev, M. 1988. Determination of the relative biological effectiveness (RBE) of the unfiltered p(66)/Be neutron beam in relation to ^{60}Co irradiation. *NAC Annual Report*, 1: 126-128.

Böhm, L., Blekkenhorst, G., Slabbert, J.P., Verheye, F., Jones, D.T.L. & Yudelev, M. 1992. RBE and OER measurements on the p(66)/Be neutron beam at Faure, South Africa. *Strahlenther Onkol.*, 168 (1): 42-47.

Böhm, L., Gueulette, J., Jones, D.T.L., et al., 1990. Radiobiological intercomparison of fast neutron beams using the regeneration of mouse jejunal intestinal crypts. *Strahlenther Onkol*, 166: 242-245.

Broerse, J.J. & Barendsen, G.W. 1973. Current Topics in Radiation. *Research Quarterly*, 8: 305-350.

Cohen, L. & Awschalom, M. 1976. Fermi National Accelerator Laboratory, Batavia - Preliminary Report, 51-60.

Elkind, M.M. & Sutton, H. 1959. X-Ray damage and recovery in mammalian cells in culture. *Nature*, 184: 1293-1295.

Griffin, T.W., Davis, R., Hendrickson, F.R., Maor, M.H., Laramore, G.E. & Davis, L.W. 1984. Fast neutron radiation therapy for irresectable squamous carcinomas of the head and neck: The results of a randomised RTOG study. *Int. J. Radiat. On-col. Biol. Phys.*, 0:2217-2223.

Gueulette, J., Slabbert, J.P., Böhm, L., De Coster, B.M., Rosier, J., Octave-Prignot, M., Ruifrok, A., Schreuder, A.N., Wambersie, A., Scalliet, P. & Jones D.T.L. 2001. Proton RBE for early intestinal tolerance in mice after fractionated irradiation. *Radiotherapy and Oncology*, 61: 177-184.

Hall, E.J. 2000. Radiobiology for the Radiologist. 5th ed. Philadelphia, PA: Lippincott Williams & Wilkins. 67-87

Hussey, D.H., Meyn, R. & Smathers, J.B. 1983. Neutron therapy, In: N. M. Bleehen, E. Galstein & J.L. Haybittle, eds., Radiation therapy planning. New York, Marcel Dekker. 393-437.

Martin, K., Potten, C.S., Roberts, S.A. & Kirkwood, T.B.L. 1998. Altered stem cell regeneration in irradiated intestinal crypts of senescent mice. *Journal of Cell science,* 111: 2297-2303.

NCRI Progress Review Group. 2003. Report of the Radiotherapy and Related Radiobiology. [Online], 27 August. Available: http://www.ncri.org.uk/publications/index.cfm?NavSub=20 [16 September 2005].

Nias, A.H.W. 1990. An Introduction to Radiobiology. London: Wiley.

Potten, C.S. 2004. Radiation, the Ideal Cytotoxic Agent for studying the Cell biology of Tissues such as the Small Intestine. *Radiat. Res.,* 161(2): 123-136.

Regaud, C. & Ferroux, R. 1927. Discordance des effects de rayons X, d'une part dans le testicile, par le peau, d'autre parts dans le fractionment de la dose. *Compt. Rend. Soc. Biol.,* 97: 431-434.

Slabbert, J.P., Theron, T., Zölzer, F., Streffer, C. & Böhm, L. 2000. A comparison of the potential therapeutic gain of p(66)/Be neutrons and d(14)/Be neutrons. *Int. J. Radiat. Oncol. Biol. Phys.* 47, 1059-1065.

Wambersie, A., Richard, F. & Breteau, N. 1994. Development of fast neutron therapy worldwide. *Acta Oncol.,* 34: 261-274.

Withers, H.R. & Elkind, M. M. 1969. Radiosensitivity and fractionation response of crypt cells of mouse jejunum. *Radiat. Res.,* 38: 598-613.

Withers, H.R. & Elkind, M.M. 1970. Microcolony survival assay for cells of mouse intestinal mucosa exposed to radiation. Int. J. Radiat. Biol., 17(3): 261- 267.

Chapter 4

IMMUNOHISTOCHEMISTRY

4.1 Introduction and literature review

After the discovery of X-radiation by Röntgen in 1895, acute irradiation changes of the

small intestine from experimental animals were reported by Krause and Ziegler (1906-

1907). Not long after, Regaud and co-workers also reported late irradiation changes of

the small intestine in dogs (Regaud *et al.*, 1912). Both acute and late radiation-induced

morphological changes of the small intestine were also evident in clinical patients treated

for abdominal cancer with X-rays (Walsh, 1897; Füth & Ebeler, 1915). Studies by Krause

and Ziegler (1906-1907) showed that X-irradiation-induced anomalies of the small

intestine in domestic animals were dose dependent. However, the authors concluded that

these anomalies and consequent mortality were the result of proliferating bacteria in the

small intestine. Quástler (1956) stated that acute radiation death is as a result of the

gastrointestinal syndrome (GI-syndrome).

GI-syndrome can be defined as signs and symptoms resulting from loss of intestinal

integrity, and represents the early response of the intestine to radiation followed by a

more complicated and irreversible insult to the haematopoietic and immune process.

Characteristic features of GI-syndrome include severe intestinal bleeding, fluid and

electrolyte imbalance, bacteraemia and endotoxaemia, anorexia, nausea and vomiting,

and diarrhoea after denudation of the intestinal villi of the irradiated individual causing acute lethality (Young, 1987; Buell & Harding, 1989; Busch, 1990).

GI-syndrome may be caused by therapeutic (intracavitary or external) radiation in the treatment of abdominal and pelvic tumours or non-therapeutic (accidental or atomic warfare) radiation (Liebow et al., 1949; Olasolo, 1989). According to Quástler (1956) there is a well-defined time course response of acute radiation death after whole body exposure of X-radiations in the doses ranging between 10-100 Gy. In the past few years researchers have also revealed that the GI-syndrome may occur following doses greater than 10 Gy (Somosy et al., 2002) and related death is accepted after sufficiently high doses of ionising radiations (Young, 1987; Hauer-Jensen, 1990; Potten et al., 1995; Langberg et al., 1996; Langberg & Hauer-Jensen, 1996). Therefore, the high sensitivity of the gastrointestinal tract to radiation damage makes it a dose limiting tissue in some radiotherapy applications (Somosy et al., 2002).

Generally it is evident that ionising radiation responses can be attributed to the activation or alteration of many intracellular signalling pathways in different tissues (Somosy, 2000; Köteles & Somosy, 2001). Therefore, the cellular response of the small intestine to ionising radiation may also be attributed, to some extent, to changes in the intracellular signalling pathways (Potten et al., 1995; Griffiths et al., 1996; Barcellos-Hoff, 1998). This may lead to either ionising radiation-related cell death or morphological and/or functional alteration; including inflammation, fibrosis, tumour development, modification of the immune system and high cell proliferation (Somosy et al., 2002).

4.2 Radiation-induced morphological change

Radiation-related morphological changes have been observed in intestinal epithelium of animals with a number of alterations after exposure to ionising radiation. Cell necrosis, loss of goblet cells, abscesses and structural changes in crypts, loss of paneth cells, mucosal alteration, increase in collagen content, and reduction of lymphocytes are amongst others (Rubio & Jalnäs, 1996). Such radiation-induced effects are time-dependent (Rubio & Jalnäs, 1996) and were classified as initial (prodormal) phase, acute (early) phase, sub-acute phase and delayed (late) phase changes (Berthrong & Fajardo, 1981; Anno *et al.*, 1989; Rubio & Jalnäs, 1996). According to Berthrong & Fajardo (1981), the early phase is considered to occur a few hours after irradiation and the late phase between six weeks to 10 years after radiation exposure. Based on the vascular changes, others considered the early phase to occur hours to a few days and late phase ranging from 4-6 months after irradiation (Fonkalsrud *et al.*, 1977; Law, 1981). Systematic analysis of dose- and/or time-dependent radiation related changes by Rubio and Jalnäs (1996) showed specific timing of histological changes with a dose dependency in 16 different morphological aspects, including the increase of collagen formation of the small intestine.

4.2.1 Collagen

A collagen fibril is one of the basic components of the extracellular matrix of connective tissue and plays an important role in providing support, strength and flexibility to surrounding tissues. Collagen is prevalent in the mucosa (submucosa, muscularis mucosa,

and subserosa) and apparently accumulations of dense extracellular matrix as early as 3 days after irradiation of the small intestine is evident (Rubio & Jalnäs, 1996; Langberg *et al.*, 1996).

According to Rubio & Jalnäs (1996), the general increase of collagen content shows a time- and dose-dependent response. A summary of the dose-time dependent response is shown in **Table 4-1** and demonstrates that the general increase of collagen content in all three parts of the mucosa is directly proportional to an increase in time after exposure, but doesn't follow the same pattern for dose response. However, studies by Tzaphlidou (2002) revealed that the collagen fibril diameter and its cluster formation follow dose dependent response with a decrease in diameter and cluster population as the dose increases.

Table 4.1. Percentage distribution of collagen content in the small intestine mucosa of Sprague-dwaley rats assessed 3, 10 and 30 days after being irradiated with low (9-12 Gy), moderate (15-18 Gy),and high (21-24 Gy) doses of X-radiation. Data obtained from Rubio and Jalnäs (1996).

Intestinal mucosa ·				
		submucosa	muscularis	subserosa
Time	3 days	70%	19%	75%
	10 days	70%	31%	81%
	30 days	100%	44%	94%
Dose	Low	50%	-	50%
	Moderate	100%	22%	100%
	High	92%	75%	92%

Any dose response of radiation-induced collagen production in the intestinal mucosa could indicate the existing relationship between radiation exposure and the related dose-dependent damage after exposure. Such investigation of collagen therefore could be indicative of early fibrosis and can play a significant role in choosing the effective dose in radiation dosimetery.

4.2.2 Apoptosis

Apoptosis is defined as a programmed process of active cell death that involves a synchronized cascade of molecular events, expressed by gross morphological alterations including condensation and clumping of nuclear chromatin, shrinkage of cytoplasmic organelles, membrane blebbing and cellular segmentation (Kerr *et al.*, 1972; Wyllie, 1992).

Apoptosis is a random effect within a given population of cells and its onset varies among cell types (Cohen-Jonathan *et al.*, 1999). Apoptosis can also be induced by ionising radiation (Blank *et al.*, 1997; Hendry & West, 1997) as interphase-linked death, known as fast apoptosis (Radford *et al.*, 1994; Merritt *et al.*, 1997) or following one or more cell divisions as mitosis-linked, known as late apoptosis (Dewey *et al.*, 1995; Yanagihara et *al.*, 1995).

Studies have shown that the response of crypt stem cells to ionising radiation is characterized by immediate cell loss and rapid repopulation (Potten *et al.*, 1983, 1994b). Any single hit on the DNA molecule initiates a p53-dependent apoptotic cell suicide as a

first choice over any DNA repair mechanism (Potten _et al._, 2003). Intestinal crypt cells

undergo fast apoptosis following irradiation (Yamaguchi, 1967) and the course of action

depends on the dose, quality of ionising radiation (Potten _et al._, 1983), time after

exposure and cell position (Ijiri & Potten, 1983 and 1987; Coopersmith & Gordon, 1997).

After exposure to ionising radiation the apoptotic response manifests within 2-3 hours,

reaching a maximum between 3-6 hours and drops over 24 hours (Hendry _et al._, 1982;

Potten, 1977; Potten & Grant, 1998).

Recent data shows that radiation-induced apoptosis is controlled by p53 (Wilson _et al.,_

1998) and has entire dependency on the gene as its expression was seen in p53-wild type

mice but not in p53-null mice between 4h and 8h after 8Gy irradiation (Merritt _et al._,

1994; Clarke _et al._, 1994). However, Merritt _et al._, (1997) reported that a delayed (G_2/M-

associated) p53-independent apoptosis was detected at 24h and 40h in small intestinal

epithelial cells taken from p53-null mice after exposure to 8Gy of gamma rays. However,

until now no p53 dependent response was observed later than 24 hours of time interval

between exposure and tissue assessment.

4.2.3 CD34 stem cell marker

Crypt stem cells are rare and their primary function is to maintain homeostasis of the

stem cell population and the internal wall lining of the intestinal epithelium by replacing

cells that die due to natural and/or cytotoxic related injury (Marshman _et al._, 2002; Potten

_et al._, 2003; Potten, 2004). Intestinal crypt stem cells are generally believed to reside at

the fourth or fifth position from the crypt base, above the Paneth cells (Booth & Potten,

2000; He, *et al.*, 2004; Sancho *et al.*, 2004). Like any other stem cells, crypt stem cells are understood to acquire markers on their cell surface.

4.2.4 Aim of study

In this study we attempted to investigate the dose response change of two specific collagens, collagen-I and –IV. Collagen-I, the most wide-spread one appears in the dermis of the skin, tendons, bone, teeth, and most connective tissue throughout the body (Kerr, 2000). Collagen-IV appears mostly in both basal and external laminae, and is produced by the cells (laminas related cells) involved in the matrix formation (Kerr, 2000). An attempt was also made to indicate late-stage radiation-induced cell death (apoptosis) which might ascribe to the decreased number of crypts in the higher doses at a time interval of more than 24 hours. A CD34 monoclonal antibody, commonly used to identify stem cells, was applied to mouse crypts in order to identify the position of stem cells. Irradiated mice tissues from single doses of 11, 12, 13 and 14Gy for ^{60}Co-gamma and 7, 8, 9 and 10Gy for p(66)/Be neutron exposures; and as split-doses (two-fractions) of 7, 7.5, 8 and 8.5Gy per fraction for ^{60}Co-gamma and 4, 4.5, 5 and 5.5Gy per fraction for p(66)/Be neutrons were stained using immunohistochemical techniques and assessed. A gap of 4 hours inbetween split-doses was allowed for cells to repair the sub-lethal damage caused by the first fraction.

4.3 MATERIALS AND METHODS

4.3.1 Experimental animals

Adult 16-week-old male Balb/C mice, weighing approximately 40g and 6-8 cm long were purchased from the Animal Unit of the University of Cape Town (UCT), South Africa, breeding facility. Prior to and after exposure to radiation the animals were maintained in plastic cages and housed at the animal house of the Cape Peninsula University of Technology. Mice were given standard clean water and food.

Both the experimental and control groups were randomized as a function of the type of radiation and/or the dose. Both control and experimental animals were maintained under identical conditions as regards room temperature ($20 \pm 2°C$), air ventilation, and 12 hours illumination.

4.3.2 Irradiation procedure

Two sources of radiation were used in this study. The gamma irradiation was performed at the Department of Radiation Oncology at Tygerberg Hospital using a ^{60}Co-gamma unit (Theratron 780C, Theratronix International). The dose-rate was 2Gy per minute at a source to surface distance (SSD) of 100 cm, a field size of 20 cm x 20 cm and a gantry angle of 0°. To ensure full charged particle equilibrium, mice were positioned behind 5 mm Perspex. Backscatter was achieved by placing the mouse jig on a 5 cm sheet of polyethylene. A similar set-up was used for neutron irradiations. Neutron irradiation was

carried out at iThemba LABS, Faure, delivering at a dose-rate of 0.4Gy per minute generated by 66 MeV protons bombarding a 19.6 mm thick beryllium target. p(66)/Be neutron radiation was applied at a field size of 29 cm x 29 cm, SSD of 150 cm and a gantry angle of 0°. Mice were placed at the centre of the beam source on a 9 cm thick Perspex, which served as a backscatter material, a 2 cm thick polyethylene block placed on spacers served as build up material. ^{60}Co-gamma rays were used as a reference beam and the p(66)/Be neutron beam as a clinical test beam.

Whole-body radiation exposures were applied with both radiation treatment modalities. During exposures the mice were stabilised in a specially designed 10 cm by 10 cm by 4 cm Perspex jig (see **Figure 3.1**A) providing enough ventilation during exposure. Three mice per dose point were positioned at the centre of the radiation field (see **Figure 3.1**B).

4.3.3   General tissue preparation and immuno-staining

A 5 cm long section of jejunum was removed 2 cm away from the pylorus from each mouse and was immediately fixed in a solution of 10% formalin, pH 7.4 overnight. Tissue samples were then cut into 3 mm pieces and placed into labelled cassettes and processed in an automated tissue processor overnight. Six small segments (3 mm each) of intestine, from the entire length of the jejunum were bundled together and embedded in wax blocks. Two blocks were prepared for each mouse.

4.3.3.1   Envision system

1μ sections of formalin-fixed, paraffin embedded jejunum from both control and radiation-exposed mice were cut for immunohistochemical detection of collagen-I, collagen-IV, and p53. Sections were placed into 40% methanol and a water bath (50°C), respectively to keep them flat and straightened. Sections were collected onto silanised glass slides coated with poly-L-lysine or positively charged slides to avoid detachment of sections from the slide during the high-pressure cooking antigen retrieval (HPCR) process. Sections were heat-fixed by incubating at 60°C, overnight. After de-waxing in xylol and hydrating through graded alcohols to water, sections were treated with 1% hydrogen peroxidase in water solution for 15 minutes to block endogenous peroxidase activity. Slides were washed well in tap water. Antigen retrieval was performed by either pressure cooking slides (Prestige stainless steel pressure cooker) in Citrate Buffer (pH 6.0) for two minutes at full pressure (15lbs at 121°C) or with the use of proteolytic enzymes incubated for 8 minutes. Slides were immediately immersed in water and washed well in tap water followed by a rinse with Phosphate Buffered Saline solution (PBS) pH 7.6. After each rinse, the area around sections was wiped with paper towel to remove excess fluid to avoid further dilution of reagents. Slides were placed in 5% normal goat serum (Dako # X0907) for 10 minutes to block non-specific binding. Serum was drained off and slides were treated with the primary antibody; namely: collagen-I, -IV and p53 (*See **Table 4.2**) at specific times and dilutions. Sections were washed well with PBS buffer and incubated with the secondary antibody, goat anti-mouse with

Envision labelled Polymer, Horseradish Peroxidase (Dako # K4003) for 10 minutes at room temperature. Slides were then washed again with PBS buffer. A positive stain was developed by applying 3,3'-diaminobenzidane (DAB, Dako # K3466) for 5-10 minutes. Slides were washed in tap water and immersed in a 1% aqueous copper-sulphate solution for 5 minutes followed by another wash in tap water. Sections were counterstained in haematoxylin, blued in Scott's tap water, dehydrated in graded alcohols and cleared in xylene. Sections were mounted in Entellen and coversliped. Slides were analysed microscopically at x 400 magnification.

In addition, a subsequent run of collagen-I and-IV immunohistochemical staining was done with a dextran labelled polymer (Envision) in an attempt to decrease the background interference observed in the initial screening of the first experiment.

*Table 4.2. List of primary antibodies used in envision system and their specific dilution and incubation time.

Type	Ag Retrieval Method	Primary Ab dilution	Primary Ab incubation time	Positive control
Collagen-I (Novocastra, NCL-COLL-Ip)	Citrate buffer HPCR	1:100	1 hour	Placenta
Collagen-IV (Dako, # M0785)	Proteolytic Enzyme	1:50	45 min	Skin
p-53 (Lab vision, #RM-9105-S0)	Citrate buffer HPCR	1:100	45 min	Gastric carcinoma

4.3.3.2   Avidin-biotin system

1µ sections of formalin-fixed, paraffin embedded jejunum from both control and radiation-exposed mice were prepared for immunohistochemical detection of CD34. Sections were placed into water bath (50°C) to keep them flat and straightened and were collected onto silanised glass slides coated with poly-L-lysine or positively charged slides to avoid detachment of sections from the slide during the high-pressure cooking antigen retrieval (HPCR) process. Sections were heat-fixed by incubating at 60°C. After de-waxing in xylol, slides were hydrated through graded alcohols to water. Antigen retrieval was performed by pressure cooking (prestige stainless steel pressure cooker) in 0.01M citrate buffer (pH 6.0) for two minutes at full pressure (15lbs at 121°C). Slides were immediately immersed in water and washed well in tap water for the first run, and for the second run sections were first stood in hot buffer for 10 minutes followed by a wash in running tap water. Sections were treated with 3% hydrogen peroxidase in water solution for 5 minutes to block endogenous peroxidase activity and then washed in distilled water. Biotinylated primary antibody, CD34 (Dako # K3954) was applied to the sections and incubated for 15 minutes at room temperature. Slides were washed in tris-buffer solution (TBS) of 0.005mol/L, wiped and incubated in Strept-avidin peroxidase for 15 minutes at room temperature followed by another TBS wash. A positive stain was developed by applying 3,3'-diaminobenzidane (DAB, Dako # K3466) for 5-10 minutes. Slides were then washed in TBS and counterstained in haematoxylin, dehydrated in graded alcohols

and cleared in xylene. Sections were mounted in Entellen and coversliped and analysed microscopically at x 400 magnification.

In a subsequent run, in an attempt to reduce the background stain interference, the primary antibody was double diluted and to avoid detachment of sections from slides the antigen retrieval was done in 0.01 M citrate buffer by boiling it in a microwave oven for 10 minutes.

4.4 Scoring system

Slides were observed under a light microscope for the presence of a brown precipitate in tissue which is indicative of a positive stain, and were subjectively scored for stain intensity using a visual comparison between controls and exposed tissues. This was supported by a live screen picture captured from a Zeiss AuxioHOME computer driven microscope.

4.5 RESULTS

4.5.1 Collagen-I

The stain for collagen-I was run on human placenta tissue and control mouse tissue (0Gy) as external and internal positive controls, respectively; both stained positive as shown in **Figure 4.1 (a)** and **(b)**. For an internal negative control two other controls were run on mouse tissue, one without the primary antibody, but with the ancillary reagents,

while the other was run with the primary antibody but without the ancillary reagents. Both stained negative as shown in **Figure 4.1 (c)** and **(d)** indicating the positive staining was true.

In the first batch experiment, our results showed high background staining as can be seen in **Figure 4.1 e, f, g** and **h** for ^{60}Co-gamma and **Figure 4.3 a, b, c** and **d** for neutron beam irradiation.

A second batch was run the same way but this time with a dextran labelled polymer containing no biotin and the primary antibody incubation time was brought down to 30 minutes to reduce background staining. Improved results with reduced background were obtained as can be seen in **Figure 4.2 a, b, c** and **d** for ^{60}Co-gamma and **Figure 4.4 a, b, c** and **d** for neutron beam irradiation. The stain gives an "amorphous" type of matrix staining. Collagen-I staining in the human tissue (placenta) and throughout the unirradiated and irradiated tissues were more or less the same in intensity and thickness.
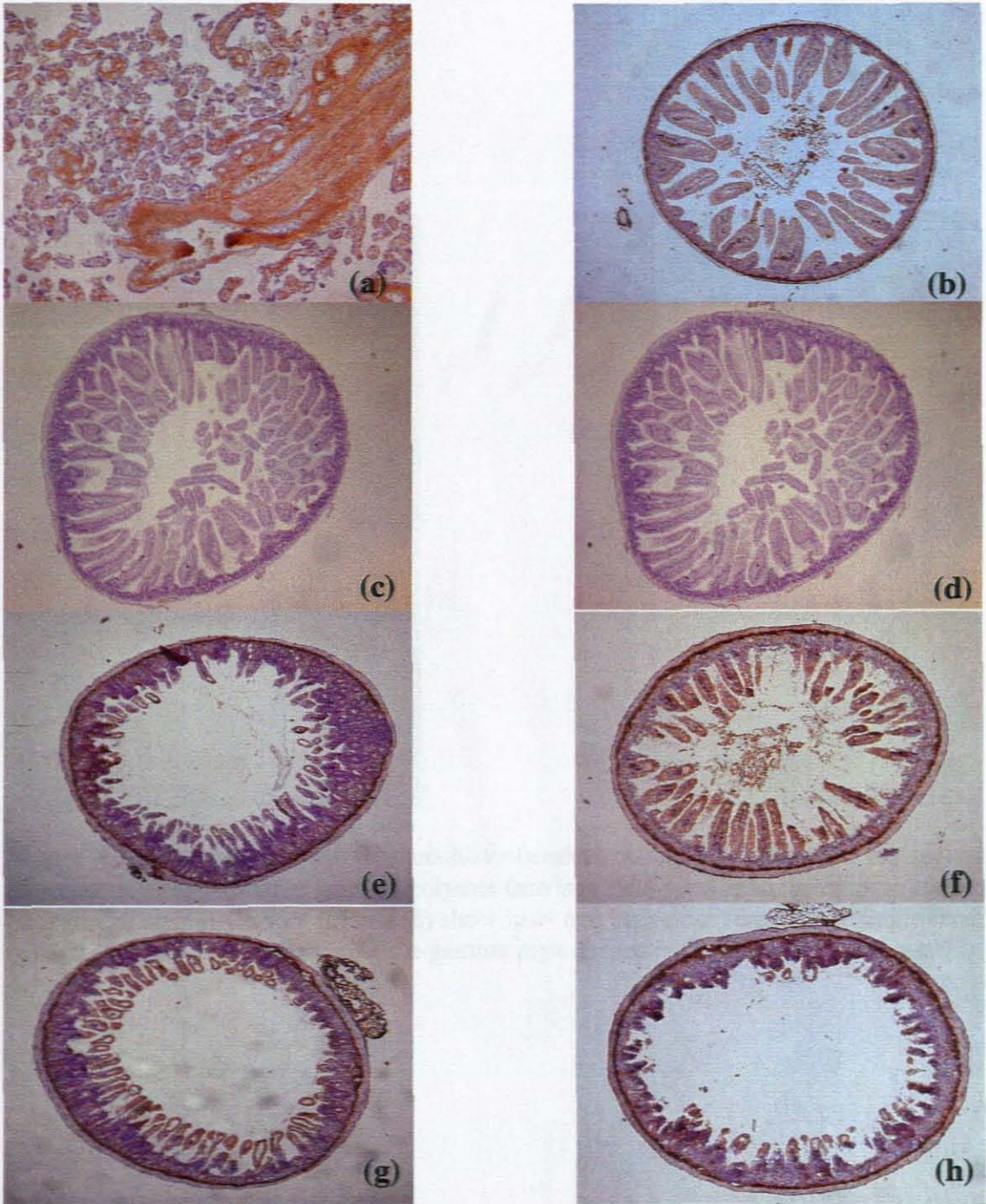
Figure 4.1. Immunohistochemical staining of collagen-I. (a) Human placenta tissue and (b) unirradiated (0 Gy) mouse tissue stained with primary antibody were used as positive control. (c) unirradiated (0 Gy) mouse tissue stained without primary antibody but with ancillary reagents and (d) vice versa were used as internal negative controls. (e), (f) and (g), (h) show collagen-I staining for low- and high-dose single-dose and split-dose exposures of ^{60}Co-gamma rays, respectively.
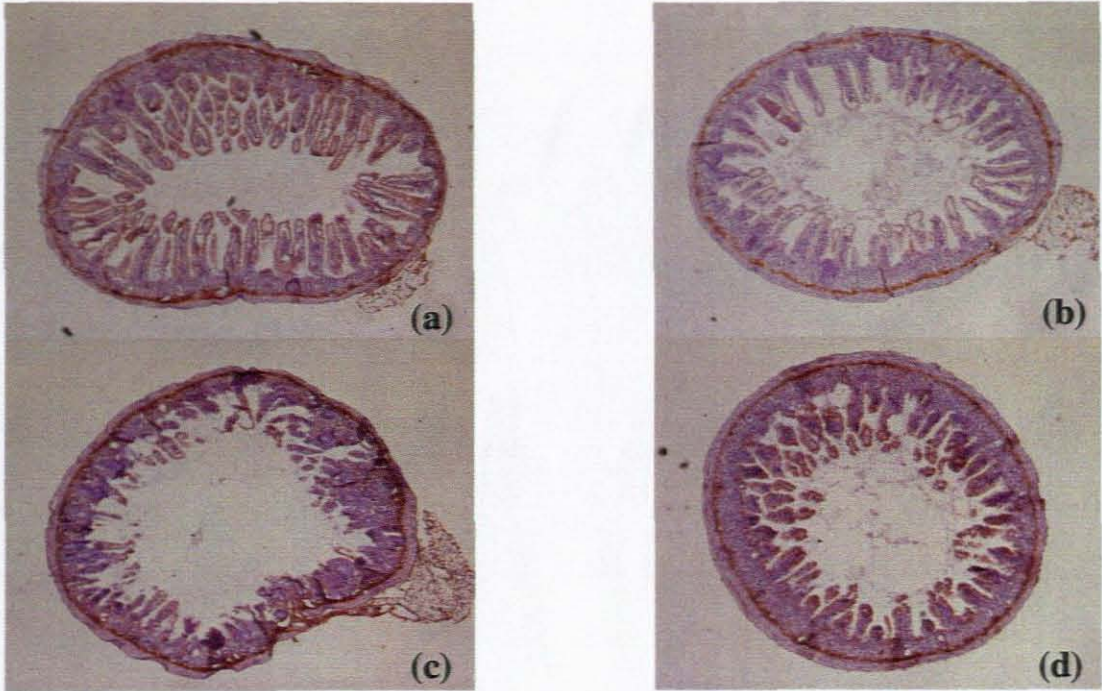
Figure 4.2. Shows subsequent immunohistochemical collagen-I staining of the second experiment when a dextran labelled polymer (envison) was used in the attempt to reduce background staining. Slides (a) and (b) show low- and high-dose response of single- and; (c) and (d) split-dose fraction of ^{60}Co-gamma rays, respectively. Controls as seen in Fig. 4.1.
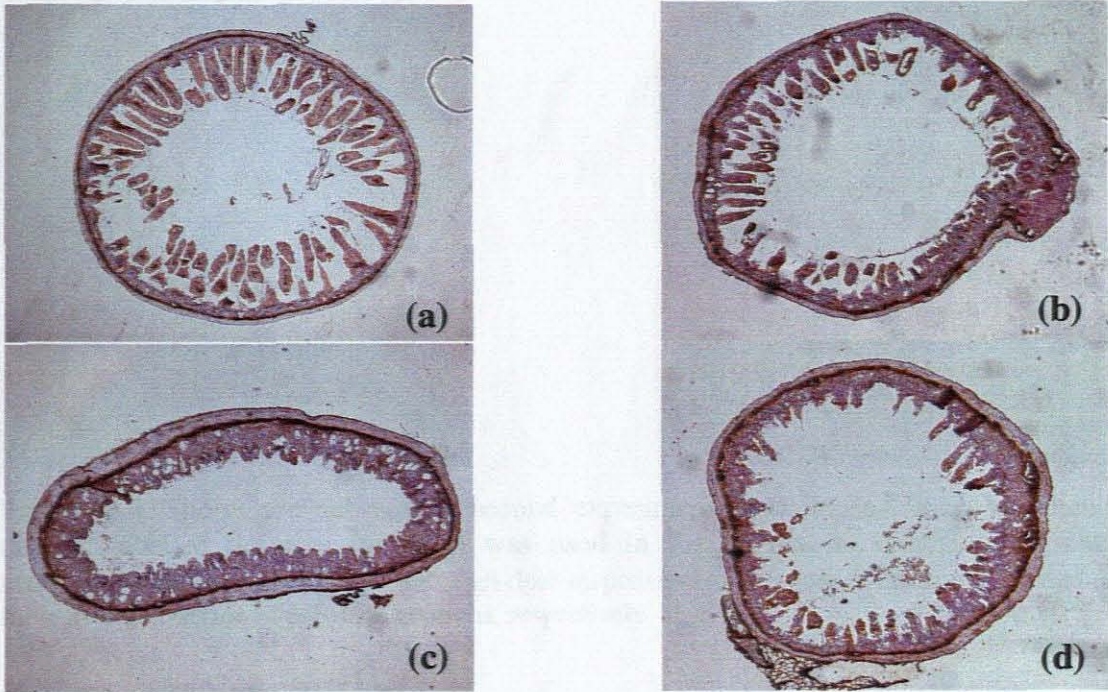
Figure 4.3. Immunohistochemical staining of collagen-I exposed to p(66)/Be neutrons.(a) and (b) shows low- and high-doses response of single-dose fraction and; (c) and (d) for split-dose fraction from the first experiment, respectively. Controls as seen in fig. 4.1.
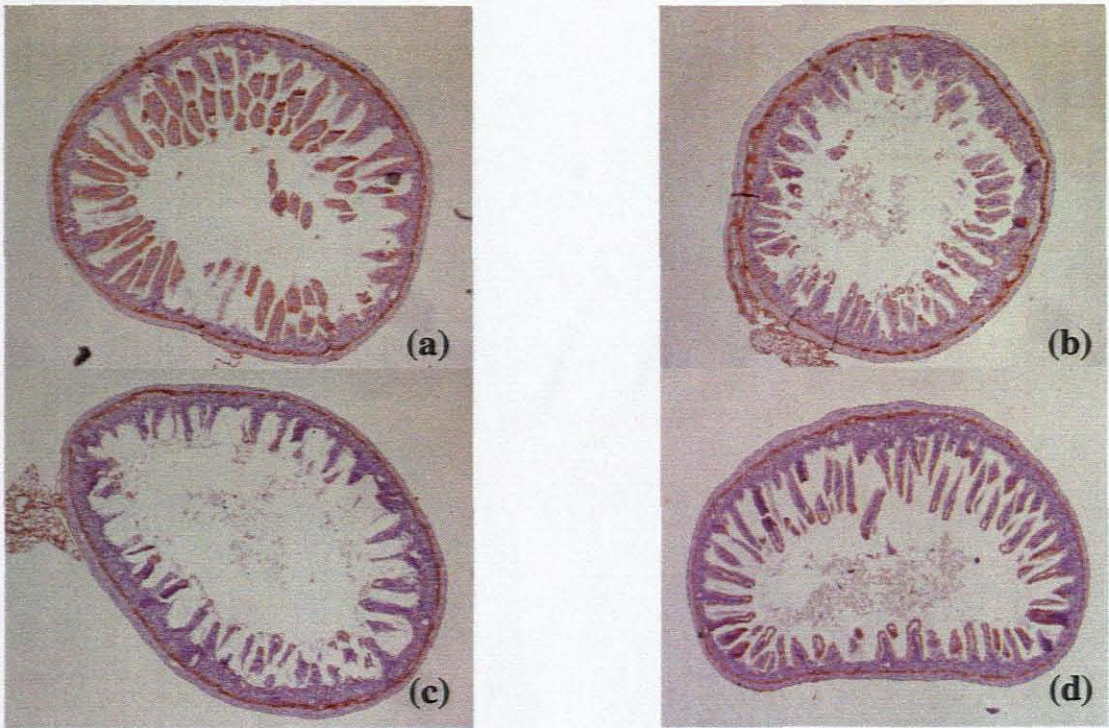
Figure 4.4. Shows the subsequent second experiment of collagen-I staining when a dextran labelled polymer (envison) was used in the attempt to reduce background staining. (a) and (b) shows low- and high-dose response of single-dose fraction and; (c) and (d) for split-dose fraction of p(66)/Be neutrons, respectively.

4.5.2 Collagen-IV

Similarly, collagen-IV unirradiated mouse controls were run parallel with the human tissue (skin) as shown in **Figure 4.5 (a)** and **(b)**, respectively. The human tissue stained positive as well as the mouse control tissue. Two other mouse control tissues, not shown in **Figure 4.5** were run as internal negative control in which one was run without the primary antibody but with the ancillary reagents, and the other one with primary antibody but with out the ancillary reagents. Both stained negative. The stain for the different dose-points of both irradiations showed non-specific with high back ground staining.
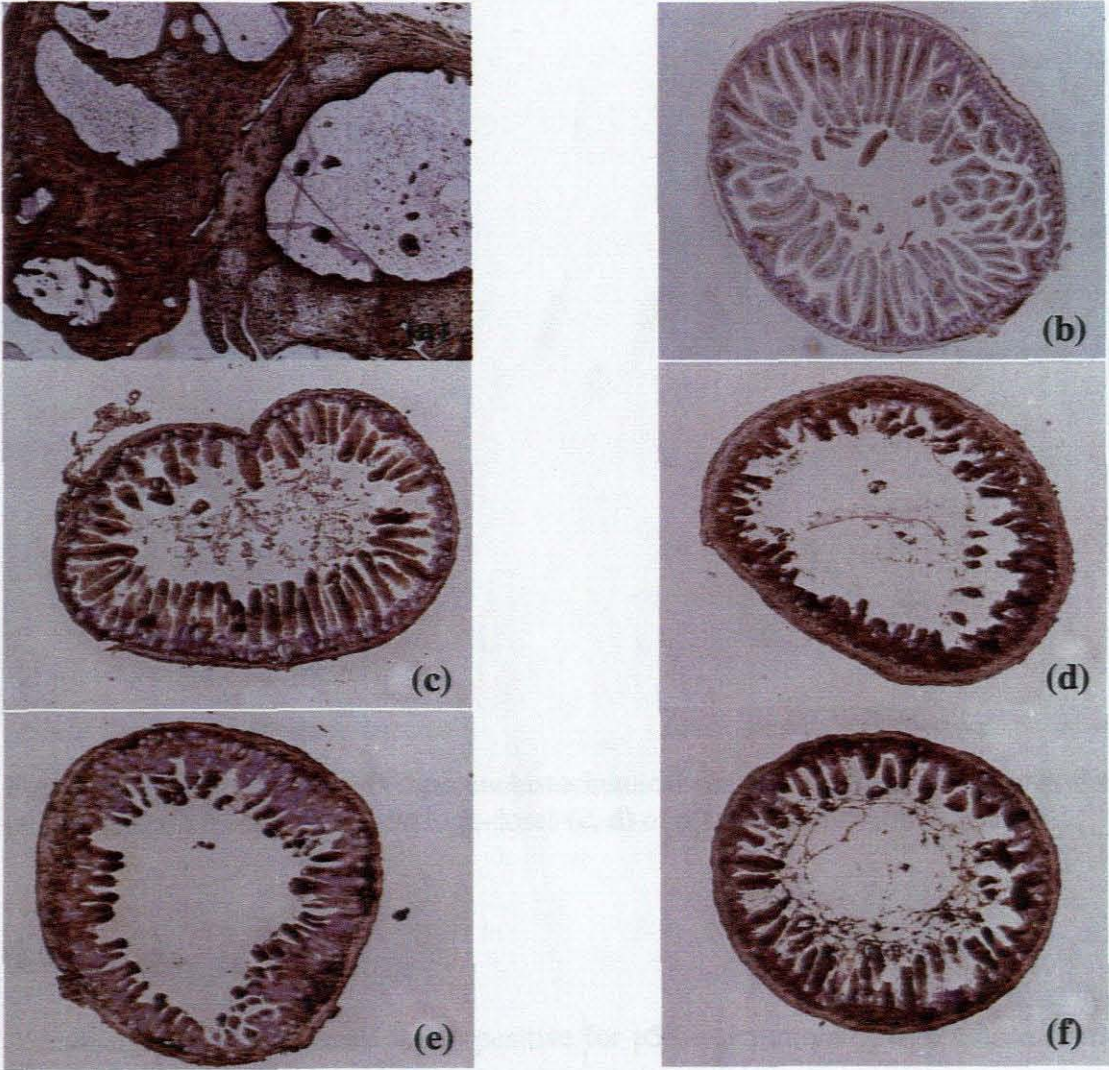
Figure 4.5. Shows collagen-IV immunohistochemical staining of single fraction low- and high-doses (c) and (d); and the same for split-dose fractions (e) and (f) of ^{60}Co-gamma rays, respectively. Skin tissue (a) and unirradiated (0 Gy) mouse tissue (b) were used as controls.

A subsequent second run made in the attempt to reduce the background staining was not successful in human tissue, control mouse tissues and irradiated mouse tissues from both irradiations.
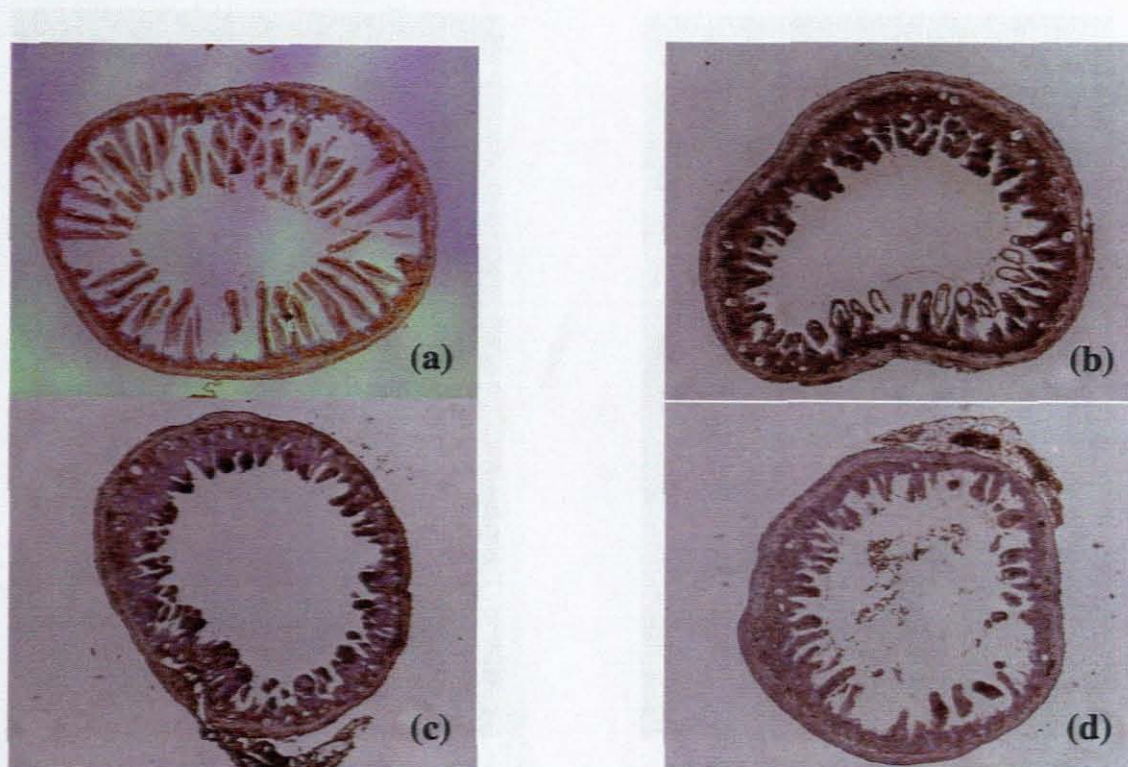
Figure 4.6. Shows collagen-IV immunohistochemical stain for single low- and high-dose (a , b) and two fraction low- and high-doses (c, d) of p(66)/Be neutron irradiation.

4.5.3 p53

A human tissue (gastric carcinoma) positive for p53 was run along with mouse control and irradiated tissues from both radiation exposures. The human gastric carcinoma stained brown, indicating positivity, as shown in **Figure 4.7(a)**. The same tissue was run without the primary antibody and showed no staining; this served as a negative control. Control and irradiated mouse tissues from both radiation exposures did not show any specific staining as shown in **Figure 4.7 b, c and d.**
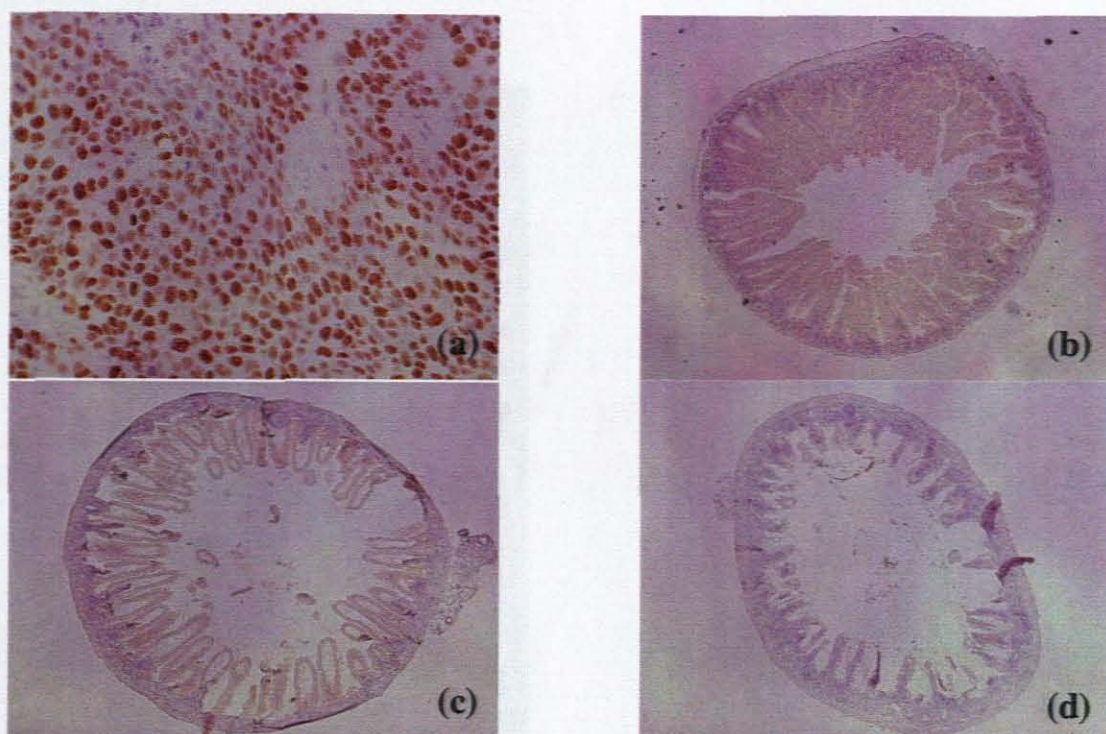
Figure 4.7. Pictures showing positive stain of p-53 in human gastric carcinoma tissue (a) and negative stain in unirradiated (0Gy) mouse tissue (b) using citrate buffer during antigen retrieval. Irradiated tissues (c, d) were also tried in different buffer, EDTA and citrate, during antigen retrieval, but both stained negative.

4.5.4 CD34

For the CD34 experiment a positive human control tissue (appendix) was run along with mouse control and irradiated tissues from both radiation exposures. A brown precipitate staining was observed in the human tissue as an indication of positivity, as shown in **Figure 4.8(a)**. The same tissue was run without the primary antibody and showed no staining confirming the positive result, **Figure 4.8(b)**. Control mouse tissue stained with the primary antibody showed up as positive. However; the same control mouse tissue stained without the primary antibody also showed positivity with high background staining, as shown in **Figure 4.8(c)** and **(d)** respectively.
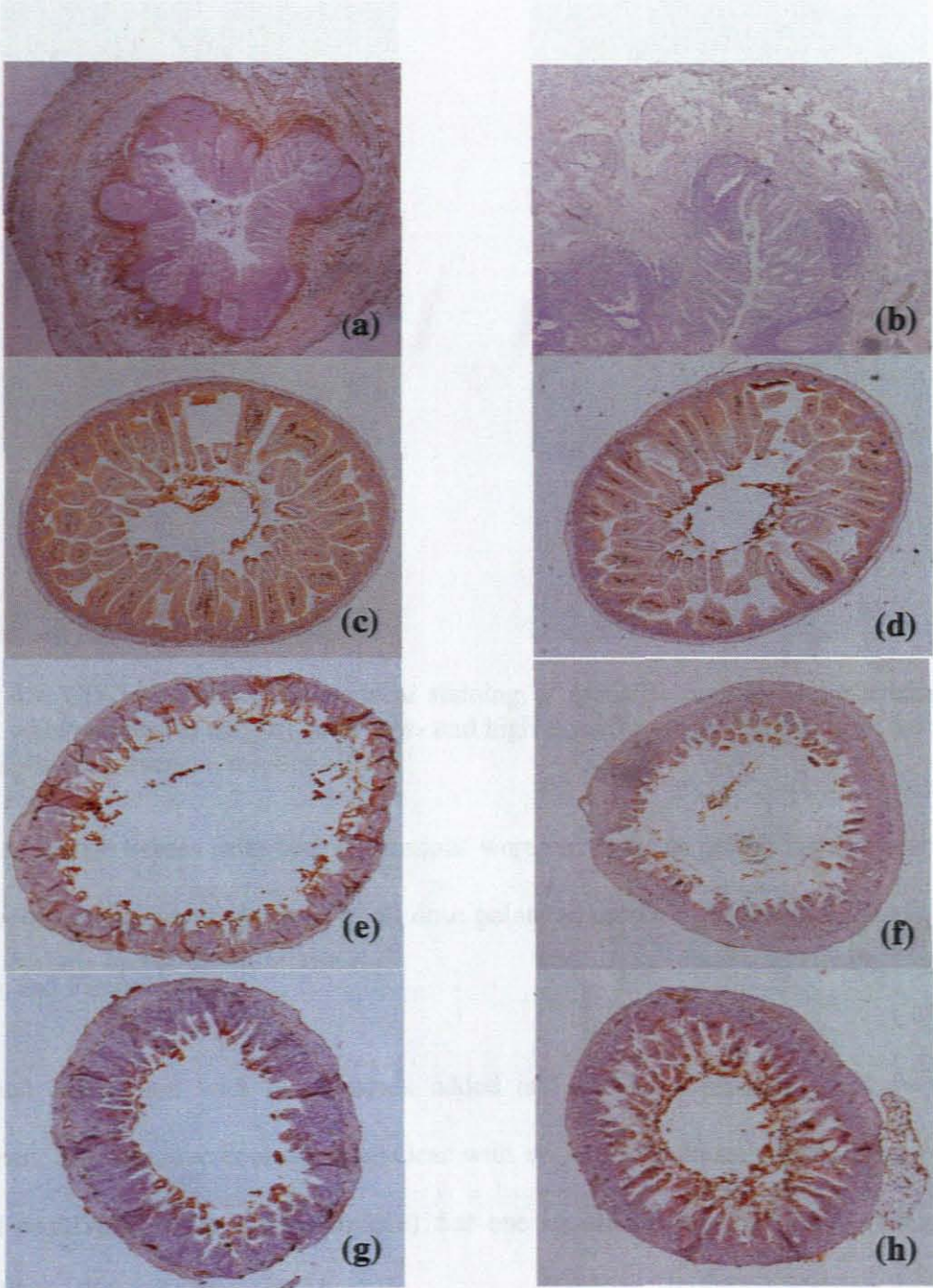
Figure 4.8. CD-34 immunohistochemical stain of human tissue appendix (a) as internal positive and (b) as internal negative control, respectively. (c) and (d) unirradiated (0Gy) mouse tissue as internal positive and negative controls, respectively. Slides (e) and (f) show low- and high-dose for single fraction and; (g) and (h) for split-dose fraction of ^{60}Co-gamma rays, respectively.
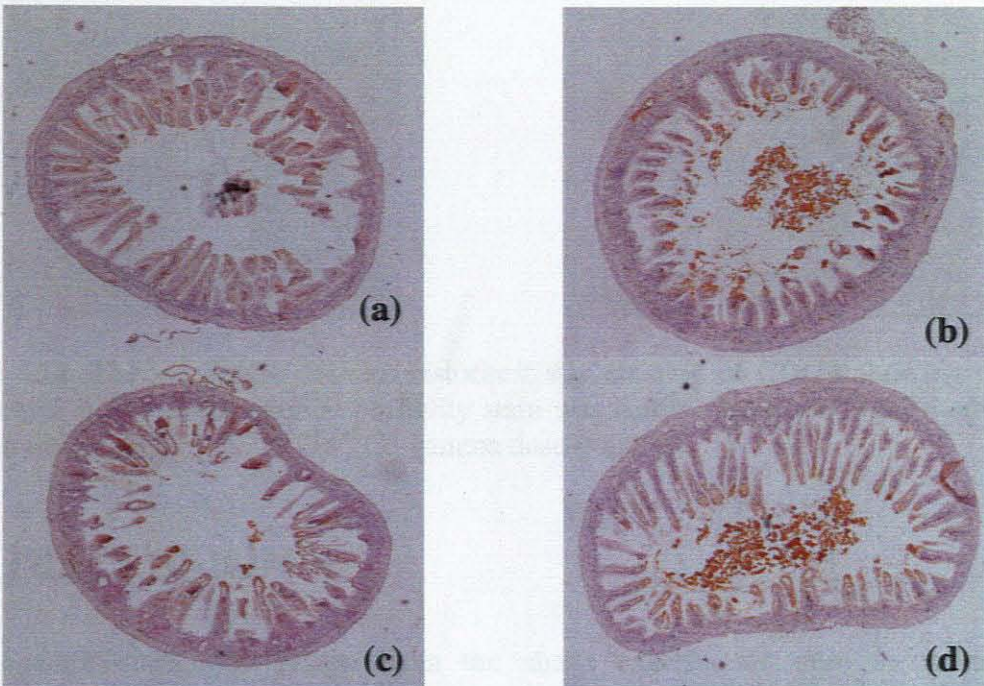
Figure 4.9. CD-34 immunohistochemical staining of p(66)/Be neutron beam irradiated tissues, where slides **(a)** and **(b)** show low- and high-dose for single fraction and; **(c)** and **(d)** for split-dose fraction, respectively.

Irradiated mouse tissues from both irradiations were run twice as per kit instructions and non-specific staining was observed in all dose points as shown in **Figure 4.8 (e)**, **(f)**, **(g)** and **(h)**; and **Figure 4.9**.

A second experiment with biotin block added and a diluted primary antibody was performed. The negative controls were clear with no background staining; however the internal positive stain (brown precipitate) that one should expect was absent or hardly noticeable as shown in **Figure 4.10**.
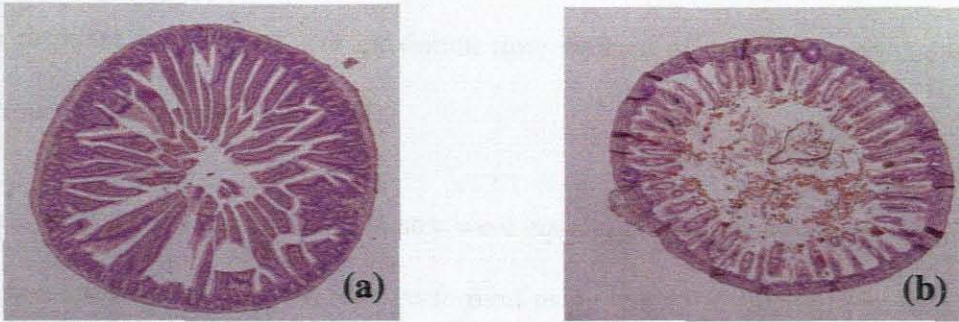
Figure 4.10. The subsequent Immunohistochemistry staining of CD-34 showing clear background, however the internal positivity stain was hardly noticeable both in control mouse tissue **(a)** and of the 13 Gy ^{60}Co-gamma dose-point **(b)**.

4.6 DISCUSSION

The immunohistochemical results from the above experiments were inconclusive. However, it is worthwhile discussing the pitfalls and technical difficulties encountered and the possible reasons behind them.

In general, the immunohistochemistry stain was difficult to quantify due to non-specific staining observed. In addition, despite all efforts to avoid the high background of non-specific staining, e.g. using dextran labelled polymer, comparisons between controls and dose points of collagen-I and -IV were very difficult. Our method of reading was to use normal light microscopy, and this appeared to showed a similar colour intensity in all dose points when compared to control tissues as shown in **Figures 4.1- 4.6**.

Immunohistochemical staining of p53 did not show any dose response after irradiation. This could be ascribed to the time interval between radiation exposure and sample collection, which was 3.5 days after irradiation. Normally, an early p53 dependent

radiation response is observed at a maximum time interval of 3-6 hours and decreases after 24 hours (Potten and Grant, 1998).

CD-34 and collagen immunohistochemistry were equally difficult to demonstrate due to the high non-specific staining. It was performed using the ARK (animal research kit). The kit failed in terms of specificity as high background staining was developed from the biotin contained within the reagent. Furthermore, the primary antibody required a heat mediated antigen retrieval method to unmask the antigens. This aggravated the problem by activating the endogenous biotin and therefore compromising the results. An attempt made to clean up the non-specific staining using a biotin block added to the primary antibody was only partially successful in clearing the background staining. The positivity of the internal control that one could expect from a human and the mouse control tissues were compromised, resulting in a false negative result. It may however be possible to improve such results with the use of poly-l-lysine (MW 3000-6000) added to the biotinylated primary antibody, but unfortunately this product is not available here in South Africa at present.

In addition to the shortcomings of the immunohistochemistry staining, the integrity of the tissue sections was compromised throughout the staining, despite being on positively charged glass slides. This could be attributed to the tissue fixation and processing procedures described in the methodology. It may be advisable for future studies to reduce processing time to a 4 hour cycle, for animal tissue particularly, when using immunohistochemistry techniques.

References

Anno, G.H., Baum, S.J., Withers, H.R. & Young, R.W. 1989. Symptomatology of acute radiation effects in humans after exposure to doses of 0.5-30 Gy. *Health Physics* 56, 821-838.

Barcellos-Hoff, M.H. 1998. How do tissues respond to damage at cellular level? The role of cytokines in irradiated tissues. *Radiation Research*, 150: s109-s120.

Berthrong, M. & Fajardo, L.F., 1981. Radiation injury in surgical pathology. Part II. Alimentary tract. Am J Surg Pathol 5:153-176.

Blank, K.R., Rudoltz, M.S., Kao, G.D., Muschel, R.J. & McKenna, W.G. 1997. Review: the molecular regulation of apoptosis and implication for radiation oncology. *International Journal of Cell Biology*, 71: 455-466.

Booth, C. & Potten, C.S. 2000. Gut instincts: thoughts on intestinal epithelial stem cells. *J. Clin. Invest.*, 105: 1493-99.

Buell, M.G. & Harding, R.K. 1989. Proinflammatory effects of local abdominal irradiation on rat gastrointestinal tract. *Digestive Disease Science*, 34: 390-399.

Busch, D.B. 1990. Pathology of the radiation-damaged bowel. In: Galland, R.B., Spencer, J. (Eds). Radiation Enteritis. Edward Arnold, London, pp. 66-87.

Clarke, A.R., Gledhill, S., Hooper, M.L., Bird, C.C. & Wylie A.H. 1994. p53 dependence of early apoptotic and proliferative responses within the mouse intestinal epithelium following gamma-irradiation. *Oncogene*, 9: 1767- 1773.

Cohen-Jonathan, E., Bernhard, E.J. & McKenna, W.G. 1999. How dose radiation kill cells? *Current Opinion in Chemical Biology*, 3: 77-83.

Coopersmith, C.M. & Gordon, J.L. 1997. Gamma-ray-induced apoptosis in transgenic mice with proliferative abnormalities in their intestinal epithelium: re-entry of villus enterocytes into the cell cycle does not affect their radioresistance but enhances the radiosensitivity of the crypt by inducing p53. *Oncogene*, 15: 131- 141.

Dewey, W.C., Ling, C.C. & Meyn, R.E. 1995. Radiation-induced apoptosis: relevance to radiotherapy. *Int J Radiat Oncol Bio Phys*, 33: 781- 796.

Fonkalsrud, E.W., Sanchez, M., Zerubavel, R. & Mahoney, A. 1977. Serial changes in arterial structure following radiation therapy. *Surg. Gynecol. Obstet.*, 145: 395-400.

Füth, H. & Ebeler, F. 1915. Röntgen und Radiumtherapie des uteruskarzinoms. *Zentralbl Gynaekol*,14: 217-227.

Griffiths, N.M., Francois, A., Dublineau, I., Lebrun, F., Joubert, C., Aigueperse, J. & Gourmelon, P. 1996. Exposure to either gamma or mixed neutron gamma field irradiation modifies vasoactive intestinal peptide receptor characteristic in membrane isolated from pig jejunum. _International Journal of Radiation_, 70: 361-370.

Hauer-Jensen, M. 1990. Late radiation injury of the small intestine: clinical, pathophysiologic and radiobiologic aspects. _Acta Oncologica_, 29: 401-415.

He, X.C., Zhang, J., Tong, W.G., Tawfik, O., Ross, J., _et al._, 2004. BMP signalling inhibits intestinal stem cell self-renewal through suppression of Wnt-beta-catenin signalling. _Nat. Genet._, 36: 1117-21.

Hendry, J.H., Potten, C.S., Chadwick, C. & Bianchi, M. 1982. Cell death (apoptosis) in the mouse small intestine after low doses: effects of dose-rate 14.7 MeV neutrons and 600 MeV (maximum energy) neutrons. _Int. J. Radiat. Biol._, 42: 611-620.

Hendry, J.H. & West, C.M.L. 1997. Apoptosis and mitotic cell death: their relative contributions to normal-tissue and tumour radiation response. _International Journal of Radiation Biology_, 71: 709-719.

Ijiri, K. & Potten, C.S. 1983. Response of intestinal cells of differing topographical and hierarchical status to ten cytotoxic drugs and five sources of radiation. _Br. J. Cancer_, 47: 175-185.

Ijiri, K. & Potten, C.S. 1987. Further studies on the response of intestinal crypt cells of different hierarchical status to eighteen different cytotoxic agents. *Br. J. Cancer*, 55: 113-123.

Kerr, J.B. 2000. Atlas of Functional Histology. London: Mosby. 59-79

Kerr, J.F.R., Wyllie, A.H. & Currie, A.R. 1972. Apoptosis: a basic biological phenomenon with wide ranging implications in tissue kinetics. *Br. J. Cancer*, 26: 239-257.

Köteles, G.J. & Somosy Z. 2001. Radiation responses in plasma membrane: review of the present state and future trends. *Biology of the Cell* (in press).

Krause, P. & Ziegler, K. 1906-1907. Experimentelle untersuchungen über die einwirkung der Röntgenstrahlen auf tierisches Gebewe. *Strahlentherapie*, 158: 50-54.

Langberg, C.W. & Hauer-Jensen, M. 1996. Influence of fraction size on the development of late radiation enteropathy: an experimental study in the rat. *Acta Oncologica*, 35: 89-94.

Langberg, C.W., Sauer, T., Reitan, J.B. & Hauer-Jensen, M. 1996. Relationship between intestinal fibrosis and histopathologic and morphometric changes in consequential and late radiation enteropathy. *Acta Oncologica*, 35: 81-87.

Law, M.P. 1981. Radiation-induced vascular injury and its relation to late effects in normal tissue. Adv Radiat Biol 9: 37-73.

Liebow, A.A., Warren, S. & De Coursey, E. 1949. Pathology of atomic bomb casualties. *Am. J. Pathol.,* 25: 853-1027.

Marshman, E., Booth, C. & Potten, C.S. 2002. The intestinal epithelial stem cell. *BioEssays,* 24: 91-98.

Merrit, A.J., Allen T.D., Potten, C.S. & Hickman, J.A. 1997. Apoptosis in small intestinal epithelia from p53-null mice: evidence for a delayed, p53-independent G2/M-associated cell death after γ-irradiation. *Oncogene,* 14: 2759-2766.

Merrit, A.J., Potten, C.S., Hickman, J.A., Kemp, C., Balmain, A., Hall, P. & Lane, D. 1994. The role of p53 in spontaneous and radiation-induced apoptosis in the gastrointestinal tract of normal and p53-defficient mice. *Cancer Res.,* 54: 614-617.

Olasolo, J.J. 1989. Severe small bowel irradiation enteritis. *Acta Oncol.,* 28: 717-720.

Potten, C.S. & Grant, H. 1998. The relationship between radiation-induced apoptosis and stem cells in the small and large intestines. *Br. J. Cancer,* 78: 993-1003.

Potten, C.S. 1977. Extreme sensitivity of intestinal crypt cells to X and γ-radiation. *Nature,* 269: 518-521.

Potten, C.S. 2004. Radiation, the ideal cytotoxic agent for studying the cell biology of tissues such as the small intestine. *Radiation Research,* 161(2): 123-136.

Potten, C.S., Booth, C. & Hargreaves, D. 2003. The small intestine as a model for evaluating adult tissue stem cell drug targets. *Cell Prolif,* 36: 115-129.

Potten, C.S., Hendry, J.H., Moore, J.V. & Chwalinski, S. 1983. Cytotoxic effects in gastro-intestinal epithelium (as exemplified by small intestine). In: Potten, C.S., Hendry, H.J. (Eds.). Cytotoxic Insult to Tissue. Effects on Cell Lineages. Churchill Livingstone, Edinburgh, London Melbourne and New York: 105-152.

Potten, C.S., Merritt, A., Hickman, J., Hall, P. & Faranda, A., 1994b. Characterization of radiation-induced apoptosis in the small intestine and its biological implications. *International Journal of Radiation Biology,* 65: 71-78.

Potten, C.S., Owen, G., Hewitt, D., Chadwick, C.A., Hendry, J.H., Lord, B.I. & Woolford, L.B. 1995. Stimulation and inhibition of proliferation in the small intestinal crypts of the mouse after in vivo administration of growth factors. *Gut,* 36: 864-873.

Quástler, H. 1956. The nature of intestinal radiation death. *Radiation Research,* 4: 303-320.

Radford, I.R., Murphy, T.K., Radley, J.M. & Ellis, S.L. 1994. Radiation response of mouse lymphoid myeloid cell lines. Part II. Apoptotic death is shown by all lines examined. *Int J Radiat Biol,* 65: 217-227.

Regaud, C., Nogier, T., & Lacassagne, A. 1912. Sur les effects redoutables de irradiation étendues de l'bomen et sur les lesions du tube digestif déterminées par les razons de Röntgen. *Archives of Electromedicine,* 21: 321-342.

Rubio, C.A. & Jalnäs, M. 1996. Dose-time-dependent histological changes following irradiation of the small intestine of rats. *Dig. Dis. Sci.,* 41(2): 392-401.

Sancho, E., Batlle, E. & Clevers, H. 2004. Signaling pathways in intestinal development and cancer. *Annu. Rev. Cell Dev. Biol,* 20: 695-723.

Somosy, Z. Horváth, G., Telbisz, Á., Réz, R. & Pálfia, Z. 2002. Morphological aspects of ionizing radiation response of small intestine. *Micron,* 33: 167-178.

Somosy, Z. 2000. Radiation response of the cell organelles. *Micron,* 31: 165-181.

Tzaphlidou, M. 2002. Collagen as a model of the study of radiation induced side effects: use of image processing. *Micron,* 33: 117-120.

Walsh, D. 1897. Deep tissue traumatism from roentgen ray exposure. *British Medical Journal,* 2: 272-275.

Wilson, J.W., Pritchard, D.M., Hickman, J.A. & Potten, C.S. 1998. Radiation-induced p53 and p21WAF-1/CIP1 expression in the murine intestinal epithelium: apoptosis and cell arrest. *American Journal of Pathology,* 153: 899-909.

Wyllie, A.H. 1992. Apoptosis and the regulation of cell numbers in normal and neoplastic tissues: an overview. *Cancer Metast Rev*, 11: 95-103.

Yamaguchi, T. 1967. Relationship between survival period and dose of irradiation in rat thymocytes in *vitro. Int J Radiat Biol,* 12: 237-242.

Yanagihara, K., Nii, M., Numoto, M., Kamiya, K., Tauchi, H., Sawada, S. & Seito, T. 1995. Radiation-induced apoptotic cell death in human gastric epithelial tumor cells; correlation between mitotic death and apoptosis. *Int J Radiat Biol*, 67: 677-685.

Young, R.W. 1987. Acute radiation syndrome. In: Conkin, J.J., Walker, R.I. (Eds). Military radiobiology. *Academic Press Inc.,* 165-190.

Chapter 5

MICRONUCLEI (MN) ASSAY

5.1   Introduction and literature review

Ionising radiation can induce the formation of different chromosomal aberrations (Hall, 2000; Travis, 2000). Chromosome fragments (acentrics, centrics and dicentrics) and whole chromosomes that are unable to attach to the spindle at metaphase lag behind at anaphase and are not included in the daughter nuclei during nuclear division, resulting in a small separate nucleus, hence the term micronuclei (Fenech *et al.*, 1999).

Countryman and Heddle (1976) first described micronuclei (MN) in lymphocytes of human peripheral blood. Fenech and Morely (1985, 1986) modified the assay using cytochalasin-B (cyt-B) to inhibit the cell cycle prior to cell division (anaphase) to have a reliable score in measuring the MN only in bi-nucleated cells that had completed one nuclear division. Therefore the cytochalasin-B micronuclei (CBMN) assay, which is an easy and fast method of cytogenetic analysis has become the standard method for biological dosimetery (Zsuzsanna *et al.*, 1987; Roux, *et al.*, 1998), human biomonitoring studies (Chang *et al.*, 1999; Kryscio *et al.*, 2001), and in the assessment of intrinsic radiosensitivity (Vral *et al.*, 2002; Widel *et al.*, 2003).

The assay is widely used in lymphocytes (Slabbert *et al.*, 1996; Brown *et al.*, 1997; Venkatachalam *et al.*, 1999) and, epithelial tissue (Fenech *et al.*, 1999) and other self-dividing cells including Chinese hamster ovarian (CHO) cells (Slabbert *et al.*, 1996; Fenech, 2000; IAEA, 2001).

Chinese hamster ovarian cells were introduced in the early 1960's as viable epithelial cells for experimental purposes. Their high plating efficiency, short cell cycle of approximately 12 hours and well-defined nuclei make CHO cells suitable for cytogenetic analysis.

Using V79 Chinese hamster fibroblast cells Jamali & Trott (1996) demonstrated that the micronucleus frequency in binucleated cells and the number of micronuclei per cell increases significantly after X-ray irradiations, reaching a maximum of 50% at 4Gy, and decreases with an increase in dose point.

Cytokinesis-blocked human peripheral blood lymphocytes were used by Vral *et al.*, (1994) to evaluate the LET dependence repair kinetics of ^{60}Co-gamma and 14.5 MeV neutrons by assessing MN frequency after irradiation. They found that the low LET ^{60}Co-gamma rays showed increased repairable damage for the range of the time interval given in between split-doses, as was indicated elsewhere by Countryman & Heddle (1976); Ramalho *et al.*, (1988); Vral *et al.*, (1992) but with no indication of repairable damage for neutrons.

For this study, two CHO cell lines with different radiosensitivities, CHO-K1 (radioresistant) and CHO–XRS1 (radiosensitive) were used to observe the sub-lethal damage repair capacity, after cell cultures were treated either with ^{60}Co-gamma rays or p(66)/Be neutrons. Cell cultures were exposed to doses ranging between 0-4 Gy of single-fraction ^{60}Co-gamma rays and p(66)/Be neutrons, or to two equal fractions of doses ranging between 0-2 Gy, of ^{60}Co-gamma and p(66)/Be neutron irradiations. Radiation-induced damage after single- and split-doses from both treatments was determined by the MN frequency in Cytochalasin-B blocked binucleated CHO cells, which is an easy, reliable assay that is not time consuming.

5.2 MATERIALS AND METHODS

5.2.1 Cell culture conditions

Chinese Hamster Ovarian cells are commonly cultured as individual cells in monolayers attaching to the surface of the culture flask and glass coverslips. **Figure 5.1** shows a monolayer of CHO cells under a positive phase contrast microscope.

In this study, two types of Chinese hamster ovarian (CHO) cell cultures were used; namely the CHO-K1 clone number 18 and CHO-XRS1. The CHO-XRS1 cells are known to be more radiosensitive than the CHO-K1 cells. Identical clones of both types of CHO cells are kept in liquid nitrogen and have been established in cultures at iThemba LABS. Chinese hamster cells were stored in liquid nitrogen (-197^{0}C) in a mixture of 10% dimethylsulfoxide (DMSO) and 90% cell suspension in pure foetal calf serum (FCS).

DMSO is an organic solvent and acts as an anti-freeze agent. Aliquots of 2 ml samples in cryogenic vials were available for use. To initiate cell culture, one ampoule stored in liquid nitrogen was placed directly into a 37^0C water bath to thaw. The cell suspension was then mixed with 8 ml Eagle Minimum Essential Medium (α-MEM) under sterile conditions. α-MEM is a growth medium containing all the essential vitamins, amino acids, buffer salts and antibiotics (penicillin and streptomycin). The working solution contained 10% foetal calf serum (FCS). A 10% FCS for CHO-K1 and 5% FCS for the CHO-XRS1 cells in α-MEM medium were used. The cell suspension was centrifuged at 1000 revolutions per minute (rpm) for 10 minutes to form a cell pellet. The supernatant was decanted and the pellet re-suspended in 5 ml α-MEM. This 5 ml cell suspension was then seeded into a T25 tissue culture flask and incubated at 37^0C in a humidified atmosphere of 5% CO_2. The tissue culture flask caps were loosened to allow for gaseous exchange.
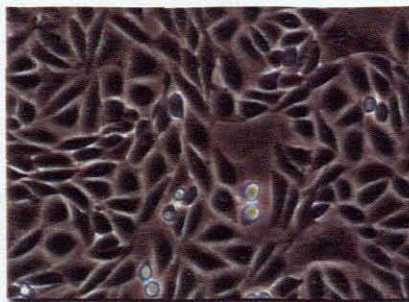
Figure 5.1. A monolayer of CHO-K1 cells under positive phase contrast microscopy.

Cell culture growth was monitored on a daily basis by observing the cells microscopically to assess if there was any bacterial contamination or abnormalities in the

cell growth. When cells reached confluence, adherent cells were detached by trypsinisation using EDTA-trypsin (1: 2.5 v/v) mixture before sub-culturing them in new flasks, as overgrowth of cells results in cell death.

5.2.2   Irradiation source

Gamma-irradiation was performed using a ^{60}Co-gamma unit (Eldorado 76, Atomic Energy of Canada Ltd.) at iThemba LABS, Faure. Vertical rays directed upwards on a field size of 30 cm x 30 cm were delivered at a dose-rate of 0.22Gy per minute, a source to surface distance (SSD) of 70 cm, and a gantry angle of 180°. The absorbed dose was measured according to the International Commission on Radiation Units and measurements (ICRU) protocol. T25 culture flasks were positioned at the centre of the radiation field on a 5 mm thick Perspex block, used as build up material and a 50 mm thick Perspex block was put above the culture flasks, separated by spacers and worked as a backscatter material (**Figure 5.2**).

Doses of 0Gy (control), 3Gy as single-fractions, and 1.5Gy as two equal fractions with a time interval of 1, 2 and 3 hours between fractions, were applied for CHO-K1 cells. Similarly for CHO-XRS1 cells, 1.5Gy as a single-dose (0 hrs) and two equal fractions of 0.75Gy as split-dose, with a time interval of 1, 2 and 3 hours in between fractions, were delivered. Split-dose cell cultures were incubated at 37^0C, between fractions in a humidified atmosphere of 5% CO_2 before being treated with the second fraction.

Figure 5-2: Photograph showing the setup procedure during ^{60}Co-gamma radiation. Note that the beam is directed from below.

p(66)/Be neutron irradiation was carried out at iThemba LABS, Faure; using a cyclotron generating a dose-rate of 0.4Gy per minute with a 66 MeV energy of protons bombarding a 19.6 mm thick beryllium target. A vertical beam directed downwards on a field size of 29 cm x 29 cm, and an SSD of 150 cm was used at a gantry angle of 0°. Cell cultures were placed at the centre of a beam source on a 9 cm thick Perspex, which served as backscatter material, and 2 cm thick poly-ethylene block on spacers used as build up material.

Doses of 0Gy (control) and higher doses of 1.5Gy as a single-fraction (0hrs) and 0.75Gy as two equal fractions, with a time interval of 3 hours inbetween fractions were applied for CHO-K1 cells. Similarly, for CHO-XRS1 cell cultures 0.5Gy as a single-dose (0 hrs) and two equal fractions of 0.25Gy as a split-dose, with a time interval of 3 hours inbetween fractions were delivered. Split-dose cell cultures were incubated at 37°C, between fractions in a humidified atmosphere of 5% CO_2, before being treated with the second fraction. p(66)/Be neutron split-dose irradiations were performed only with a time interval of 3 hours for logistical reasons.

5.2.3 Cell preparation for MN assay

After irradiation, cell cultures were incubated at 37^0C, 5% CO_2 for 20 minutes. Adherent cell monolayers were trypsinised to detach from the substrate by treatment with trypsin (Highveld Biological (PTY), Ltd., RSA), a proteolytic enzyme derived from beef pancreas. To facilitate the process, EDTA mixed with trypsin was used. EDTA adsorbs heavy ions like Mg^{++} and Ca^{++} involved in the attachment of cells to each other and to the substrate. The medium, which covers the cell monolayers, was removed from the tissue culture flask and then rinsed twice with 1.5 ml of trypsin-EDTA mixture, and discarded. The flask was returned to the incubator for 3 minutes. During this time the cells detached and became spherical as a result of the enzyme action of trypsin. The flask was then tapped in the palm of the hand in order to further loosen the cells to yield a single cell suspension. The enzymatic action of the trypsin was halted by adding 10 ml α-MEM to the cell cultures. Cell suspensions were now ready for dilution and seeding. All cell cultures were carried out under sterile conditions in a laminar flow cabinet.

5.2.4 Cell suspension and seeding

3 ml of α-MEM growth medium and 6 ml of cell suspension were mixed in a plastic test tube. Using a haemocytometer the number of cells per 1 ml was estimated and seeded at a concentration of 6-7 x 10^4 cells in a 35 mm plastic Petri dish (Corning, NY) containing a 22 mm glass cover slip (Chance Propper, England). Cytochalasin-B (C-6762; Sigma) was added immediately after seeding cell samples to each Petri dish to give a final concentration of 2 μg/ml and incubated at 37^0C for 24 hours.

5.2.5 Cell fixation and staining

Before cell samples were fixed, the growth medium was removed and a fixative of methanol-acetic acid (3:1 v/v) was added and left for 10 minutes. After discarding the fixative, samples were left to air dry before staining.

Glass coverslips with CHO-K1 and -XRS1 cells attached were stained with 1% acridine-orange for 1 minute, rinsed with distilled water twice and de-stained in buffer solution (BDH Lab., England), pH 6.8 for 1 minute. A drop of buffer solution was placed on a microscope slide and the coverslip was carefully mounted upside down avoiding any bubble formation. To prevent the cell sample from drying, the coverslip edges were sealed with nail vanish. Four slides were prepared for counting of MN for each dose-point.

5.2.6 Microscopic analysis and scoring system

The scoring system for micronuclei in this study was adapted from Fenech *et al.*, (2003) and was limited to binucleated cells. Scoring criteria included: the cell should be bi-nucleated with nuclei more or less the same size and stain intensity; the micronuclei should be one third of the main nuclei and the same stain intensity as the main nuclei; a clear border should exist between nuclei and micronuclei, and micronuclei not linked or connected to the main nucleus were included. **Figure 5.3** shows a diagrammatic representation of the micronuclei scoring system.
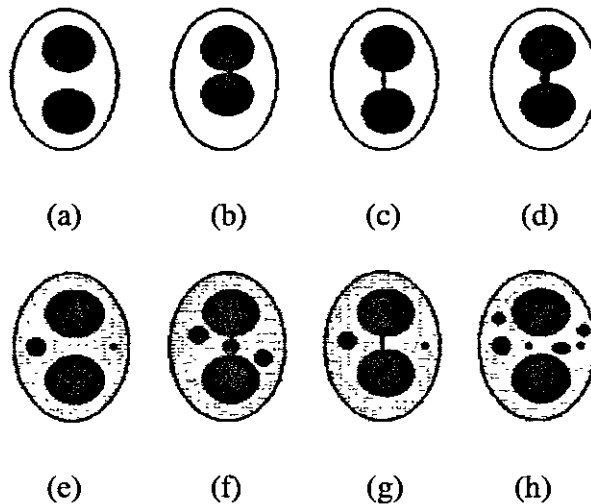
Figure 5.3. Diagrammatic representation of the micronuclei scoring system. Cells scored as binucleated are shown in diagrams with; (a) two separate nuclei; (b) slightly touching nuclei; (c) and (d) different size of nucleoplasmic bridge. Diagrams (e),(f),(g), and (h) show binucleated cells with 2, 3, 2 and 6 micronuclei, respectively.

A minimum of 500 BN cells in each of 4 slides per experimental dose-point were analysed for the presence of micronuclei and were scored as 0, 1, 2, 3, 4 or more MN per BN cell. A Zeiss Axioskop fluorescent microscope equipped with a fluorescein isothiocyanate (FITC) filter was used. Micronuclei formation due to radiation exposure were easily identified and enumerated at x600 objective **(Figure 5.4)**.

Micronuclei per 500 binucleated cells were calculated as follows:

$$\text{MN/500 BN cells} = \frac{[(\text{MN1} \times 1) + (\text{MN2} \times 2) + \ldots\ldots + (\text{MNn} \times \text{n})] \times 500}{N}$$

where **MN1** to **MNn** represent the number of binucleated cells with one to 'n' numbers of micronuclei and **N** is the total number of viable binucleated cells scored.
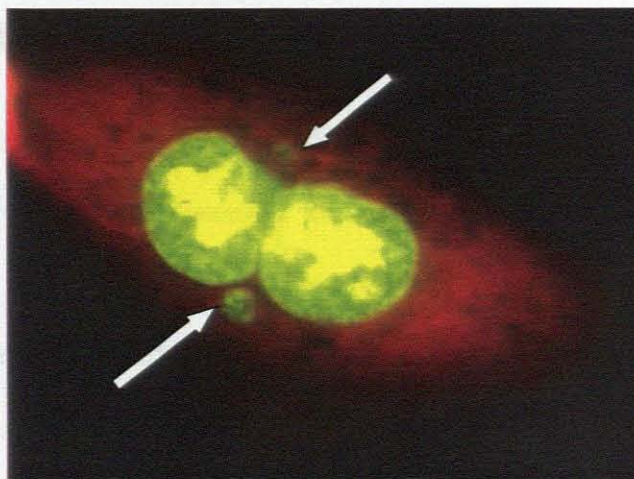
Figure 5.4. Photograph picture showing a binucleated CHO-K1
cell with two micronuclei (arrows) as a result of radiation exposure.
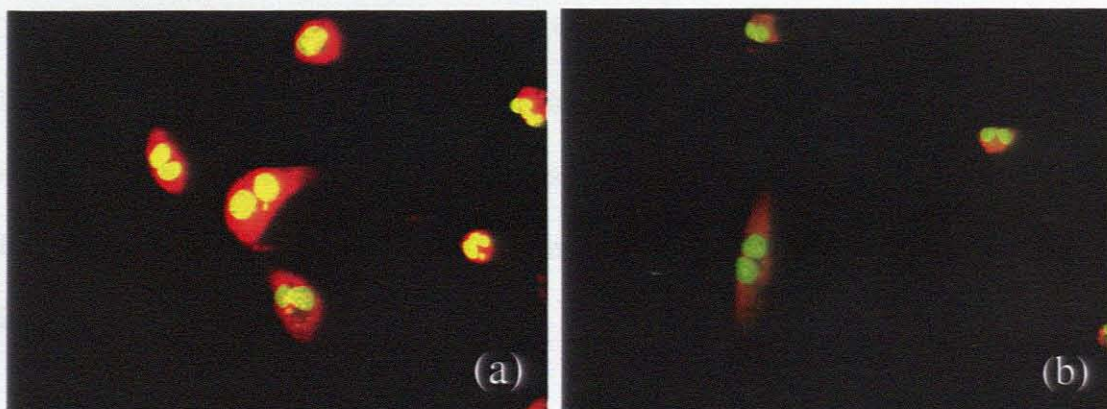
Figure 5.5. Photograph picture showing CHO-K1 cell survival, at x600 magnification
after (**a**) 3Gy of ^{60}Co-gamma rays and (**b**) 1.5Gy p(66)neutron beam irradiation. Notice
more cells are counted per field for ^{60}C0-gamma radiation than p(66)/Be neutron beam
irradiation.

5.3   RESULTS

The micronuclei background frequency in unirradiated (0Gy) control CHO-K1 and CHO-XRS1 cells were counted and data generated are shown and presented in **Table 5-1**. Similarly, micronuclei formation for irradiated CHO-K1 and –XRS1 cells were enumerated on slides per dose point for the two treatment modalities of both ^{60}Co-gamma rays and p(66)/Be neutrons. Results are tabulated and dose response curves are shown in **Figure 5.5** and **5.6**. Data represent results of radiation-induced micronuclei in BN cells after micronuclei background frequency has been subtracted from the calculation of MN per 500 BN cells.

Dose-dependent response data was obtained for single-doses of 3Gy (CHO-K1) and 1Gy (CHO-XRS1); and split-doses of 1.5Gy (CHO-K1) and 0.5Gy (CHO-XRS1) given a time window of 1, 2 and 3 hours after ^{60}Co-gamma irradiation. However, for p(66)/Be neutrons MN were scored after a single-dose of 1.5Gy (CHO-K1) and 0.5Gy (CHO-XRS1); and after a 3hr time interval between split-doses of 0.75Gy (CHO-K1) and 0.25Gy (CHO-XRS1).

Table 5.1. Micronuclei background frequency data for control CHO-K1 and –XRS1 cells no irradiation was applied.

Control CHO-K1									
	DOSE	BN	1MN	2MN	3MN	4MN	Total	Total MN	MN/500 BN cells
	0 Gy	1000	7	0	0	0			
		1000	1	0	0	0			
		1000	4	0	0	0			
Total		3000	12	0	0	0	3012	12	2
Control CHO-XRS1									
	DOSE	BN	1MN	2MN	3MN	4MN	Total	Total MN	MN/500 BN cells
	0 Gy	1000	27	2	0	0			
		1000	32	0	0	0			
		1000	50	1	1	0			
Total		3000	109	3	1	0	3113	118	19

Table 5.2. Micronuclei score in CHO-K1 cells after single-dose of 3Gy (0hr) and split-dose of 1.5Gy given at a time interval of 1, 2 and 3hrs after ^{60}Co-gamma irradiation.

^{60}Co-gamma CHO-K1									
Dose	Time	BN	1MN	2MN	3MN	4MN	Total Cell	Total MN	MN/500 BN cells
3 Gy	0hr	637	110	13	0	1			
		637	115	22	2	0			
		637	95	16	2	0			
Total		1911	320	51	4	1	2287	438	93.8
1.5 + 1.5 Gy	1hr	655	101	13	2	0			
		637	79	22	3	1			
		667	92	14	4	0			
Total		1959	272	49	9	1	2290	401	85.6
1.5 + 1.5 Gy	2hr	637	100	11	1	0			
		648	85	12	1	1			
		639	100	11	2	0			
Total		1924	285	34	4	1	2248	369	80.1
1.5 + 1.5 Gy	3hr	773	148	18	1	0			
		806	140	20	3	0			
		831	136	18	2	0			
Total		2410	424	56	6	0	2896	554	93.6

Table 5.3. Micronuclei score in CHO-XRS1 after 1Gy single-dose (0Hr) and split-dose of 0.5Gy given a time window of 1, 2 and 3 hrs of ^{60}Co-gamma irradiation.

^{60}Co-gamma CHO-XRS1									
Dose	Time	BN	1MN	2MN	3MN	4MN	Total Cell	Total MN	MN/500 BN cells
1 Gy	0hr	825	189	29	4	0			
		854	141	38	4	1			
		829	221	48	10	3			
Total		2508	551	115	18	4	3196	851	114.1
0.5+0.5 Gy	1hr	875	245	44	2	0			
		875	218	64	6	3			
		875	199	46	9	3			
Total		2625	662	154	17	6	3464	1045	131.8
0.5+0.5 Gy	2hr	863	251	47	9	3			
		893	185	28	7	2			
		793	218	36	5	3			
Total		2549	654	111	21	8	3343	971	126.2
0.5+0.5 Gy	3hr	852	190	38	4	1			
		737	228	59	9	2			
		419	139	34	5	1			
Total		2008	557	131	18	4	2718	889	142.5

Using the CHO-K1 cells, the score for ^{60}Co-gamma exposure was found to be 93.8 for the single-dose of 3Gy, and 85.6; 80.1 and 93.6 for the split-dose of 1.5Gy after a time window of 1, 2 and 3 hours respectively. Results are shown in **Table 5.2** as both single- and split-dose. Using the CHO-XRS1 cells, the score was found to be 114.1 for the single-dose (0 hrs) of 1Gy, and 131.8, 126.2 and 142.5 for the split-dose of 0.5Gy after a time window of 1, 2, and 3 hours, respectively and are shown in **Table 5.3** as single- and split-doses.

Table 5.4. Micronuclei scores in CHO-K1 cells after p(66)/Be neutron beam irradiation shown as single- versus split-dose exposure.

p(66)/Be neutrons CHO-K 1									
Dose	Time	BN	1MN	2MN	3MN	4MN	Total Cell	Total MN	MN/500 BN cells
1.5 Gy	0hr	720	219	30	8	0			
		459	179	28	12	3			
		602	175	44	5	0			
Total		1781	573	102	25	3	2484	864	171.9
0.75+0.75Gy	3hr	859	232	31	4	3			
		708	174	28	5	3			
		649	181	25	5	2			
Total		2216	587	84	14	8	2909	829	140.5

Table 5.5. Micronuclei scores in CHO-XRS1 cells after p(66)/Be neutron beam irradiation shown as single- versus split-dose exposure.

p(66)/Be neutrons CHO-XRS 1									
Dose	Time	BN	1MN	2MN	3MN	4MN	Total Cell	Total MN	MN/500 BN cells
0.5 Gy	0hr	849	271	69	9	1			
		811	277	59	7	0			
		839	252	41	6	1			
Total		2499	800	169	22	2	3492	1212	154.5
0.25+0.25Gy	3hr	863	228	22	1	0			
		801	184	32	6	2			
		751	250	44	3	0			
Total		2415	662	98	10	2	3187	896	121.6
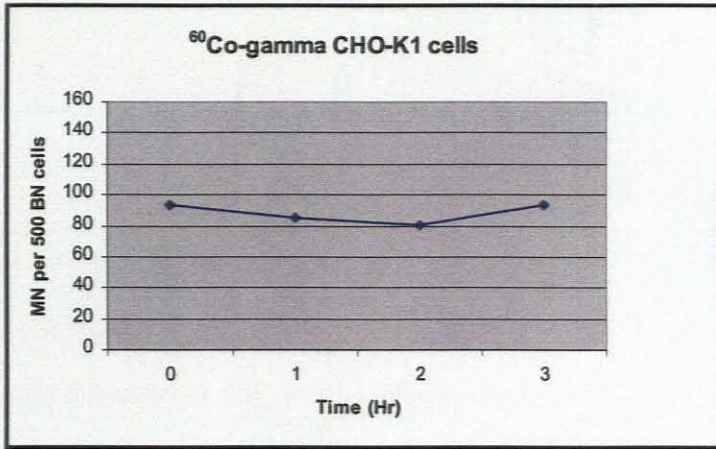
(a)
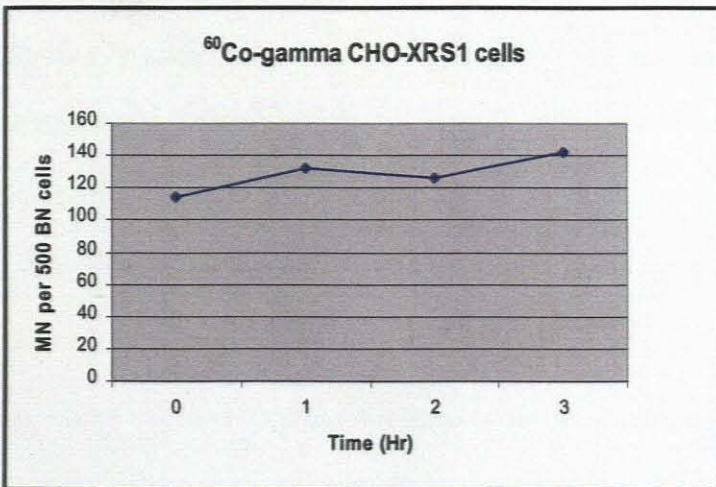
(b)

Figure 5.6. Two graphs showing the dose response after
^{60}Co-gamma irradiation. (a) shows the response using the
CHO-K1 cells and (b) using CHO-XRS1 cells.

5.4 DISCUSSION

Neutrons and other high-LET radiations cause more biological damage than sparsely ionising radiation, such as X-and gamma-rays. This phenomenon is observed in both CHO-K1 and CHO-XRS1 cells. The micronuclei, viewed under ideal magnification, reveal a higher MN score after irradiation with particle neutrons than ^{60}Co-gamma irradiation, as expected from this result. This phenomenon is supported by the data generated from both experiments and is in keeping with published work. This is indicated by the relatively high MN score obtained for particle neutrons than for ^{60}Co-gamma irradiations.

Dose response curves of both CHO and XRS in ^{60}Co-gamma irradiation showed internal MN score differences, allowing comparison of cell line sensitivity and dose application. CHO-XRS1 cells are more sensitive to radiation-induced damage indicated by high MN scores than the CHO-K1 cells at the same dose. Similarly, dose response curves of both CHO cell lines irradiated with neutrons both followed the same pattern although the same radiation dose resulted in higher MN scores than the CHO-K1 cells. However, for an equivalent radical dose given they scored almost the same as CHO-K1 cells.

A time-dependent response is observed in both CHO cell lines for both irradiations and dose agreement ^{60}Co-gamma irradiation. (a) shows the response using the data for ^{60}Co-gamma radiation-induced damage was relatively constant for the equivalent dose given between the two cell lines, as the sensitive of both cell lines responded correspondingly.
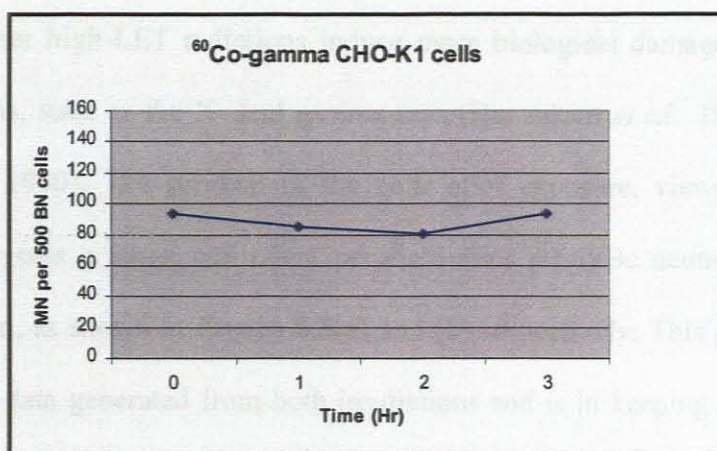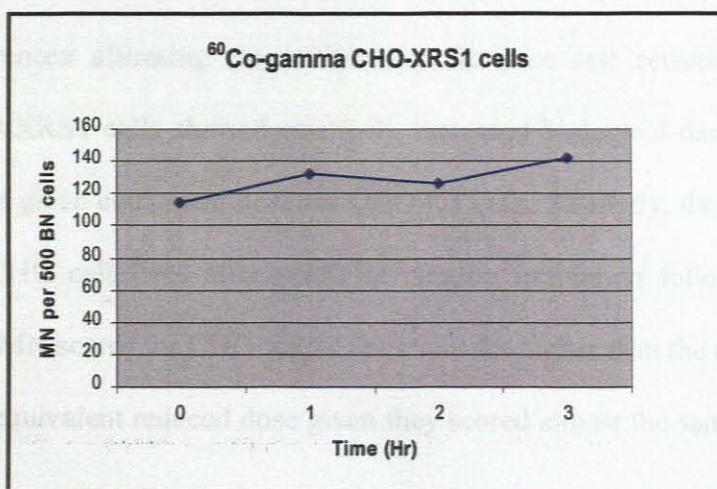

(a)

(b)

Figure 5.6. Two graphs showing the dose response after ^{60}Co-gamma irradiation. (a) shows the response using the CHO-K1 cells and (b) using CHO-XRS1 cells.

- 118 -

5.4   DISCUSSION

Neutrons and other high-LET radiations induce more biological damage than sparsely ionising radiations, such as the X- and gamma-rays (Barendsen *et al.*, 1968, Spotheim-Maurizot *et al.*, 1990). The survival of the cells after exposure, viewed under x600 magnification, reveals a lower cell count per field after p(66)/Be neutrons than ^{60}Co-gamma irradiation, as shown in **Figure 5.5(a)** and **(b)** respectively. This phenomenon is supported by the data generated from both irradiations and is in keeping with published work. This is indicated by the relatively high MN score obtained for p(66)/Be neutrons than for ^{60}Co-gamma irradiations.

Dose response curves of both CHO cell lines for ^{60}Co-gamma irradiation showed internal MN score differences affirming the relationship between cell sensitivity and dose application. CHO-XRS1 cells showed relatively increased biological damage indicated by high MN score given equivalent doses to CHO-K1 cells. Similarly, the dose response curves of both CHO cell lines after p(66)/Be neutron irradiation followed the same pattern, although MN scores for CHO-XRS1 cells was not higher than the CHO-K1 cells. However, for an equivalent reduced dose given they scored almost the same as CHO-K1 cells.

A time-dependent response is observed in both CHO cell lines for both irradiations and close agreement is observed according to their sensitivity. This explains that for ^{60}Co-gamma radiation-induced damage was relatively constant for the equivalent doses given between the two cell lines, as the sensitive of both cell lines responded correspondingly

between time intervals of 0,1,2 and 3 hours. The same trend was also followed by the p(66)/Be neutrons, though the reading was only done at 0 and 3 hours because of some logistic reason.

Cell repair kinetics for both radiation exposures were measured following the application of various time intervals between split-doses. For ^{60}Co-gamma irradiations the repair kinetics showed insignificant difference using the CHO-K1 cell line and negative repair kinetics was observed using the CHO-XRS1 cell line. The time-dependent response in Figure 5.6(a) revealed a curve close to a straight line verifying that no repair had occurred during the time interval between the split-doses for the CHO-K1 cells. Nonetheless, the MN score for CHO-XRS1 cells increased by 25% showing negative repair kinetics as a drop in MN was only observed at 2 hours, as shown in Figure 5.6(b). However, Vral *et al.*, (1994) showed clear cell repair kinetics for ^{60}Co-gamma irradiations with time intervals of 30 minutes to 7 hours between split-doses.

On the other hand, for p(66)/Be neutron irradiations significant cell repair kinetics was observed in both CHO cell lines. A decrease in MN of 18% and 21% was obtained in CHO-K1 and CHO-XRS1 cells, respectively, after 3 hour time interval between split-doses. Although explained by Vral *et al.*, (1994), no repair kinetics was observed after a split-dose of 1.5Gy given a time interval of 30 minutes to 7 hours. The possible reason for this could be the energy source of the radiation and has played a role in the repair

kinetics of both cell lines. Vral and colleagues applied a 5.5 MeV mean energy neutron source to blood lymphocytes which is lower than the 66 MeV energy source we used. This could explain that either high energy radiation overkill cells, where the radiation-induced damage is not detected as all cells with MN will not be scored, or they have the potential to activate more cell repair than low energy radiation.

Throughout the experiment only once did there exist an overkill of cells. This is shown in CHO-XRS1 cells exposed to ^{60}Co-gamma radiation. The biological damage expected at 0 hour after a 1Gy single dose was less than the 3 hour split-dose. For an acute exposure radiation-induced damage this is not the case. However, with p(66)/Be neutrons it proved otherwise, which made us question whether high energy radiation has the potential to initiate more repair than low energy radiation.

References:

Brown, J.K., Williams, A., Withers, H.R., Ow, K.T., Gramacho, C., Grey, R. & Amies, C. 1997. Sources of variability in the determination of micronuclei in irradiated peripheral blood lymphocytes. *Mutation research/ Genetic Toxicology and Environmental Mutagenesis*, 389(2-3): 123-128.

Barendsen, G.W., Koot, C.J. & Van Kersen, G.R. 1968. Responses of cultured cells, tumors and normal tissue to radiation of different linear energy transfer. *Current Topics of radiation Research*, 4: 293-356.

Chang, W.P., Tsai, M., Hwang, J., Lin, Y., Hsieh, W.A. & Shao-Yi, H. 1999. Follow-up in the micronucleus frequencies and its substitutes in human populations with chronic low-dose gamma irradiation exposure. *Mutation Research*, 428: 99-105.

Countryman, P.I. & Heddle, J.A. 1976. The production of micronuclei from chromosome aberrations in irradiated cultures of human lymphocytes. *Mutation Research*, 41:321-331.

Fenech, J. 2000. The in vitro micronucleus technique. *Mutation Research*, 455: 81-95.

Fenech, J., Holland, N., Chang, W.P., Zeiger, E. & Bonassi, S. 1999. The Human Micronuclei Project-An international collaborative study on the use of the micronucleus techniques for measuring DNA damage in humans. *Mutation Research*, 428:271-283.

Fenech, J., Chang, W.P., Kirsch-Volders, M., Holland, N., Bonassi, S. & Zeiger, E. 2003. HUMAN project: detailed description of the scoring criteria for the cytokinesis-blocked micronucleus assay using isolated human lymphocyte cultures. *Mutation Research*, 534: 65-75.

Fenech, M. & Morley, A.A. 1985. Measurement of micronuclei in lymphocytes, *Mutation Research*, 147: 29–36.

Fenech, M. & Morley, A.A. 1986. Cytokinesis-blocked micronucleus method in human lymphocytes: Effect of in vivo ageing and low-dose X-irradiation. *Mutation Research*, 161: 193–198.

Hall, E.J. 2000. Radiobiology for the Radiologist. 5th ed. Philadelphia, PA: Lippincott Williams & Wilkins. 67-87.

International Atomic Energy Agency (IAEA), 2001. Cytogenetic Analysis for Radiation Dose Assessment, A manual, Technical Report Series No. 405, Vienna

Jamali, M. & Trott, K.R. 1996. Increased micronucleus frequency in the progeny of irradiated Chinese hamster cells. *International Journal of Radiation Biology*, 69(3): 301-307.

Köksal, G., Dalci, D.Ö. & Pala, F.S. 1996. Micronuclei in human lymphocytes: the ^{60}Co-gamma-ray dose-response. *Mutation research*, 359: 151-157.

Kryscio, A., Müller, W-U., Wojcik, A., Kotschy, N., Grobelny, S. & Streffer, C. 2001. A cytogenetic analysis of the long term effect of uranium mining on peripheral lymphocytes using the micronucleus-centromere assay. *International Journal of Radiation Biology*, 77(11): 1087-1093.

Le Roux, J., Slabbert, J.P., Smit, B. & Blekkenhorst, G. 1998. Assessment of the micronucleus assay as a biological dosimeter using cytokinesis-blocked lymphocytes from cancer patients recovering fractionated partial body radiotherapy. *Strahlenther. Onkol.* 174(2): 75-81.

Ramalho, A., Sunjevaric, I. & Natarajan, A.T. 1988. Use of the frequencies of micronuclei as quantitative indication of X-ray-induced chromosomal aberrations in human peripheral blood lymphocytes: comparisons of two methods. *Mutation Research*, 207: 141-146.

Slabbert, J.P., Theron, T., Serafin, A., Jones, D.T.L., Böhm, L. & Schmitt, G. 1996. Radiosensitivity variation in human tumor cell lines exposed in vitro to p(66)/Be neutrons or ^{60}Co γ-rays. *Strahlenther. Onkol.*, 172(10): 567-572.

Spotheim-Maurizot, M., Charlier, M. & Sabattier, R. 1990. DNA radiolysis by fast neutrons. *International Journal of Radiation Biology*, 57: 301-313.

Travis, E.L. 2000. Primer of Medical Radiobiology. 2nd ed. St. Louis: Mosby

Venkatachalam, P., Paul Solomon, F.D., Karthikeya Prabhu, B., N. Mohankumar, M., Gajendiran, N. & Jeevanram, R.K. 1999. Estimation of dose in cancer patients treated with fractionated radiotherapy using translocation, dicentrics and micronuclei frequency in peripheral blood lymphocytes. *Mutation research/ Genetic Toxicology and Environmental Mutagenesis*, 429(1): 1-12.

Vral, A., Thierens, H. & De Ridder, L. 1992. Study of dose-rate and split-dose effects on the *in vitro* micronucleus yield in human lymphocytes exposed to X-rays. *International Journal of Radiation Biology*, 61: 777-784.

Vral, A., Thierens, H., Baeyens, A. & De Ridder, L. 2002. The micronucleus and G2 phase assays for human blood lymphocytes as biomarkers of individual sensitivity to ionizing radiation: Limitations imposed by intra-individual variability. *Radiation Research,* 157: 472-477.

Vral, A., Verhaegen, F., Thierens, H. & De Ridder, L. 1994. Micronuclei induced by fast neutrons versus ^{60}Co γ-rays in human peripheral blood lymphocytes. *International Journal of Radiation Biology,* 65(3): 321-328.

Widel, M., Jedrus, S., Lukaszczyk, B., Raczek-Zwierzycka, K. & Swierniak, A. 2003. Radiation-induced micronucleus frequency in peripheral blood lymphocytes is correlated with normal tissue damage in patients with cervical carcinoma undergoing radiotherapy. *Radiation Research,* 159: 713-721.

Zsuzsanna, A., Krepinsky, A.B., Bianco, A. & Köteles, G.J. 1987. The present state of perspectives of micronuclei assay in radiation protection. A review. *Appl. Radiat. Isot.,* 38(4): 241-249.

Chapter 6

DIRECTION FOR FUTURE STUDY

Changing the fractionation protocol of the radiation dose given influences the biological factor of the radiation in addition to the total dose and overall time increase (NCRI, 2003). The aim of an increased number of fractions in p(66)/Be neutron therapy is to separate the early and late effects of radiation. While the overall treatment time stays the same, the total dose may increase as the dose per fraction decreases. This results increased early effects but reduced late effects. Manipulation of the trend of fractionation along with the increase of the total dose and its distribution should lead to a better neutron therapeutic gain.

The primary focus of this study was to increase the iso-effectiveness of fractionated p(66)/Be neutron radiations by increasing the number of fractions and lowering the dose-per-fraction, *i.e.* to attain the same biological effect when radiation is given as a single fraction. This may result in an increase of the total dose and it is assumed there would be sub-lethal damage repair, thus requiring an additional dose to compensate the repair after irradiation.

Intestinal crypt regeneration used in the *in vivo* assessment of repairable damage after p(66)/Be neutrons showed considerable repair. This was also supported by the *in vitro*

experiments using CHO-K1 and –XRS1 cells, where the repair kinetics were defined more clearly for p(66)/Be neutrons than for ^{60}Co-gamma irradiations.

This is very important as the protocol for neutron patient treatments is under debate and there are clinical indications suggesting a lower dose per fraction should be given to increase the number of treatment fractions to complete the course of neutron therapy. Moreover, when lowering the dose per fraction, the α/β ratio needs to be correctly estimated for p(66)/Be neutrons as the early effects of the therapy may vary with the protocol. Therefore, it was observed that it is possible to estimate a reasonable α/β ratio for p(66)/Be neutrons using values previously determined for photons.

However, the immunohistochemistry experiments for collagen-I and IV, p53 and CD34 for stem cell marker assessment were inconclusive and did not support the above conclusion. Not withstanding the pitfalls, and making suggested changes to the protocol of the experiment, some therapeutic importance for p(66)/Be neutrons could be gained as an indicator of early effect; such as fibrosis. In view of the current work it is recommend flowcytometry be used to assess collagen after irradiation. It is also advisable to follow a 4 hour cycle for animal tissue processing as the integrity of the tissue was compromised for over night processing.

In conclusion, this work has proven beyond a reasonable doubt that there exists a chronological difference in cell repair kinetics for p(66)/Be neutrons between single- and split-dose irradiation; and it is important for therapeutic purposes that further investigation is carried out as some patients may benefit from it.